COOPERATIVE SPECTRUM SENSING/ACCESS IN COGNITIVE RADIO NETWORKS

BY

RAZA UMAR

A Dissertation Presented to the

DEANSHIP OF GRADUATE STUDIES

KING FAHD UNIVERSITY OF PETROLEUM & MINERALS

DHAHRAN, SAUDI ARABIA

In Partial Fulfillment of the
Requirements for the Degree of

DOCTOR OF PHILOSOPHY

In

ELECTRICAL ENGINEERING

MAY 2014

KING FAHD UNIVERSITY OF PETROLEUM & MINERALS
DHAHRAN 31261, SAUDI ARABIA

DEANSHIP OF GRADUATE STUDIES

This thesis, written by **RAZA UMAR** under the direction of his thesis adviser and approved by his thesis committee, has been presented to and accepted by the Dean of Graduate Studies, in partial fulfillment of the requirements for the degree of **DOCTOR OF PHILOSOPHY IN ELECTRICAL ENGINEERING**.
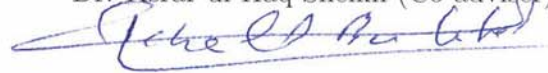
Dissertation Committee

Dr. Wessam Mesbah (Adviser)

Dr. Asrar-ul-Haq Sheikh (Co-adviser)

Dr. Khaled Ben Letaief (Member)

Dr. Mohamed Adnan Landolsi (Member)

Dr. Muhammad Ashfaq Bokhari (Member)

Dr. Ali A. Al-Shaikhi
Department Chairman

Dr. Salam A. Zummo
Dean of Graduate Studies

26/5/14

Date

Dedicated to my
loving parents for their never-ending prayers,
beloved wife for her affection and support, and
adorable children for their immense love.

ACKNOWLEDGMENTS

Allah, I start in His name, who is the Most Beneficent, the Most Merciful.

All praise be to Allah for His boundless blessings. May Allah bestow peace and His choicest blessings on His last prophet, Hadhrat Muhammad (Peace Be Upon Him), his family (May Allah be pleased with them), his companions (May Allah be pleased with them) and his followers.

First of all, I would like to acknowledge that the fours years I spent at KFUPM have been a great learning experience. I am thankful to my advisors, Dr. Wessam Mesbah, and Dr. Asar-ul-Haq Sheikh, for their great mentorship, for the patience and trust they showed in me, and above all for their guidance in persevering under hardship. I am thankful to Dr. Asrar for teaching me to recognize and formulate important questions, and to Dr. Wessam for guiding me to be precise and always try to simplify things rather than to complicate them!

I thank Dr. Khaled Ben Letaief, Dr. Mohamed Adnan Landolsi and Dr. Muhammad Ashfaq Bokhari for serving on my dissertation committee. Dr. Khaled's enthusiastic encouragement helped in achieving my research goals. I am also grateful to him for guiding me to focus on game-theoretic tools as my problem solving approach. Dr. Adnan's comments on the emerging trends in my

research area helped me explore interesting works related to my field of interest. Dr. Ashfaq's feedback on my research work helped greatly in the presentation of my contributions.

I would like to make a special acknowledgement to Dr. Mohamed Deriche, who always encouraged me to have confidence in my research outcomes, and guided me about various research dimensions to explore during my PhD. I strongly believe that his confidence in me played a vital role in accomplishing my research objectives. I am also thankful to all the professors at KFUPM. In particular, I benefited a lot from very useful discussions with Dr. Maan Kousa, Dr. Salam Zummo, Dr. Samir Ghadban, Dr. Ali Muqaibel, and Dr. Ashraf Mahmoud.

I would also like to appreciate the support of all my friends at KFUPM. Thanks to Khurram Masood, Imran Akram, Hussein Ali, Moaz Rais, Omer Bin Saeed, and all fellow students at KFUPM whom I shall not be able to name here. Their friendship made my stay at KFUPM pleasant and enjoyable.

Last but not least, I am very thankful to my parents for their prayers and well wishes. I would also like to thank my wife for making my job very easy. She took care of all the family responsibilities and offered me the moral support to focus on my PhD. Finally, my children were always a source of relaxation, after spending weekends with whom, I used to come up with interesting solutions to my research problems.

I pray to Allah subhana wa ta'aala that He may make this work beneficial for the society! (Ameen).

TABLE OF CONTENTS

CHAPTER 4 THROUGHPUT-EFFICIENT SPECTRUM ACCESS IN CENTRALIZED CRNS   96

CHAPTER 5 THROUGHPUT-EFFICIENT SPECTRUM ACCESS IN DISTRIBUTED CRNS   121

LIST OF TABLES

LIST OF FIGURES

Nomenclature

ADC   :   Analog to Digital Converter

ADP   :   Asynchronous Distributed Pricing

AM   :   Amplitude Modulation

AWGN   :   Additive White Gaussian Noise

BC   :   Blind Combining

BCED   :   Blindly Combined Energy Detection

BPF   :   Band Pass Filter

BSS   :   Blind Source Separation

BW   :   Bandwidth

CBD   :   Covariance Based Detection

CDR   :   Constant Detection Rate

CF   :   Coalition Formation

CFAR   :   Constant False Alarm Rate

CPC   :   Cognitive Pilot Channel

CR   :   Cognitive Radio

CRN   :   Cognitive Radio Network

CS   :   Compressed Sensing/Sampling

CSI   :   Channel State Information

CSS   :   Cooperative Spectrum Sensing

CSSA   :   Cooperative Spectrum Sensing and Access

DOSA : Dynamic and Opportunistic Spectrum Access

DSAP : Dynamic Spectrum Access Protocol

EBD : Eigenvalue Based Detection

ED : Energy Detection

EGC : Equal Gain Combining

EME : Energy to Minimum Eigenvalue

FC : Fusion Center

FCC : Federal Communications Commission

FDM : Frequency Division Multiplexing

GC : Grand Coalition

GLRT : Generalized Likelihood Ratio Test

GT : Game Theory

IID : Independent Identically Distributed

ILP : Integer Linear Programming

ITU-R : International Telecommunication Union, Radiocommuication Sector

MF : Matched Filter

MME : Maximum to Minimum Eigenvalue

MRC : Maximum Ratio Combining

NE : Nash Equilibrium

OCED : Optimally Combined Energy Detection

OFDM : Orthogonal Frequency Division Multiplexing

POMDP : Partially Observable Markov Decision Process

PSD   :   Power Spectral Density

PU   :   Primary User

RF   :   Radio Frequency

ROC   :   Receiver Operating Characteristics

SA   :   Spectrum Access

SC   :   Secondary Coordinator

SCS   :   Singleton Coalition Structure

SNR   :   Signal to Noise Ratio

SS   :   Spectrum Sensing

ST-SR   :   Secondary Transmitter-Receiver pair

SU   :   Secondary User

UWB   :   Ultra Wide Band

VCG   :   Vickery-Clark-Groves

xG   :   Next Generation

WiMAX   :   Worldwide Interoperability for Microwave Access

WLAN   :   Wireless Local Area Network

THESIS ABSTRACT

NAME: Raza Umar

TITLE OF STUDY: Cooperative Spectrum Sensing/Access in Cognitive Radio

                       Networks

MAJOR FIELD: Electrical Engineering

DATE OF DEGREE: May 2014

Cognitive radio (CR) technology is expected to be a key component in future wireless systems. The principal objective of CR is to optimize the use of under-utilized spectrum through efficient spectrum sensing/access. This thesis contributes to the field of CR with respect to both spectrum sensing (SS) and spectrum access (SA).

The first part of the thesis focuses on SS. A comprehensive comparative study of various SS techniques is provided in terms of achievable sensing accuracy and the required computational complexity. Since energy detection based SS offers the lowest complexity and is blind in nature, it is investigated in detail. A general structure of the test statistic and its corresponding threshold are presented to address some of the existing ambiguities in the literature, and to unveil some of the hidden assumptions on the primary user signal model. In-depth analysis of ED

highlights the roles of signal to noise ratio, performance constraints (probability of detection/false-alarm), and the observed number of samples, in approximating the exact distribution of the test statistic with Gaussian distribution.

The second part of the thesis addresses the problem of throughput-efficient spectrum access in cognitive radio networks (CRNs). A cooperative game theoretic (GT) model for joint coalition formation (CF) and bandwidth (BW) allocation is developed and the throughput of a CRN is improved at two levels: First, in the process of choosing best partners to collaborate, and second, in the process of optimally allocating and efficiently accessing the available BW. Both centralized and ad hoc network models are considered, and efficient CF algorithms, that maximize spectrum reuse efficiency subject to interference constraints, are proposed. For centralized CRNs, the sum-rate maximizing network partitioning problem is formulated as a coordinated CF game. On the other hand, for ad hoc CRNs, a fully distributed CF game is designed in which rational distributed CRs self-organize into throughput-efficient disjoint coalitions. A closed-form expression of the optimal BW allocation among the coalition members is obtained and the convergence/stability analysis of a variety of proposed CF rules is carried out.

Detailed analyses of the proposed centralized and distributed CF algorithms is performed which shows the effectiveness and the gains of the joint CF and BW allocation approach, in terms of average payoff (rate) per CR, over existing CF techniques.

CHAPTER 1

INTRODUCTION

The emerging wireless multimedia applications are leading to an insatiable demand for radio spectrum. Cognitive radio (CR) has emerged as a promising solution to the current spectral congestion problem by embedding intelligence to the conventional radio that allows opportunistic spectrum access. This thesis identifies spectrum sensing (SS) and spectrum access (SA) as the two most critical concerns for the establishment of cognitive radio networks (CRNs) and proposes efficient sensing and access strategies for NeXt Generation (xG) communication networks based on CR technology.

This introductory chapter reviews the fundamentals of CR, presents SS as a key concept in CR, and introduces coalitional game theory (GT) as a useful tool to analyze cooperation strategies among distributed CRs in CRNs. Existing work in the areas of spectrum sensing and access is discussed and the gaps therein are identified. The chapter concludes with an outline of thesis contributions followed by the thesis layout.

1.1 Background

NeXt Generation wireless services are facing a crisis of spectrum availability at
frequencies that can be economically used for wireless communications. This is
evident from the Federal Communications Commission (FCC) spectrum allocation
chart [1] shown in Figure 1.1, that indicates that most of the usable frequencies are
already allocated to multiple wireless operators and that there is very little room
for future innovative services. As a result, several spectrum regulatory authorities
around the world have carried out studies on current spectrum scarcity with an
aim to optimally manage the available radio spectrum. Interestingly, these studies
revealed that a large portion of assigned spectrum in most places is under-utilized
most of the time.
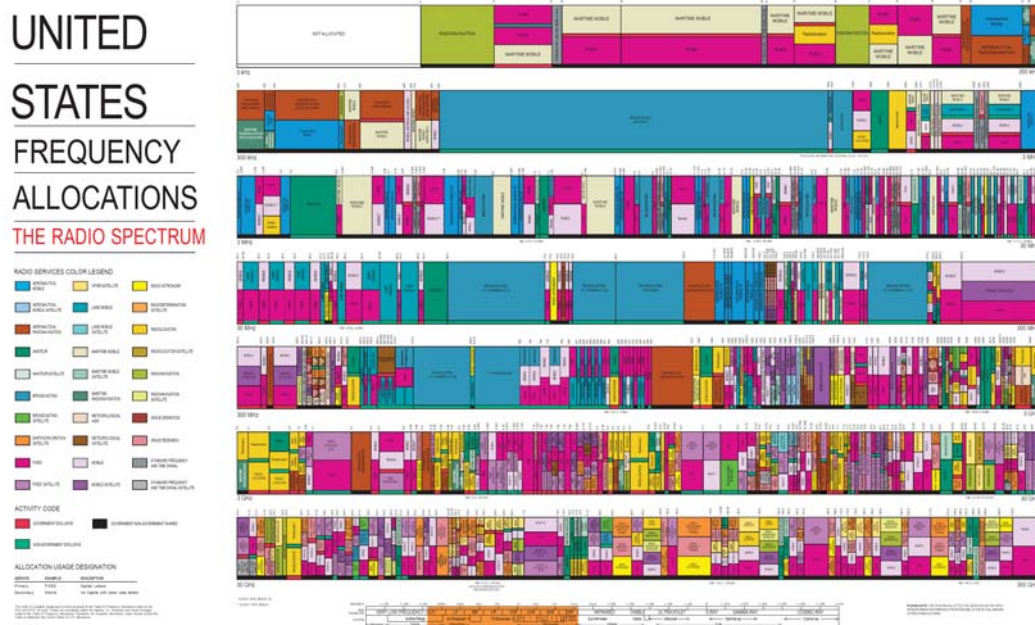
Figure 1.1: FCC spectrum allocation chart for the United States [1].
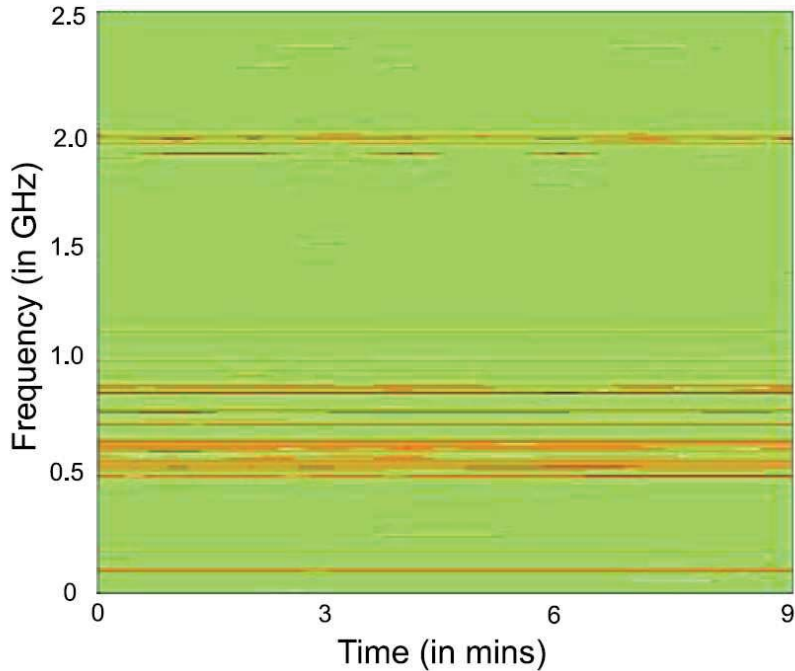
Figure 1.2: A ten minute snapshot of the spectral activity in downtown Berkeley, USA over the $0 - 2.5$ GHz band [2].

Figure 1.2 shows a ten minute snapshot of the spectral activity ('brown/dark' regions) in an urban area over the $0 - 2.5$ GHz band [2], which indicates that there is actually very little usage at the time and place at which this measurement was taken. Several spectrum-measurement studies; e.g., [3]-[5], have been conducted and have concluded that spectrum utilization varies from 15% to 85% with wide variance in time and space. It also has been inferred that the apparent spectrum shortage is in part an artificial result of the inefficient use of spectrum due to the current static and exclusive-use allocation model. These findings have opened doors to a new communication paradigm of sharing the under-utilized radio spectrum through dynamic and opportunistic spectrum access (DOSA) [6].

The technology that enables un-licensed users to dynamically and opportunis-

3

tically access the licensed spectrum, without affecting the existing users, with legacy rights to that spectrum, is the cognitive radio technology. The key component of CR technology is the ability to sense and ultimately adapt to the continuously changing radio's operating environment. In CR terminology, the incumbents of a frequency band are called primary users (PUs) while the term secondary users (SUs) is reserved for low-priority un-licensed users equipped with a cognitive capability to exploit this spectrum without affecting operation of PUs. Therefore, the most crucial task of SUs (also termed as simply CRs in literature) is to reliably identify available frequency bands across multiple dimensions (such as time, space, frequency, angle and code etc.), and efficiently exploit them by dynamically updating its transmission parameters under the stringent requirement of avoiding interference to the licensed users of that spectrum. To accomplish this, secondary users rely on robust and efficient spectrum sensing to identify vacant frequency bands under uncertain radio frequency (RF) environment and to detect primary users with high probability of detection, as soon as they become active in the band of interest.

In essence, CR introduces intelligence to conventional radio such that it senses the information from its environment by monitoring spectrum bands and capturing temporal and spatial variations. In this way, CR tracks a *spectrum hole* which represents a licensed band not being used by a licensed user at a particular time over a selected area. With an objective to exploit this spectrum availability, CR adjusts its transmitter parameters, such as modulation, frequency and

access technique, on the fly and makes use of the available band as long as no spectrum activity is detected. If this band is re-acquired by the PU, the SU must halt its transmission or move to another spectrum hole if available. A typical CR operation is depicted in Figure 1.3.
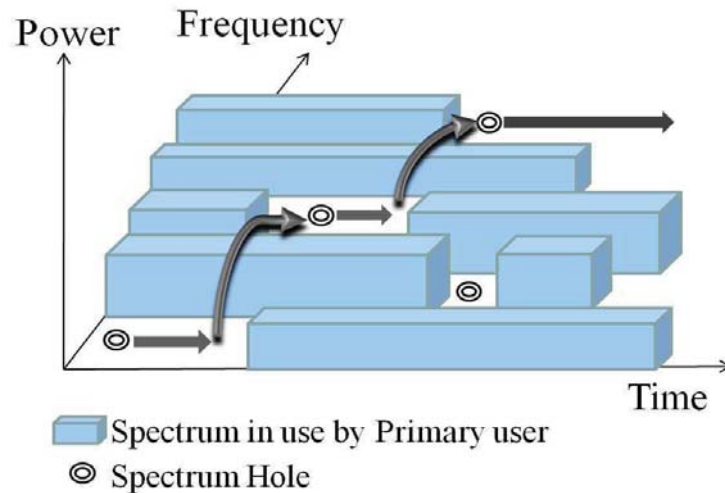
Figure 1.3: CR operation.

It is also important to point out that the cognitive functionality can allow SUs to simultaneously operate along with PUs. This is achieved by reconfiguring CR transmission parameters to ensure non-interfering coexistence with higher priority PUs. Hence, two modes for the operation of CR can be identified: (1) **Spectrum overlay**, wherein SUs only transmit over the licensed spectrum when PUs are not using that band, and (2) **Spectrum underlay**, wherein SUs are allowed to transmit concurrently with PUs under the constraint that secondary communications do not interfere with primary transmission.

The key concept in CR is the provision of opportunistic and dynamic spectrum access of licensed frequency band to unlicensed users. Hence, the main function-

ality of CR is to opportunistically *sense* the spectrum with high accuracy, and *access* it in a most efficient manner

Spectrum sensing is the task of obtaining spectrum occupancy information which is usually accomplished through primary transmitter detection. Variety of transmitter detection based SS techniques exist in literature with their own merits and demerits, but they all suffer from degraded performance under multi-path fading and shadowing. An attractive approach to improve the spectrum sensing reliability is to exploit the inherent spatial diversity in CRNs through cooperative spectrum sensing (CSS). In comparison to non-cooperative primary transmitter detection, cooperative sensing offers a more relaxed detection sensitivity requirements for cooperating users, and at the same time, it can provide a high sensing accuracy in scattering rich RF environment. However, CSS incurs an overhead in terms of cooperation delay and increased complexity. As a result, there is a dire need to perform an in-depth comparative analysis of different spectrum awareness techniques to identify a low-complexity detection scheme that can be applied locally at each radio in CRN.

The ultimate objective of CR is to utilize the un-used spectrum. Hence, throughput-efficient spectrum access is the next challenge in a distributed network of competing CRs, once the spectrum usage opportunities are identified. In this regard, how the distributed CRs cooperate to access the available bandwidth (BW), sets the limits on the average achievable transmission rate per CR.

1.2 Literature Survey and Problem Identification

The history of *"Cognitive Radio"* dates back to the article published in 1999 by Joseph Mitola [7], the same person who coined the term *"Software-defined radio"*. Over the passage of time, several formal definitions of CR have been proposed in literature owing to the required degree of *cognition* in several contexts [8]. Keeping in mind that CR aims at improved utilization of available spectrum, all the available definitions overlap in some common features/capabilities of the CR which are highlighted in the definition adopted by International Telecommunication Union, Radiocommunication Sector (ITU-R) [9] as:

"A radio or system that senses, and is aware of, its operational environment and can be trained to dynamically and autonomously adjust its radio operating parameters accordingly."

In essence, this implies that CR needs to track a **spectrum hole** defined as [10]:

"A spectrum hole is a band of frequencies assigned to a primary user, but, at a particular time and specific geographic location, the band is not being utilized by that user."

As most of the spectrum is already assigned to PUs with legacy rights, the key task is to share licensed spectrum without producing harmful interference to its licensees, which relies on robust and efficient radio-scene analysis. Radio-scene

7

analysis or spectrum sensing is the fundamental cognitive task, as identified by Haykin [11], and it primarily comprises of securing precise and accurate tracking of spectrum holes. Tandra et al., in their landmark paper [12], titled "What is a spectrum hole and what does it take to recognize one? ", have provided detailed discussion on this topic. The identified spectrum usage opportunity is then exploited by CR as long as no spectrum activity is detected. If this band is re-acquired by a PU, then the CR, being a low-priority secondary user, must either vacate the band or adjust its transmission parameters to accommodate the PU or , if available/possible, shift to another spectrum hole. The fundamental features and the main functionality of CR along with key references are presented in [13].

The first objective of this thesis is to explore various dimensions of spectrum sensing with an aim to review ongoing and emerging trends in SS and compare different SS techniques to identify low-complexity detection scheme with minimum required *apriori* information about primary transmissions.

1.2.1 Spectrum Sensing

Spectrum sensing, lying at the heart of CR, is the task of obtaining spectrum occupancy information. Literature survey on SS revealed three main approaches that can be adopted to obtain this spectrum occupancy knowledge. They are:

1. Spectrum sensing using geolocation and database [14],[15].

2. Spectrum sensing by listening to cognitive pilot channel (CPC) or PU bea-

cons [16],[17].

3. Spectrum sensing by employing signal detection techniques [18],[19].

As the scope of this research focuses on SS techniques that are able to sense PU activity with minimum required *apriori* information about primary transmissions, it was decided to explore local spectrum sensing at CR by employing signal detection techniques. In this regard, the most efficient and simple approach to identify spectrum opportunity with low infrastructure requirement is to detect the primary receiver within operative range of CR [13]. Practically, however, this is not feasible since the CR cannot locate the PU receiver, and hence, spectrum sensing techniques usually rely on primary transmitter detection [20].

Review of SS literature lead us to categorize sensing methods into different groups by focussing on various features of SS [21]. The main features of SS include: what (primary receiver or transmitter) to sense, how (non-cooperatively or cooperatively) to sense, when (periodic or on-demand) to sense and what a priori information is available about primary transmission that needs to be detected. Fundamental classification of spectrum sensing techniques is highlighted in Figure 1.4 [21].

Based on the sensing mechanism, SS can be classified into three detection approaches. In a *non-cooperative primary transmitter detection* approach, CR makes a decision about the presence or absence of PU signal based on its local observations of primary transmitter signal [6]. In comparison, *cooperative detection* refers to transmitter detection based SS methods where multiple CRs cooperate
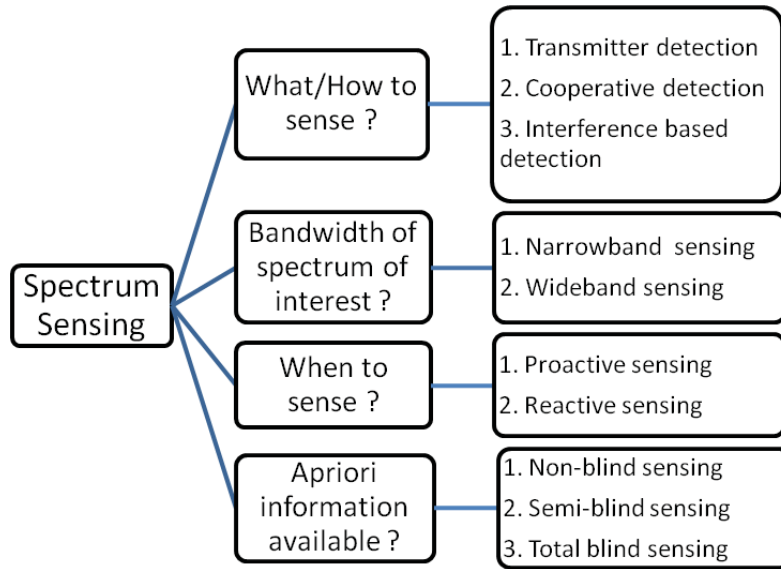
Figure 1.4: Classification of spectrum sensing techniques.

in a centralized or decentralized manner to decide about the spectrum hole [112]. Each cooperating node in CRN may apply any sensing method locally, and then share its raw/refined sensing information with other node(s), depending on a selected cooperation strategy. Both of these approaches fall under the category of *spectrum overlay*. The third detection approach, based on *spectrum underlay*, relies on the estimation of interference temperature of the RF environment during the radio-scene analysis as pointed out by Haykin [11]. Interference temperature based sensing was analyzed and declared to be non-implementable by FCC [23] and thus was crossed out from the list of open avenues to explore during the course of this thesis. This lead us to focus on spectrum overlay approach.

The review of sensing techniques [18], [19] from the perspective of BW of spectrum of interest highlighted two main SS categories: (1) *Narrowband* sensing, and (2) *Wideband* sensing. Thus, the focus of CR might be on identifying a

narrowband hole or a free wideband spectrum, based on the application at hand. With the objective in mind to come up with a low-complexity detection scheme and use it in CSS, it was decided to concentrate on narrowband sensing.

Depending on the application at hand, CR can opt for a *proactive* (periodic) or *reactive* (on-demand) sensing strategy [13]. Either of the two approaches may be employed in the absence or presence of cooperation among CRs.

Apriori information required for PU detection is another important criterion upon which SS methods are classified [24]. In this category, different transmitter detection based sensing techniques are categorized as *non-blind, semi-blind* or *total blind* [21]. Non-blind schemes require primary signal signatures as well as noise power estimation to reliably detect PU. Semi-blind schemes are relaxed in the sense that they need only noise variance estimate to detect a spectrum hole. The most general detection schemes are total blind, requiring no information on source signal or noise power to determine PU activity.

A great body of literature has been amassed in recent years on SS techniques [25], [26]. Specifically, plenty of research efforts in the past have been devoted to develop efficient sensing schemes able to offer high sensing accuracy [21]. A careful comparison of these techniques reveal that improved sensing performance is achieved at the cost of either some *apriori* known information about primary transmissions or extended sensing time/energy consumption owing to computational complexity of the adopted sensing technique [21]. Both of these hidden factors limit the application of sophisticated spectrum sensing techniques in coop-

erative detection where time/energy becomes the most critical factor in evaluating the cooperative gain. Given the tradeoff between the achievable cooperative gain and the incurred cooperation overhead in different stages of cooperative sensing, it is extremely important to conduct an in-depth comparative numerical analysis of various SS approaches. A review of both classical and emerging trends in SS along with a comparative study of spectrum awareness techniques is presented in Chapter 2, which provides a detailed overview of the existing work and the key publications on SS.

Comparison of SS techniques identifies energy detection (ED) as the simplest sensing scheme that can be exploited in cooperative sensing, owing to its low computational complexity and semi-blind nature [27]. An in-depth performance analysis of ED is presented in Chapter 3, which provides an exact and approximate distribution of ED test statistic [28] and unveils the hidden assumptions on the PU signal model in the existing literature on ED based SS [29]-[32].

1.2.2 Spectrum Access

Once the spectrum availability is identified for secondary access in a CRN, a challenging problem is to devise a coordination strategy for preventing harmful collisions among multiple SUs trying to access the available bandwidth. The existing solutions to spectrum access problem in CRNs can be mainly classified based on three main aspects: (1) network architecture, (2) spectrum access behavior, and (3) spectrum access technique. Classification of spectrum access solutions is

depicted in Figure 1.5 [6].
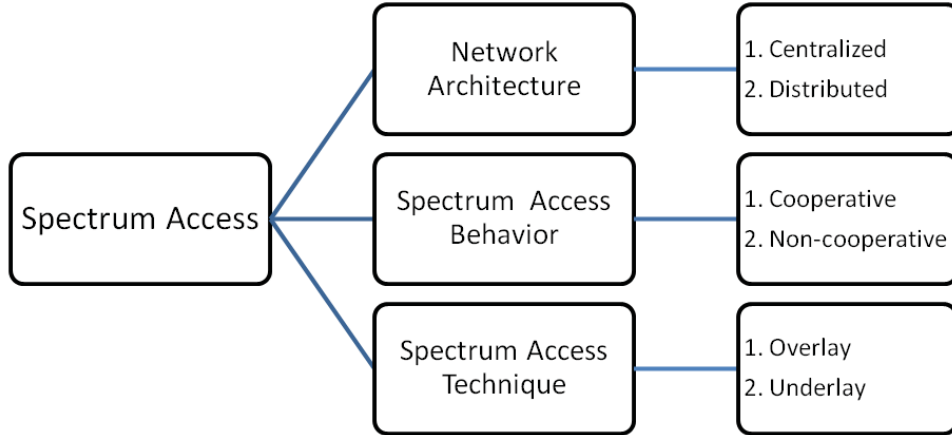
Figure 1.5: Classification of spectrum access solutions.

The first classification of SA solutions is based on the network architecture. In centralized CRNs, the central controller acts as s secondary coordinator (SC) to control the spectrum allocation and access procedures [33], [34] [35]. This leads to *centralized SA*, in which distributed SUs forward their local measurements about the spectrum allocation to a SC which constructs the spectrum allocation map for all the users in CRN. In [33], authors have proposed a centralized spectrum brokering mechanism to assign portions of large available spectrum to competing users. A dynamic spectrum access protocol (DSAP) is proposed in [34] that enables lease-based dynamic spectrum access through a centralized coordinator. Similarly, a centralized spectrum server is considered in [35] to find an optimal scheduling for a group of links sharing a common spectrum with an objective of maximizing the average sum-rate subject to a minimum average rate constraint

for each link. In comparison to centralized approach, distributed solutions to spectrum access problem are also proposed in literature to cater for the cases where a SC is not preferable (e.g. in ad hoc CRNs) [36]-[39]. In *distributed SA*, each CR determines spectrum access mechanism based on local/global policies. A low-complexity, local bargaining approach to self organize distributed CRs is presented in [36], while the authors in [37] have modeled the distributed coordination problem in ad hoc CRNs as a group-based coordination scheme where the distributed CRs adaptively select the locally available control channels. In [38], a partially observable Markov decision process (POMDP) based framework is used to derive optimal and suboptimal decentralized SA strategies to maximize the overall network throughput. A different approach, called an asynchronous distributed pricing (ADP), is proposed in [39], in which each distributed link selects a single channel and transmission power by considering the effect of its transmission on other links.

Looking from the spectrum access behavior, all centralized SA techniques fall into the category of *cooperative access* in which the distributed links exchange interference measurements among themselves and SA algorithms consider the effect of the transmission of each link on other links [33], [34]. In addition, many distributed SA techniques [36], [37], [39] are also cooperative in nature, when the access strategy is not based exclusively on the local policy of each link. As a result, cooperative solution to SA problem offers improved spectrum utilization and network throughput as compared to non-cooperative spectrum access. On

14

the other hand, *non-cooperative SA* techniques are inherently *selfish*, since the access is based only on the link at hand, as proposed in [38], [40], [41]. While the non-cooperative access may result in reduced spectrum utilization and network throughput, the minimal communication requirements among the distributed CRs introduce a tradeoff for practical implementations.

A comprehensive comparison of cooperative and non-cooperative SA in terms of spectrum utilization and fairness is presented in [42]. SA problem is modeled as a graph coloring problem and an optimization framework is developed to investigate both centralized and distributed SA approaches. Simulation results show that cooperative access outperforms non-cooperative access and closely reaches the global optimal performance. Furthermore, distributed solution closely follows the centralized solution.

Spectrum access technology is another important dimension based on which SA schemes are classified as *spectrum overlay* and *spectrum underlay*. Overlay SA is characterized by minimum interference to the primary system provided the underlying SS technique tracks PU activity with high detection probability [34],[36], [37], [38], [40]. On the other hand, underlay SA is principally based on sophisticated spread spectrum techniques [39]. An interesting comparison between the overlay and underlay spectrum access is provided in [43]. In this work, authors have compared spreading based underlay access, interference avoidance based overlay access and a hybrid SA approach combining underlay with interference avoidance. The comparison is made in terms of outage probability in each

access scenario under no system knowledge, perfect system knowledge and limited system knowledge. Results show that the hybrid access approach outperforms both pure underlay and overlay access techniques under a realistic case of limited system knowledge. Furthermore, the performance of overlay schemes strongly depend on spectrum sensing accuracy while underlay SA with interference avoidance offers minimum interference to PUs under practical conditions.

Spectrum access problem has been widely investigated using established optimization techniques [33]-[43]. A dynamic programming approach is proposed in [44] to maximize the utility function which rewards SU for successful packet transmission and penalize it for colliding with PU. In this manner, inherent trade-off between sensing and transmission resulting from the required PU protection and SU throughput maximization is investigated. An integer linear programming (ILP) approach has been used in [45] to maximize the network sum-rate with respect to both channel assignment and transmission rate.

More recently, game theoretical analysis has been used to find optimal/stable spectrum sharing strategies in CRNs under different network settings [46],[47]. Non-cooperative SA is investigated in [48] where the SUs are treated as selfish players who play the game independently to maximize their own rate in the system. In [49], each player estimates the spectrum conditions based on its history, and choose the spectral allocations which maximize its utility in a non-cooperative game. In comparison to non-cooperative SA, cooperative access approach is analyzed in [50] where the distributed players form groups/coalitions to maximize

their utility. Two models are proposed to maximize channel capacity. In the first model, multiple available channels are allocated to SUs subject to availability and interference constraints. Available channels are characterized based on the PU activity over neighboring channels to minimize adjacent channel interference with PUs. The second model allocates a single channel to each SU by defining the reward functions based on idle duration of each available channel, transmission time for an allocable SU, and the signal energy limited to each channel. Both models are shown to maximize the overall allocation of all users.

GT tools have also been used in evaluating the performance of SA techniques in CRNs. Cooperative and non-cooperative access schemes are compared in [51] for distributed adaptive channel allocation. The cooperative access problem is modeled as an exact potential game and convergence to pure strategy Nash equilibrium (NE) solution is shown. For non-cooperative access, a learning algorithm is proposed which converges to a mixed strategy NE. Furthermore, it is shown that cooperative access approach converges quickly to NE point and offers relatively fair spectrum allocation with improved throughput as compared to non-cooperative access. Cooperative and non-cooperative access solutions are also investigated in [52] where multiple systems coexist in the same area. The results indicate that frequency division multiplexing (FDM) is optimal in case of high interference among the systems cooperating to maximize a global utility. When the systems have different objectives, non-cooperative GT is utilized to analyze the system performance and it is shown that the performance degradation resulting from lack of

cooperation vanishes with increasing signal to noise ratio (SNR).

Since the spectrum access strongly depends on sensing results, SS and SA are closely interlinked and hence, a joint SS and SA is an attractive approach to optimize the spectrum utilization in CRNs. In this regard, a coalitional GT framework is proposed in [53] to increase the achievable throughput in CRNs under detection probability constraint. However, it is important to point out that the authors have focused here on sensing-throughput tradeoff and proposed to improve the average throughput per CR by reducing the average false alarm probability. Both selfish coalition formation (CF) based on the individual preferences of rational CRs, and altruistic CF maximizing the overall gain of the group/coalition of CRs, are investigated. In comparison to this work, where the authors have assumed a constant transmission rate for all cooperating CRs, a more realistic utility function, capturing the average sensing time as well as the variable achieved data rate on the identified frequency band, is considered in [54]. The joint spectrum sensing and access problem is modeled as a CF game in partition form and the distributed CRs are proposed to share their local sensing results and jointly coordinate their order of access over multiple available channels to reduce the probability of interfering with each other. In contrast, a simple approach to avoid interference in a multi-channel access problem is proposed in [55], where only one CR is chosen to transmit over each identified idle channel. In this work, the authors have proposed a cooperative spectrum sensing and access (CSSA) scheme by modeling the multi-channel sensing and access problem as a hedonic CF game.

Although joint optimization of SS and SA parameters [53]-[55] has shown throughput improvement in CRNs, its scope has proven to be limited after the FCC ruling [56] which obviated the SS requirement in CRNs. As a result, there has been a dire need to explore stand-alone efficient SA schemes in a competitive environment where SUs do not solely rely on SS performance for their throughput improvement. Furthermore, GT has emerged as an efficient tool to model the competition and conflict of interest of distributed SUs while designing the cooperation strategies in CRNs.

Hence, in this thesis, we use coalitional GT framework to determine which SUs should cooperate with each other to efficiently share the available spectrum resources. In this regard, both centralized [58], [59] and ad hoc CRNs [60], [61] are considered and efficient CF algorithms are developed.

A coordinated CF game is set up in Chapter 4 to organize distributed CRs into disjoint coalitions in centralized CRNs. The global utility function is defined as the network throughput and a search for stable coalition structure is assumed to be executed centrally at secondary coordinator (SC) node, under the assumption that available spectrum opportunities are known a priori. SC node serves as an information aid to share the available spectrum resources among competing CRs. In comparison to the centralized SA approach in which a SC node advises a group of distributed links to make a coalition and share the total available BW among themselves, Chapter 5 addresses the problem of distributed CF in ad hoc CRNs. Variety of CF rules based on individual/group rate improvement are proposed

through which distributed CRs may self-organize into throughput-efficient disjoint coalitions.

1.3 Review of Fundamentals

This section presents some fundamental concepts related to cognitive radio characteristics and spectrum sensing, and provides a comprehensive review of the fundamentals of GT and CF games.

1.3.1 Cognitive Radio and Spectrum Sensing

Cognitive Radio Characteristics

Cognitive radio is essentially an evolution of software defined radio (SDR) with two main characteristics: (1) **Cognitive capability**, and (2) **Reconfigurability**. *Cognitive capability* refers to the ability of the radio technology to interact with its radio environment in real time to identify and exploit "un-occupied" licensed spectrum bands called *spectrum holes* or *white spaces* [11]. The observations published by FCC in [5], categorizes spectrum holes into two groups: temporal spectrum holes and spatial spectrum holes. This gives rise to two secondary communication schemes [62] of exploiting spectrum opportunities in time and space which are depicted in Figures 1.6(a) and 1.6(b) respectively.

A *temporal spectrum hole* occurs when no primary transmission is detected over the scanned frequency band for a reasonable amount of time and hence this frequency band is available for secondary communication in current time slot. A
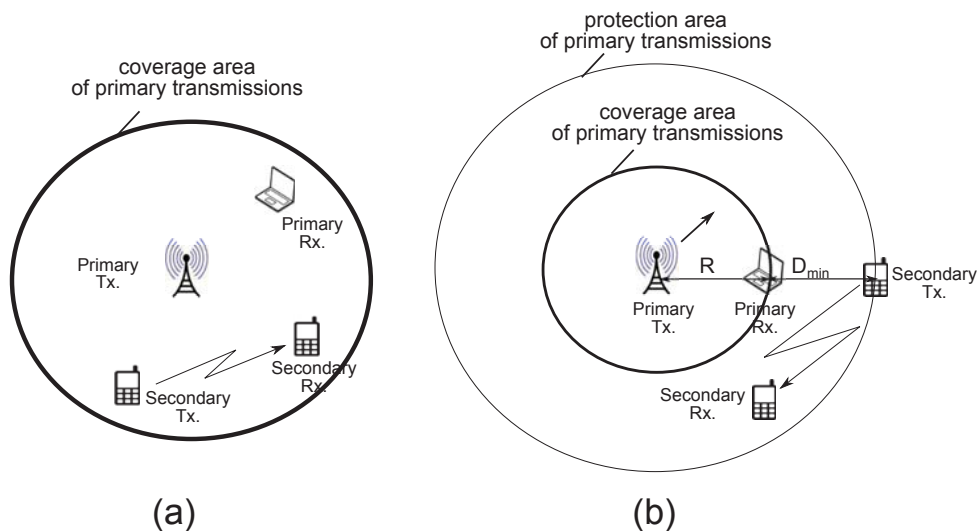
Figure 1.6: A spectrum hole: (a) Temporal hole (b) Spatial hole

temporal spectrum hole is depicted in Figure 1.6(a). A *spatial spectrum hole* is generated when the primary transmissions are confined to a certain area as shown in Figure 1.6(b) and hence this frequency band is available for secondary communication (may be in the same time slot) well outside the coverage area of PU to avoid any possible interference with primary communication. The secondary transmission over the spatially available licensed spectrum is allowed if and only if it remains transparent to presumably nearby primary receiver. This puts a stringent requirement on the SU to be able to successfully detect the PU at any place where secondary communication may cause interference to primary transmission. Therefore, a protection area of the PU is defined wherein the SU must be able to detect any PU activity to avoid harmful interference with the primary receiver at a distance of D_{min} from the SU [63],[64]. The cognitive capability is not limited to only monitoring power in some frequency band, rather it demands spectrum monitoring in time, space, code, angle etc. [25]. This requires the CR to be able

to reconfigure its communication parameters on the fly in order to adapt to its dynamic radio environment, calling for the *reconfigurability* characteristic of CR.

Spectrum Sensing: A Binary Hypothesis Testing Problem

The key concept in CR is the provision of opportunistic and dynamic spectrum access of licensed frequency band to unlicensed users. Hence, the main functionality of CR lies in efficient SS so that whenever an opportunity of unused spectrum band is identified, CR may make use of it. In general, SS is analyzed using as a binary hypothesis testing model, defined as:

$$x(t) = \begin{cases} n(t), & 0 < t \leq T \quad H_0 \\ hs(t) + n(t), & 0 < t \leq T \quad H_1 \end{cases} \tag{1.1}$$

where $x(t)$ is the signal received by CR during observation window T, $n(t)$ represents the additive white Gaussian noise (AWGN) with zero mean and variance σ^2, $s(t)$ represents the transmitted signal from primary user which is to be detected, and h is the channel gain. This is a classic binary signal detection problem in which CR has to decide between two Hypothesis, H_0 and H_1. H_0 corresponds to the absence of primary signal in scanned frequency band while H_1 indicates that the spectrum is occupied. It is important to point out here that under H_1, spectrum may be occupied by an incumbent or a secondary user. Hence, a sensing scheme is generally required not only to detect but also to differentiate between the primary and secondary user signal. Conventionally, the performance of a detection algorithm is evaluated by its *sensitivity* and *specificity* [25] which

are measured by probability of detection P_d and probability of false alarm P_f, respectively. P_d is the probability of correctly detecting the PU signal present in the considered frequency band. In terms of hypothesis, it is given as:

$$P_d = P(\text{signal is detected}|H_1) \tag{1.2}$$

P_f is the probability that the detection algorithm falsely decides that PU is present in the scanned frequency band when it actually is absent, and it is written as:

$$P_f = P(\text{signal is detected}|H_0) \tag{1.3}$$

Thus, we target at maximizing P_d while minimizing P_f. Another important parameter of interest is the probability of missed detection P_m which is the complement of P_d. P_m indicates the likelihood of not detecting the primary transmission when PU is active in the band of interest and can be formulated as:

$$P_m = 1 - P_d = P(\text{signal is not detected}|H_1) \tag{1.4}$$

Total probability of making a wrong decision on spectrum occupancy is given by a weighted sum of P_f and P_m. Hence the key challenge in SS is to keep both P_f and P_m under certain threshold, since high P_f corresponds to poor spectrum utilization/exploitation by CR and high P_m may result in increased interference at primary receiver if the missed signal belongs to the incumbent.

1.3.2   Game Theory and Coalition Formation Games

Game theory is a branch of mathematics that targets modeling and analyzing resource conflict problems. In the context of CRNs, the limited spectrum and power, and especially the scenario where multiple SUs try to access the same available spectrum, creates a resource conflict. GT provides the necessary tools to analyze the interactions between rational SUs to reach a stable, throughput-efficient operating point from network perspective.

Although, the fundamental developments of GT occurred in the middle of 20th century with the major works by Von Neuman, Morgenstern, and John Nash, it is only recently that GT has been used to analyze communication networks. In general, GT can be divided into two branches: (1) Non-cooperative [65], and (2) Cooperative game theory [66]. The distinction between the two is whether or not the players in the game can make joint decisions to choose a particular strategy. In non-cooperative games, the players strictly compete such that each player chooses its strategy independently to improve its own performance (payoff/utility). In contrast, cooperative GT studies the behavior of rational (selfish) players when they cooperate. Principally, cooperative games describe the formation of cooperating groups of players, called *coalitions* [66], that can strengthen the players' positions in a game. Since cooperation is considered as an effective approach to throughput improvement in CRNs, this thesis focuses on an important class of cooperative games, known as coalition formation games [67], that provide analytical tools for designing practical and efficient cooperation strategies in CRNs. In the following,

the fundamental components of a CF game are presented and different forms of CF games are introduced to model and analyze the throughput-efficient grouping of rational players in CRNs.

Player, Coalition and Network Partition

A set of players, $\mathcal{N} = \{1, 2, \cdots, N\}$, who seek to form coalitions, constitutes the basic element of a CF game. In CRNs, the players are secondary transmitter-receiver (ST-SR) pairs (secondary links or simply CRs) that try to efficiently access the available spectrum. In general, all *players* of the game are assumed to be *truthful* (report observations correctly) and *myopic*; i.e. care only for their *current* utility/payoff (to be defined later) *only*. Furthermore, it is also intuitive to consider players to be *individually rational*; i.e. they seek to improve their utility.

A *Coalition*, S, is defined as a subset of $\mathcal{N}$, $S \subseteq \mathcal{N}$, which represents an agreement between the players in S to act as a single entity. A coalition comprised of a single player is called a *singleton coalition* while a coalition comprised of all the players in the network is termed as a *grand coalition*.

A *partition* Π of $\mathcal{N}$ is the set of coalitions $\Pi = \{S_1, S_2, \cdots, S_{|\Pi|}\}$ such that all the coalitions in Π are mutually disjoint ($S_m \bigcap S_n = \emptyset \ \forall \ m, n \in \{1, 2, \cdots, |\Pi|\}, m \neq n$) and *span* all the players of $\mathcal{N}$ ($\bigcup_{m=1}^{|\Pi|} S_m = \mathcal{N}$). $|\Pi|$ represents the total number of coalitions in Π. A *network partition* is also referred to as a *coalition structure* [67] and this thesis uses the two terms interchangeably. The set of all possible partitions of $\mathcal{N}$ is denoted by $\mathcal{P}$, and the number of possible

partitions; $|\mathcal{P}|$, is given by the Bell number [68].

Player Utility and Coalition Value

In general, $\phi_i(S, \Pi)$ describes the *payoff/utility* of player $i \in S$ which it receives being the member of Coalition S when partition Π is in place. However, for a Coalition $S \subseteq \mathcal{N}$, $S \in \Pi$, the *coalition value* $\mathcal{V}(S, \Pi)$ describes the overall utility that the *entire* Coalition S receives under the partition Π. Formally, $\mathcal{V}(S, \Pi)$ is defined as a mapping given by a vector $\mathbf{v}(S, \Pi) \in \mathbb{R}^{|S|}$ where each element $v_i \in \mathbf{v}(S, \Pi)$ represents the payoff $\phi_i(S, \Pi)$ of player $i \in S$; i.e.,

$$\mathcal{V}(S, \Pi) = \left\{ \mathbf{v}(S, \Pi) \in \mathbb{R}^{|S|} \mid v_i(S, \Pi) = \phi_i(S, \Pi) \right\}. \qquad (1.5)$$

Characteristic and Partition form CF games

The form of the CF game is governed by the definition of the coalition value $\mathcal{V}$. The most common form of a CF game is the *characteristic form* [69]. In characteristic form, the value of Coalition S depends solely on the members of that coalition, with no dependence on externalities $\mathcal{N} \backslash S$ (members outside the Coalition S). Hence, for CF games in characteristic form, the value of a Coalition S is represented as $\mathcal{V}(S)$. On the other hand, CF games in *partition form* [70] consider the effect of externalities in evaluating the value of a Coalition S, and hence, for such games, the value of a Coalition S is represented as $\mathcal{V}(S, \Pi)$.

CF games with Transferable and Non-transferable Utility

The theory of CF games splits into the cases of *transferable utility (TU)* and *non-transferable utility (NTU)* based on whether the coalition value can be arbitrarily distributed among the coalition members or not. CF games with transferable utility were introduced by Von Neuman and Morgenstern [69], along with the characteristic form games. The TU property defines the coalition value as a mapping (*characteristic function* $\mathcal{V}: 2^{\mathcal{N}} \to \mathbb{R}$) that associates with every coalition $S \subseteq \mathcal{N}$, a real number quantifying the worth of S. The implicit assumption is that the total utility of the coalition, represented by this real number can be divided in any manner among the coalition members. However, in many cases, assigning a single real number to the coalition value is not sufficient, and strict constraints, on the distribution of the coalition value, exist. Such types of games are referred to as CF games with non-transferable utility and were first introduced by Aumann and Peleg [71]. The value of a coalition S in an NTU game, $\mathcal{V}$, is no longer a function over the real line, rather it is a set of payoff vectors, $\mathcal{V}(S) \subseteq \mathbb{R}^{|S|}$, where each element v_i of a vector $\mathbf{v}(S) \in \mathcal{V}(S)$ represents a payoff that a player $i \in S$ can obtain within Coalition S.

Main Properties of CF games

Many cooperative games are built on the underlying assumption that forming a coalition is always beneficial. This property of cooperative games is called *super-additivity*, which always yields grand coalition as an optimal structure. Unlike

27

such class of games, CF games incorporate a cost for forming coalitions and in general, CF games are not superadditive. As a result, in contrast to superadditive cooperative games where formal solution concepts exist, CF games are difficult to handle as the optimal network partition is not known. Furthermore, finding an optimal network partition is an NP-hard problem [72], as the number of possible partitions (given by Bell number B_N [73]) grows exponentially with the number of communication links, N, in the network. Hence, there is a need to develop algorithms to organize links into non-overlapping coalitions that are at least stable, if not optimal. In the following, we present the fundamental stability concepts [137] that can be used to study the *stability* of the final network partition Π_f resulting from the CF process.

Nash Stability: A network partition $\Pi = \{S_1, S_2, \cdots, S_{|\Pi|}\}$, is *Nash stable (NS)* if $\forall\, i \in \mathcal{N}$ with $i \in S_k, S_k \in \Pi$, we have $(S_k, \Pi) \succeq_i (S_l \cup \{i\}, \acute{\Pi})$ for all $S_l \in \Pi \cup \{\phi\}$, $l \neq k$ where $\acute{\Pi} = \{\Pi \backslash \{S_k, S_l\}\} \cup \{S_k \backslash \{i\}, S_l \cup \{i\}\}$.

Hence, a network partition Π is *NS* if there does not exist a player $i \in \mathcal{N}$ who has an *incentive* to move from its current coalition to another coalition in Π or to deviate and act *singleton*. In other words, no player can obtain a higher payoff by performing a switch operation when the current partition is *Nash stable*.

Individual Stability: A network partition $\Pi = \{S_1, S_2, \cdots, S_{|\Pi|}\}$, is *individually stable (IS)* if there does not exist a player $i \in \mathcal{N}, i \in S_k, S_k \in \Pi$ and a coalition $S_l \in \Pi \cup \{\phi\}$, $l \neq k$ such that $(S_l \cup \{i\}, \acute{\Pi}) \succ_i (S_k, \Pi)$, and $(S_l \cup \{i\}, \acute{\Pi}) \succeq_j (S_l, \Pi) \,\forall\, j \in S_l$.

Hence, a network partition Π is *IS* if $\forall\, i \in \mathcal{N}$, either a player i does not find a coalition to switch in order to improve its payoff or if it finds, it is not *welcomed* by that coalition i.e. the players in that coalition get hurt (their payoff is decreased) when player i joins them to form the new coalition $S_l \cup \{i\}$.

Contractual Individual Stability: A network partition $\Pi = \{S_1, S_2, \cdots, S_{|\Pi|}\}$, is *contractually individually stable* (CIS) if there does not exist a player $i \in \mathcal{N}, i \in S_k, S_k \in \Pi$ and a Coalition $S_l \in \Pi \cup \{\phi\}$, $l \neq k$ such that $(S_l \cup \{i\}, \acute{\Pi}) \succ_i (S_k, \Pi)$, $(S_l \cup \{i\}, \acute{\Pi}) \succeq_j (S_l, \Pi) \; \forall\, j \in S_l$, and $(S_k \backslash \{i\}, \acute{\Pi}) \succeq_j (S_k, \Pi) \; \forall\, j \in S_k, \; j \neq i$.

Hence, a network partition Π is *CIS* if $\forall\, i \in \mathcal{N}$, either a player i does not find a coalition to switch in order to improve its payoff or if it finds, it is not *welcomed* by that coalition i.e. the players in that coalition get hurt (their payoff is decreased) when player i joins them to form the new coalition $S_l \cup \{i\}$ or if a player i finds a coalition where its rate is improved as well as its movement does not decrease the rate of any of the other players in the new coalition $S_l \cup \{i\}$, it is not *allowed* by its current coalition S_k i.e. the other players in its current coalition get hurt (their payoff is decreased) when player i leaves them forming $S_k \backslash \{i\}$.

Remark: The following relation between the stability concepts can be observed [137]:

- IS *implies* CIS

- NS *implies* IS *implies* CIS

1.4   Thesis Contributions

The main contributions of the thesis can be summarized as follows:

1. A comparative numerical analysis of prominent SS techniques is conducted in terms of their sensing accuracy and computational complexity. Merits/demerits and limitations of different spectrum awareness approaches are outlined and required a priori information about the primary system is highlighted [13], [20], [21].

2. An in-depth performance analysis of ED based sensing is carried out. Derivations of the exact distribution of ED test statistic are shown and the validity conditions for the Gaussian approximations to exact test statistic are established in terms of SNR, P_d and P_{fa}. A general structure of the ED threshold is highlighted and the hidden assumptions on the PU signal model in the existing literature on ED are unveiled [27], [28], [130].

3. A closed form expression for the optimal BW allocation among distributed CRs is obtained for fixed transmission power [57].

4. A throughput-efficient CF algorithm is developed for centrally-controlled spectrum access in centralized CRNs. Nash stability of the proposed CF algorithm is proved. Significant improvements in average network throughput as compared to GS, SS and existing CF techniques are shown to be achieved via proposed CF algorithm. Two variants of a heuristic initialization algorithm are proposed and analyzed for improving the convergence speed of

proposed CF algorithm [58], [59].

5. A distributed CF algorithm to self organize selfish/altruistic radios in ad hoc CRNs is developed and its convergence/stability properties are analyzed. Variety of CF rules are proposed and means to guarantee stability are presented. The scenarios leading to oscillation in CF process under different CF rules are identified and graceful exit procedures are provided when a CF cycle is inevitable. Probabilistic analysis to study the stability of grand and singleton structure is performed and a lower bound on the probability that a different coalition structure other than GS and SS is stable, is evaluated. Substantial gain in terms of average payoff per radio over existing CF techniques is shown through MATLAB simulations [60], [61].

1.5   Thesis Layout

This thesis is organized as follows: An introduction to CR technology and a review of existing work in the field of SS and SA was presented in Chapter 1. Fundamental concepts/definitions of GT focussing on CF games were given and thesis contributions were clearly laid out in this chapter. A comparative study of spectrum awareness techniques is presented in Chapter 2, while Chapter 3 provides an in-depth performance analysis of ED based spectrum sensing. Throughput-efficient game-theoretic solutions to spectrum access problem in CRNs are provided in Chapter 4 and Chapter 5 for different network architectures. In particular, Chapter 4 considers an centralized CRN and proposes a centralized joint CF and BW

allocation algorithm to organize distributed SUs into disjoint coalitions. In Chapter 5, a distributed CF algorithm is developed to self organize selfish/altruistic CRs and variety of CF rules are proposed to analyze the convergence/stability properties of proposed distributed algorithm. Finally, Chapter 6, concludes the findings of the research and provides recommendations for future work.

COMPARATIVE STUDY OF SPECTRUM SENSING TECHNIQUES

This chapter undertakes an in-depth comparative study of various spectrum sensing (SS) techniques in terms of their sensing accuracy and computational complexity and shows the performance of differen detection algorithms through numerical results.

A comprehensive classification of SS techniques based on transmitter detection approach is provided in Section 2.1. This is followed by brief overview of different SS techniques, from Section 2.2-2.6. The chapter concludes with a detailed comparison of SS techniques presented in Section 2.7.

2.1 Classification of SS Techniques

Practically, spectrum sensing techniques rely on primary transmitter detection [20] in a non-cooperative or cooperative manner. Figure 2.1 illustrates the SS classification where different borders are used to group representative transmitter detection techniques as non-blind, semi-blind and blind schemes.

Figure 2.1 shows variety of schemes to identify any spectrum usage opportunity in the scanned frequency band ranging from very simple energy detection to quite advanced cyclostationary feature extraction and waveform based sensing. Recent work mainly focuses on further sophistication of these basic techniques with an aim to make sensing results more robust and accurate at the same time [19], [26]. The following sections provide a brief overview of principles of spectrum sensing techniques based on the observation of PU signal, followed by a detailed comparison of these schemes in terms of their favorable aspects and limitations.

2.2 Energy Detection (ED)

Energy detection is a naive signal detection approach which is referred in classical literature as *radiometry*. In practice, energy detector (ED) is especially suitable for wideband SS when CR cannot gather sufficient information about the PU signal. First, received primary signal is pre-filtered with a band pass filter (BPF) of bandwidth W to select the desired frequency band. Filtered signal is then squared and integrated over observation window of length T. This gives an estimated energy content of signal which is then compared with a threshold value depending
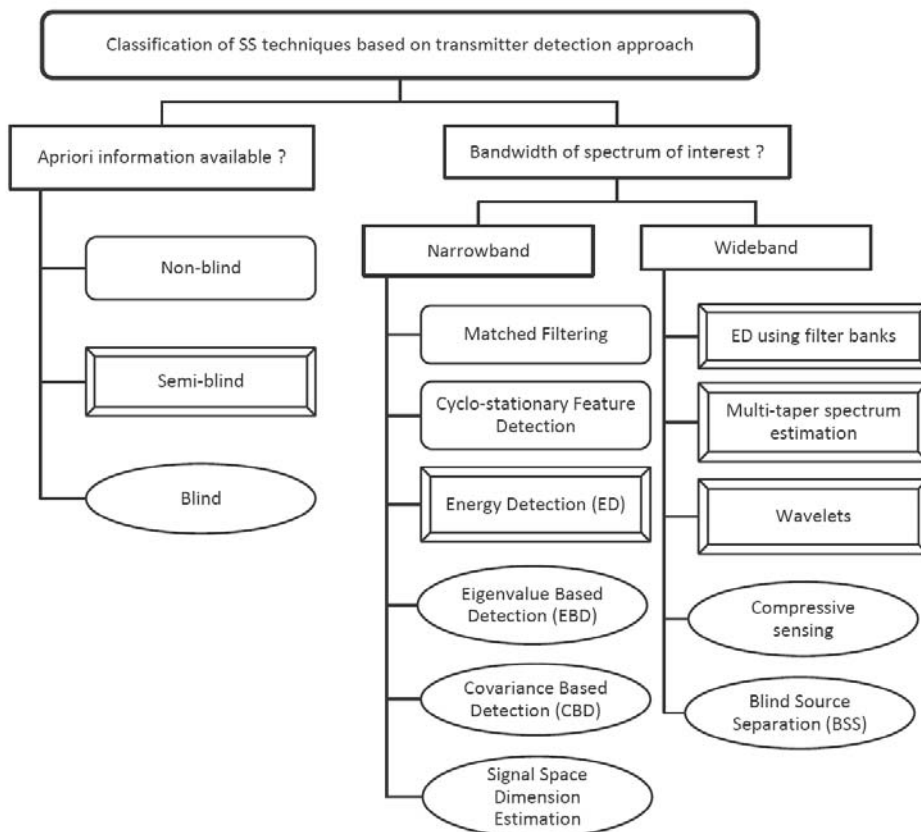
Figure 2.1: Classification of spectrum sensing techniques.

on noise floor to decide about the presence of PU signal in scanned sub-band [29]. When the spectral environment is analyzed in frequency domain and power spectral density (PSD) of the observed signal is estimated, this approach is termed as *periodogram* [75].

General performance analysis of ED is outlined in [62] with some discussion on advanced power spectrum estimation techniques while its performance in fading environments is analyzed in [76]. Setting the right *threshold* value is of critical importance [77]. If *threshold* is kept high to achieve minimum P_f, P_d is decreased, on the other hand, if value of *threshold* is kept low, with an aim to get maximum P_d, corresponding P_f exceeds the acceptable limits [20]. Hence, a careful trade off has to be considered while setting the ED threshold.

2.2.1   Noise Uncertainty Problem in ED

The uncertainty in ED threshold originates from its strong dependence on the accurate estimation of the noise power. It is well established that under practical conditions, (receiver) noise power changes with time and location, and it is very difficult to obtain an accurate knowledge of noise power level. Hence, the assumption of known noise power σ_n^2 is not realistic, rather, what may be known at best is an estimated noise variance: $\hat{\sigma}_n^2 = \alpha \sigma_n^2$. α is called the *noise uncertainty factor* with a given upper bound B (in dB), where $B = sup\{10 \log_{10} \alpha\}$ defines *noise uncertainty bound*. This problem has been well investigated in literature as energy detector's inherent noise uncertainty problem which was identified as SNR wall

by Tandra and Sahai in [78].

In general, for noise uncertainty factor (α), the performance metric probabilities $(P_d \rightarrow P_d(\alpha)$ and $P_f \rightarrow P_f(\alpha))$ give the *instantaneous* probability measure as a function of uncertain statistic (originating from the noise variance estimate). Thus, in this case, average probabilities are needed to be evaluated by averaging already derived probabilities over the varying noise power. Hence,

$$\overline{P}_d = \int_x P_d(\alpha) f_\alpha(x) dx, \tag{2.1}$$

$$\overline{P}_f = \int_x P_f(\alpha) f_\alpha(x) dx, \tag{2.2}$$

where $f_\alpha(x)$ represents the pdf of the noise uncertainty factor α [31]. It is important to point out here that in most of the cases, no closed-form solutions of (2.1) and (2.2) exist, and average probabilities are numerically evaluated.

Figure 2.2 shows the performance degradation of ED under noise uncertainty (with typical uncertainty bound of $B = 0.5$ dB) for different sample size ($N_s = 3000$ & 30000). It is observed that the performance of ED improves by increasing the sample size if the noise power is assumed to be known *apriori*. Theoretically, cooperative sensing can increase the reliability to some extent [31] but it cannot conquer the SNR wall with limited number of sensors.
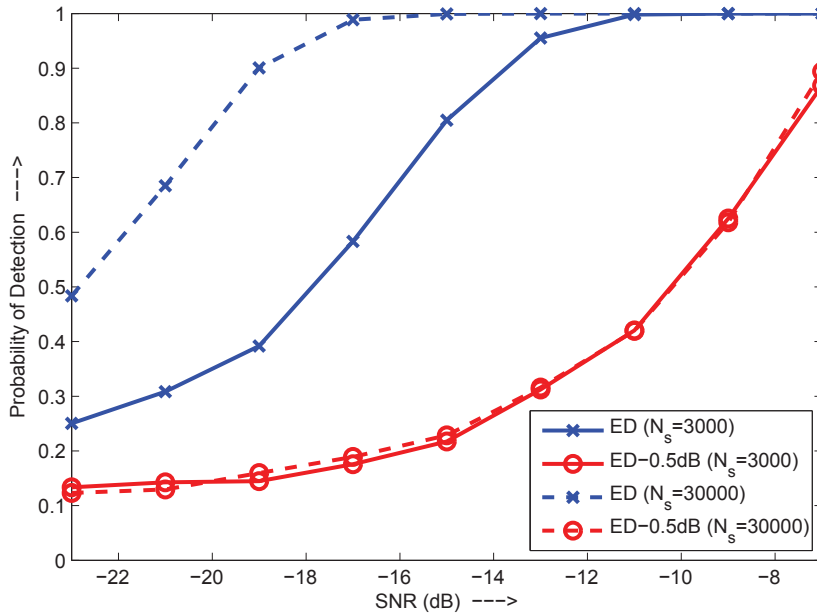
Figure 2.2: Performance degradation of ED under noise uncertainty.

2.2.2 Applications of Advanced Power Estimation Techniques to ED

It is important to point out that variety of sophisticated power estimation techniques are proposed in literature with an aim to improve over all sensing performance particularly while scanning a wide frequency band. The techniques include filter bank approach [79], multitaper spectrum estimation [80], wavelet based spectrum sensing [81] and spectrum detection employing compressed sensing [82].

2.3 Feature (Cyclostationary) Detection

The idea of feature detection is based on capturing a specific signature of PU signal. Wireless (digitally modulated) signals are in general coupled with sine

wave carriers, pulse trains, repeating spreading or hopping sequences or cyclic prefixes, which induce periodicity in the signal making them cyclostationary. This periodicity may result from modulation or even be deliberately generated to assist channel estimation (regularly transmitted pilot sequences) and synchronization (preambles, mid-ambles etc). Cyclostationary feature detection exploits built-in periodicity of received signal to detect primary transmissions in a background of noise and other modulated signals [83]-[90]. Features that can be extracted include RF carrier, symbol rate and modulation type etc. [91].

Recent work [92] has reported to combine ED with feature detection to benefit from complementary advantages of both the schemes by doing coarse detection using ED which is then made more reliable by fine detection employing cyclostationary detection.

2.4   Coherent Sensing: Pilot Based Detection

Coherent sensing makes use of known patterns in PU signal to coherently detect the presence of active PU. These known patterns, sometimes termed as *pilot signals*, are usually transmitted periodically by PU to assist channel estimation and achieve time and frequency synchronization at primary receiver. When CR has *apriori* knowledge of these known signal patterns in primary transmission, it can detect the PU signal by either passing the received signal at CR through a filter (matched filter: MF) having impulse response matched to the incoming signal [62], or correlating it with a known copy of itself. Thus there are two main approaches

of coherent sensing namely: Matched filtering and correlation (waveform-based) detection [93].

2.5 Covariance Based Detection (CBD)
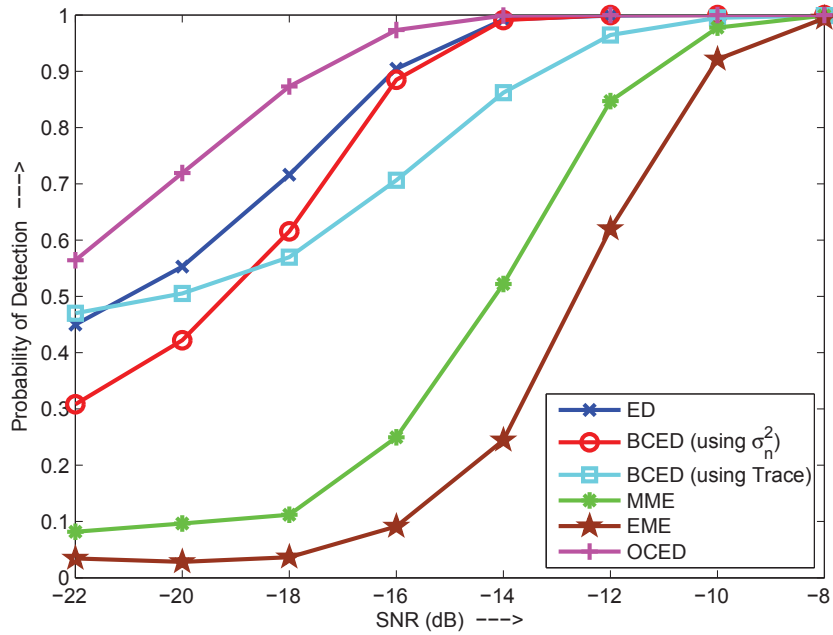
Figure 2.3: Performance comparison of conventional energy detector with eigenvalue based detection under no noise uncertainty.

Covariance based detection exploits the inherent correlation in received PU signal samples resulting from the time dispersive nature of wireless channel and oversampling of received signal [24]. If CR uses multiple antennas, received signal samples are also spatially correlated as they originate from the same source (primary) signals.

In multi-antenna CR, multiple copies of the received PU signal can be coherently combined to maximize the SNR of received (combined) signal. The diversity

40

combining approaches of maximum ratio combining (MRC) and selection combining (SC) are analyzed for ED in [94]. Although, MRC gives optimal detection performance but is difficult to implement as it requires channel between transmitter (primary) and receiver (secondary) to be known at the receiver. In comparison, blind detection calls for equal gain combining (EGC) or blind combining (BC). In [95], authors revisited the combining strategies for PU signal samples received at different CR antennas during different time intervals. An optimal combining approach (MRC), requires *apriori* information about the primary signal and channel in the form of eigenvector corresponding to maximum eigenvalue of the received source (primary) signal covariance matrix. However, this eigenvector can be estimated using the received signal samples only without requiring any information of primary transmitted signal. In this way, temporal spatial combining of received samples may be achieved blindly. After combining, ED is used to identify any vacant spectrum band in the received wideband signal. The authors have named MRC based ED as optimally combined energy detection (OCED) and BC based ED as blindly combined energy detection (BCED) in [95].

There are different possible ways to utilize eigenvalues of received sample covariance matrix for SS. In [96], authors have indicated that number of significant eigenvalues is directly related to presence/absence of data in received signal and may be exploited to identify vacant spectrum bands. The ratio of maximum eigenvalue to minimum eigenvalue (MME) and the ratio of average eigenvalue (energy of received signal) to minimum eigenvalue (EME) are used in [97] to detect the
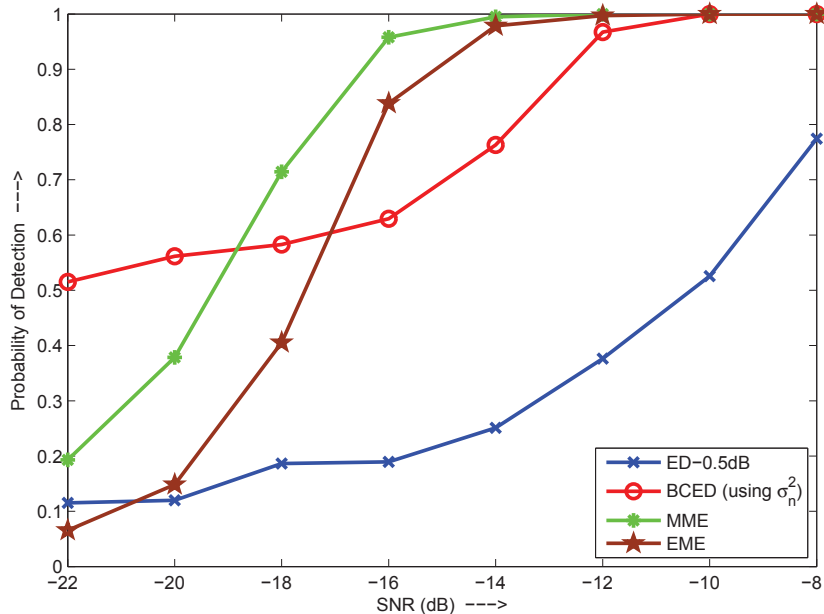
Figure 2.4: Performance comparison of conventional energy detector with eigen-value based detection under 0.5dB noise uncertainty factor.

presence of primary signal. Figure 2.3 and Figure 2.4 provide a comparison of semi-blind ED with variety of blind eigenvalue based detection (EBD) algorithms under no noise uncertainty and 0.5dB noise uncertainty case respectively. It is evident that EBD not only outperforms ED for correlated PU signals by capturing the inherent correlation in source signals but is also robust to noise uncertainty. However, it is important to point out here that EBD relies on the distribution of ratio of extreme eigenvalues of received covariance matrix whose closed form expressions are still mathematically untractable and asymptotic assumptions are usually employed to set the detection threshold [98],[99]. More recently, an up-per bound on the joint probability density function of the largest and smallest eigenvalues of the received covariance matrix is used to derive analytically sim-

ple expression for the required distribution of the ratio of extreme eigenvalues as reported in [100],[101]. Eigenvalue based detection is discussed in detail in [102]-[104].

If the signals exhibit time correlation as well, the concept of EBD can be extended to incorporate joint space time processing. This approach is generally known as covariance based detection, EBD being its one special case where the eigenvalues of received signal sample covariance matrix are used for PU signal detection. Covariance based detection has been addressed in [105]-[107].

2.6   SS Based on Blind Source Separation (BSS)

Blind source separation (BSS) technique is discussed for the CR system model with multiple antennas in [108] to simultaneously detect active PUs in the scanned spectrum. For the sake of illustration, four channels/PU signals are analyzed in [109] and performance of BSS in CRN is simulated using simple PU signal models. In this setup, channel one and two are occupied by pure tones of 5 Hz and 20 Hz, respectively, channel three is amplitude modulated (AM) with carrier centered at 50 Hz while channel four is kept idle and hence contains only noise. These four primary signals are observed at four antennas/sensors and appear to be noisy linear mixture of active PU signal samples, represented by $r_i[k]$ ($i = 1, 2, 3, 4$) in Figure 2.5. The mixed observed samples are then passed through a whitening filter before applying a low complexity, non-iterative BSS approach for multiuser detection. Finally, the inherent channel sequence uncertainty in BSS is resolved
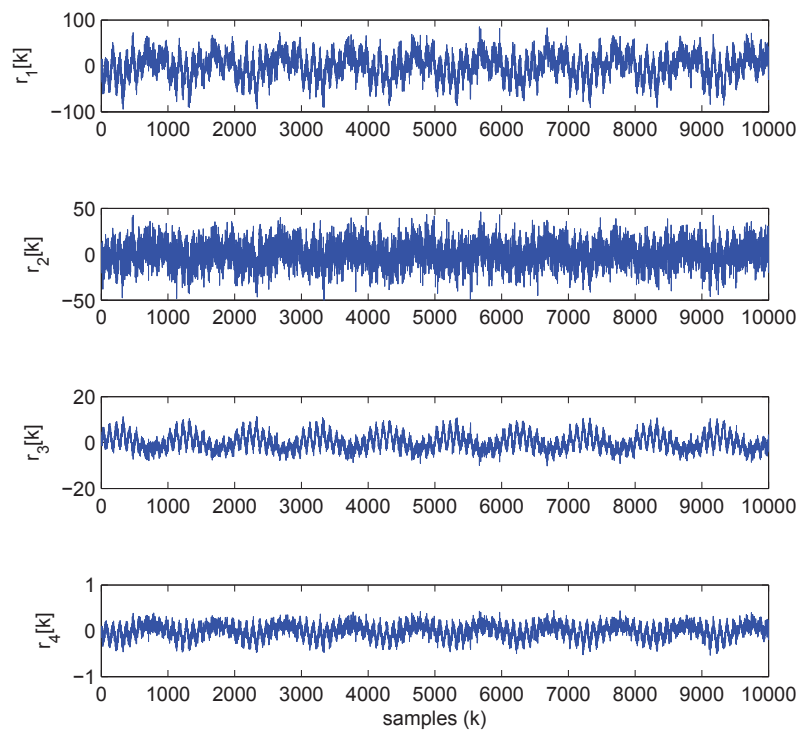
Figure 2.5: SS using BSS: Observed noisy mixed signals at four antennas of CR.
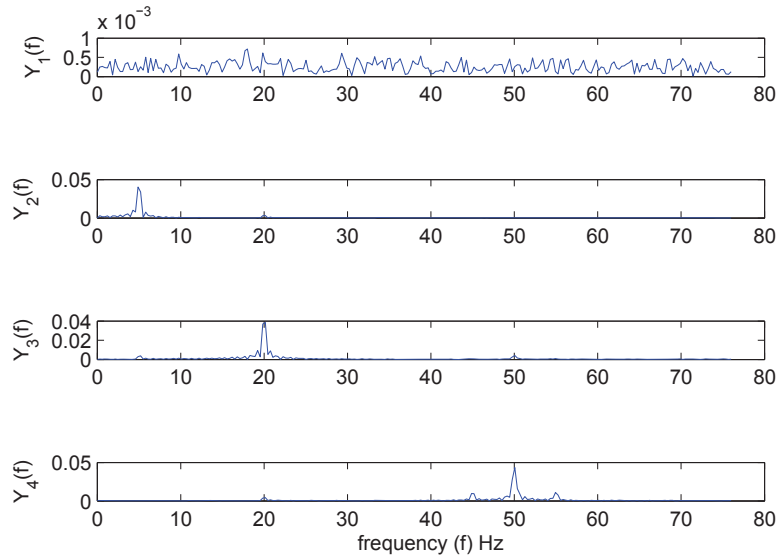
Figure 2.6: SS using BSS: Frequency spectrum of noisy recovered signals after pre-whitening.

by looking at the frequency spectrum of separated signal samples shown by $Y_i(f)$ $(i = 1, 2, 3, 4)$ in Figure 2.6.

2.7 Comparison of Sensing Methods

The selection of a sensing method comes with a tradeoff between accuracy and complexity. A concluding comparison of spectrum sensing techniques is presented in Table 2.1 to identify key factors in deciding on a sensing strategy.

Figure 2.7 compares different SS methods in terms of their implementation, computational complexities and sensing accuracies. When nothing is known about the PU signal, ED happens to be most simple approach but it fails in the presence of fading and noise uncertainties. Advanced power spectrum estimation techniques

Table 2.1: Comparison of spectrum sensing methods.

SS approach	Advantages	Disadvantages	Comments
Energy Detection	+ Implementation simplicity + Low computational complexity + optimal for detecting IID primary signals + Semi-blind (No *apriori* PU signal information required)	- Non Robust • Threshold strongly depends on Noise uncertainties - Low accuracy/reliability • Unable to differentiate interference from PU signal and noise • poor performance under low SNR (due to shadowing and multipath fading) • Inability to detect spread spectrum signals - Inefficient for detecting correlated primary signals - More susceptible to Hidden Terminal problem	Advanced power estimation techniques become feasible for wideband spectrum sensing • multitapering [80] • wavelets [81] • compressive sensing [82]
Feature Detection	+ Robust to Noise uncertainty + High Accuracy/reliability • able to differentiate PU signal from interference and noise • able to differentiate among PU signals + High Prob. of detection + Less susceptible to Hidden Terminal problem	- Implementation complexity -Non-blind - High Prob. of miss-detection resulting from large observation time	Hybrid schemes employing coarse detection using ED and fine sensing using Feature detection give complementary advantages of both ED and Feature detection
Pilot based Detection	+ Less complex than cyclostationary feature detection + Higher Agility than cyclostationary feature detection + Less susceptible to Hidden Terminal problem	- (Matched filtering) High complexity and high sensitivity to inaccurate PU signal information - (Waveform based sensing) High sensitivity to synchronization errors - Non-blind	Benefits from all advantages of feature detection at reasonable complexity cost but susceptible to errors in *apriori* information
Covariance based Detection	+ High Accuracy + Medium computational complexity + Blind	- performance degrades for uncorrelated PU signals	• Detection accuracy can further be increased by making use of available *apriori* information about PU signal correlation • Computational complexity depends on blind detection algorithm • Hidden Terminal problem points to cooperation among CRs for sensing performance improvement

achieve accuracy while sacrificing the simplicity of energy detection. As a matter of fact, some *apriori* knowledge about primary transmissions is necessary to distinguish primary signal from secondary signal and interference/noise. Processing of this known information achieves reliability in detection at the cost of additional computational complexities. Such schemes are classified as non-blind and the type of the detection approach depends on the available information about primary signal. In particular, cyclostationary detector is suitable when cyclic frequencies associated with primary transmissions are known while coherent detector is preferred when pilot transmissions of primary system are known. Blind sensing, based on received signal covariance matrix and other approaches achieves high accuracy with its computational complexity dependent on sensing algorithm used.

2.8 Cooperative Spectrum Sensing

All the single-user centric sensing schemes discussed so far, are based on the detection of primary transmitted signal. However, in practice, the locations of PUs are unknown, and hence the SU may lie outside the PU coverage area, or it may be located within the PU's transmission range, but primary signal might be obscured due to deep fading or shadowing. These practical scenarios are referred to as *primary receiver uncertainty problem* (Figure 2.8(a)) and *hidden primary transmitter problem* (Figure 2.8(b)), respectively. In both cases, the limited sensing capability of the underlying single-user centric sensing approach results in the

47
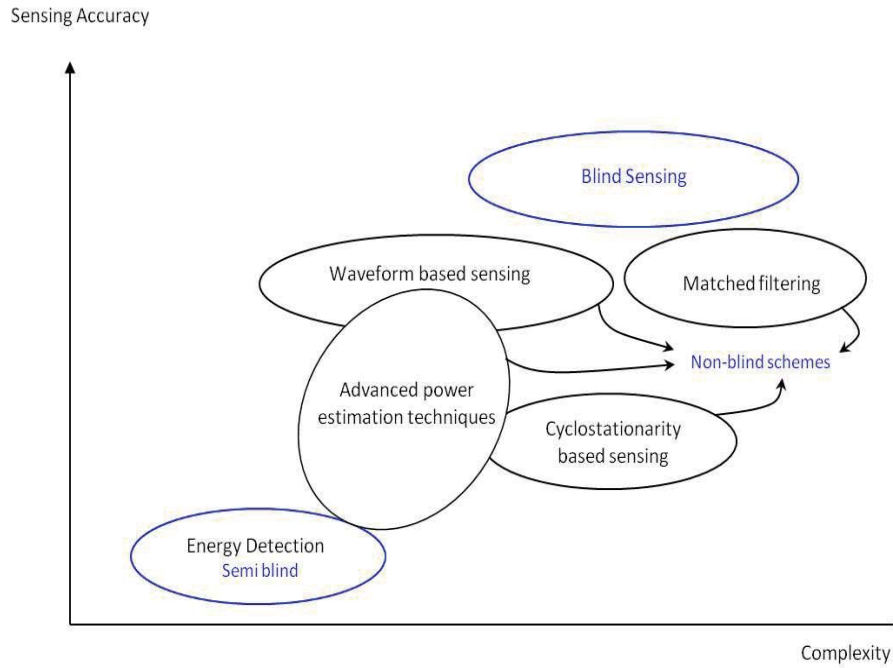
Figure 2.7: Comparison of spectrum sensing methods.

harmful interference to primary transmissions.

This problem can be solved by exploiting the inherent spatial diversity in a multi-user environment; where if some CRs experience primary receiver uncertainty problem, or they are in deep fade or observe severe shadowing, as shown in Figure 2.9, there might be other CRs, in the network, with relatively strong signal from primary transmitter. Consequently, combining the sensing information from different CRs gives a more reliable spectrum awareness. This leads to the concept of cooperative spectrum sensing (CSS) wherein CRs employing different technologies, exchange information about the time and frequency usage of spectrum to avail more efficiently any vacant spectrum usage opportunity [110], [111].
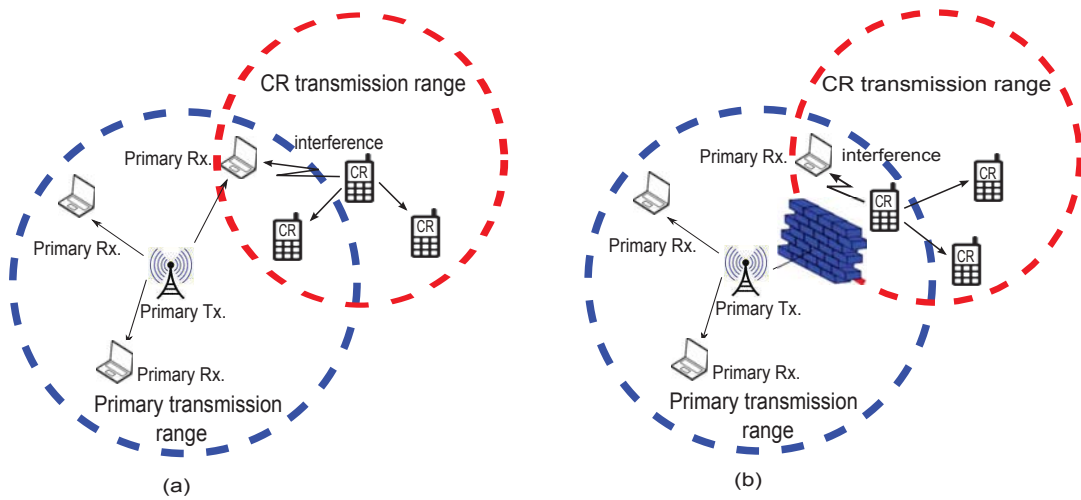
Figure 2.8: Vulnerability of primary receivers to secondary transmissions (a) Receiver uncertainty (b) Hidden primary transmitter.

2.8.1 Classification of Cooperative Sensing

Cooperative sensing can be classified based on different criteria. The key questions in this regard include: who performs sensing, who makes the final decision about spectrum opportunity, how the sensing information is shared and what information is shared among the cooperating CRs. Classification of cooperative spectrum
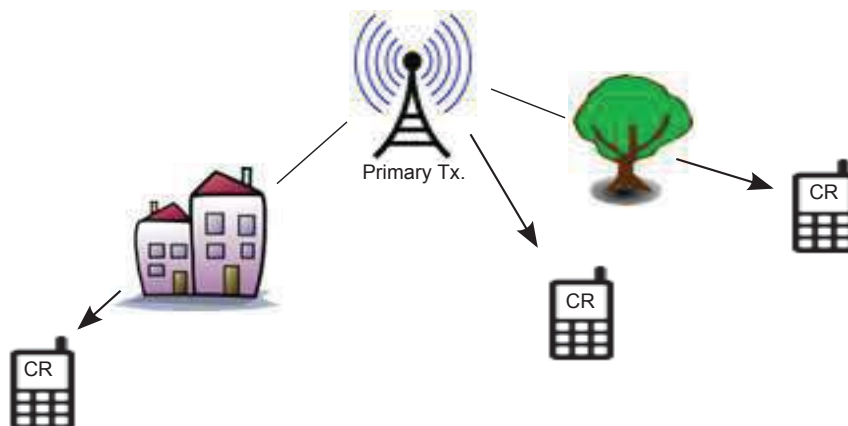
Figure 2.9: Cooperative SS in a shadowed environment.

sensing based on these questions is depicted in Figure 2.10.
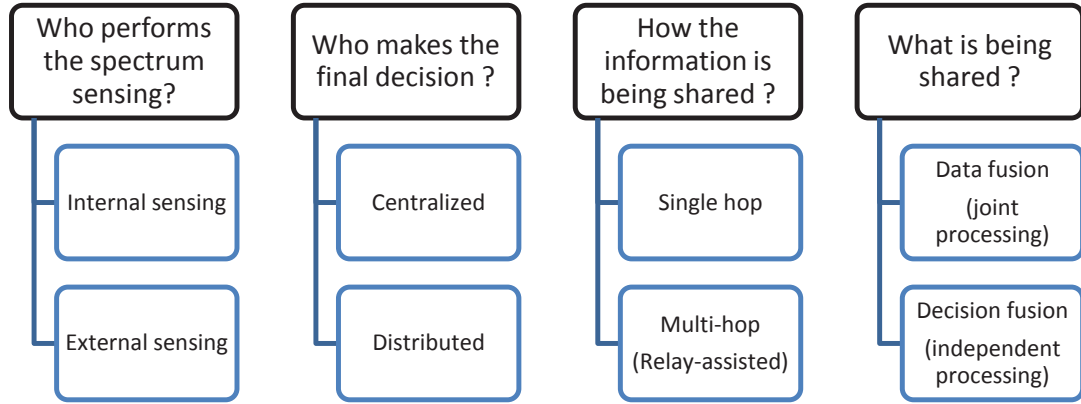
Figure 2.10: Classification of cooperative spectrum sensing.

A comprehensive survey on CSS is provided in [112]. In essence cooperative spectrum sensing is a series of actions involving **Local Sensing**, **Reporting** and **Information Fusion**. The following sections highlight the distinguishing features of cooperation strategies.

2.8.2 Centralized and Distributed Cooperative Sensing

The conventional cooperation strategy completes the three above mentioned steps based on centralized approach which is the most popular cooperation scheme. In **centralized cooperation**, a central unit, also called the *fusion center* (FC), decides about the spectrum hole after collecting local sensing information from cooperating SUs [113],[114]. This spectrum usage opportunity is then either broadcast to all CRs or central unit itself controls the CR traffic by managing the detected spectrum usage opportunity in an optimum fashion. This central node is an access point (AP) in a wireless local area network (WLAN) or a base station (BS) in a

cellular network while in CR ad hoc networks, any CR can act as a master node to coordinate CSS. Hence, centralized cooperation can take place in both centralized and distributed network architectures. On the other hand, in **distributed cooperation**, CRs do not rely on a FC to make a cooperative decision. Instead, CRs communicate among themselves and converge to a joint global decision on the presence or absence of PU in an iterative manner [115]-[117]. This is accomplished in three basic steps defined by a distributed algorithm as follows:

1. Each cooperating CR sends its local sensing data to other CR users in its neighborhood (defined by transmission range of CR user).

2. Each cooperating CR combines its data with received sensing information from other users to decide on presence or absence of PU based on its local criterion. The shared spectrum observations are usually in the form of *soft* sensing results or quantized (binary/*hard*) version of local decisions about spectrum hole availability.

3. If spectrum hole is not identified, CRs send their combined sensing information to other secondary users in next iteration. The process continues until the scheme converges and a final unanimous opinion on spectrum availability is achieved.

In this way, each CR in distributed cooperation partially plays the role of FC. The significant features of centralized and distributed cooperation are highlighted in Table 2.2.

Table 2.2: Comparison of centralized and distributed cooperative sensing.

CSS approach	Advantages	Disadvantages
Centralized Sensing	+ Bandwidth efficient for same number of cooperating CRs as compared to distributed cooperation	- One CR i.e. FC becomes very critical as well as complex to carry the burden of all cooperating CRs
Distributed Sensing	+ No need of backbone infrastructure resulting in low implementation cost	- Large control bandwidth required for information exchange among all cooperating CRs - Finding neighbors in itself is a challenging task for CRs - Large sensing duration resulting from iterative nature of distributed algorithm

The working principle of centralized and distributed cooperation is shown in Figure 2.11 (a) and (b) respectively.
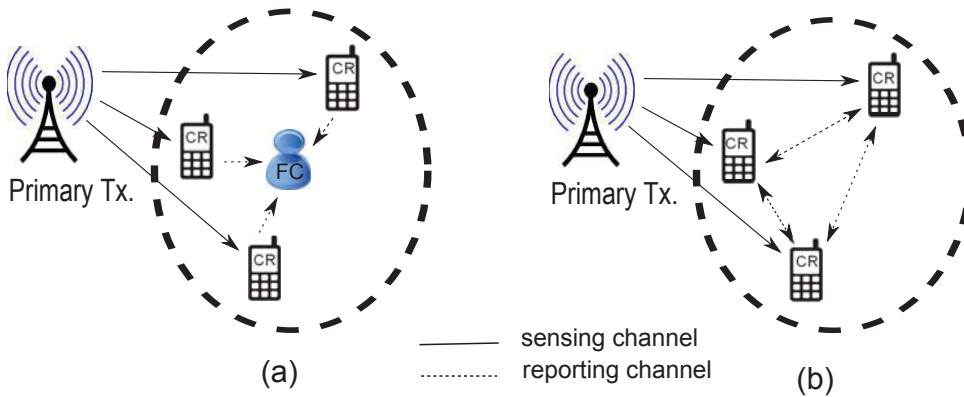
Figure 2.11: Cooperative SS (a) Centralized approach (b) Distributed approach.

As shown in Figure 2.11, CRs make use of sensing and reporting channels to arrive at a cooperative decision. At first, CRs establish a link with primary Tx. to perform local sensing over the selected licensed frequency band. This physical channel between primary Tx. and each cooperating CR is termed as *sensing channel*. During the reporting phase, CRs need a control channel, also known as

reporting channel to share local spectrum sensing data with FC or each other. This control channel, depending upon system requirements, can be implemented using a dedicated spectrum, an un-licensed band such as ISM or an underlay approach such as ultra wide band (UWB) [118]. Usually, a medium access protocol governs the shift between the sensing and control channel.

2.8.3   Data and Decision Fusion in Cooperative Sensing

In both centralized and distributed sensing, a control channel is required for sharing sensing information within CRN to reach a cooperative decision on spectrum hole availability. The bandwidth of the control channel limits the amount of sensing information that can be reported to FC or shared among cooperating CRs. If the entire local sensing data or the complete local test statistics are shared, joint processing of the raw sensing data offers the best detection performance at the cost of control channel communication overhead. This fundamental component of cooperative sensing is termed as **data fusion**. In comparison to *soft combining* based data fusion, *hard combining* is another alternative to perform cooperation under control channel bandwidth constraint. In this approach, sensing data is processed locally before transmitting it over the control channel and the one-bit local decision from each of the cooperating secondary users is combined using linear fusion rules. This leads to **decision fusion** based cooperative detection which requires much less control channel bandwidth at the cost of depreciated sensing performance when compared with data fusion based CSS. Typically, *OR*, *AND*,

and *MAJORITY* rules are used for decision fusion which can be considered as special instances of generalized k out of N rule. It has been shown in [119] that *OR* (k=1) rule outperforms when number of cooperating secondary users is large while *AND* (k=N) rule gives optimal performance for small number of CRs.

2.8.4 Relay-assisted Cooperative Sensing

It is noteworthy that under realistic transmission conditions, both sensing and reporting channel are not ideal. Such a scenario is illustrated in Figure 2.12 where CR1 and CR2 observe strong sensing channels but weak reporting channels (to FC) due to possible shadowing or multipath effect. In this case, sensing data from these CRs is forwarded to CR3 and CR4 who suffer from shadowed sensing channels but strong reporting channels. Hence, CR3 and CR4 act as relays to transmit sensing information from CR1 and CR2 to FC through them and thus the reporting channels between CR3, CR4 and FC are termed as *relay channels*. This scheme is popularly known as **Relay-assisted cooperative sensing** and has been discussed in [120].

2.8.5 Single hop and Multi-hop Cooperative Sensing

It is important to point out that Figure 2.12 shows a centralized network for sake of simplicity, however, relay-assisted cooperation is equally applicable in distributed sensing where each cooperating CR plays the role of FC. In fact, when sensing data reaches the intended secondary user through multiple hops, all the intermediate
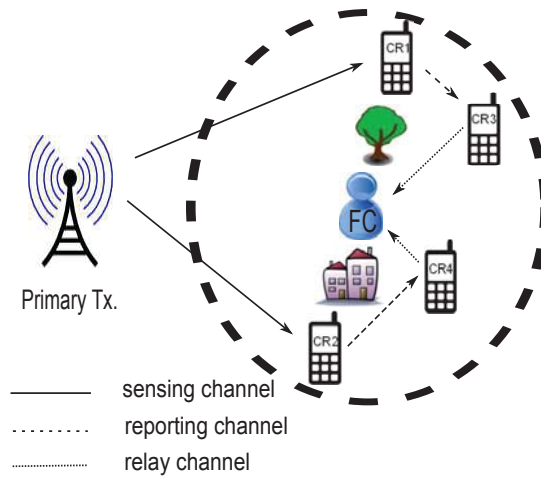
Figure 2.12: Relay-assisted cooperative SS.

hops act as relays. Hence, centralized and distributed sensing schemes depicted in Figure 2.11 are classified as **single hop cooperative sensing**, while relay-assisted cooperation, shown in Figure 2.12, falls under the category of **multi-hop cooperative sensing**.

2.8.6 Internal and External Sensing

From the network perspective, both centralized and distributed sensing, involving either single hop or multi-hop (relay-assisted), fall under the category of **internal sensing**, which results in suboptimal utilization of spectrum usage opportunity as both the spectrum sensing and subsequent data transmission on the detected frequency band are collocated at a single CR. In [121], CR network architecture based on two distinct networks; i.e., the *sensor network* and an *operational network* has been proposed as a third approach for cooperative PU detection, known as *External sensing*. In **external sensing**, a dedicated network composed of only sensing nodes is employed to scan the targeted frequency band continuously or

periodically. The sensing results are then passed on to the master sensor in this external network which optimally combines the sensing data and shares the PU activity information in the sensed area with *operational network*.

Detailed comparative analysis of SS techniques and the inevitable requirement of cooperation among the sensing nodes, discussed in this chapter, identifies energy detection as the most suitable sensing scheme that can be applied in cooperative sensing, due to its low computational complexity and semi-blind nature. Robustness of ED can be achieved and other limitations of ED can be overcome through cooperative detection. The next chapter undertakes an in-depth performance analysis of ED.

CHAPTER 3

ENERGY DETECTION BASED

SPECTRUM SENSING

Based on the comparative analysis of SS techniques from the previous chapter (Chapter 2), which identifies energy detection (ED) as the most appropriate sensing scheme that can be applied in cooperative spectrum sensing, this chapter presents an in-depth performance analysis of ED.

The chapter is organized as follows: Section 3.1 reviews the existing work on ED, and highlights some of the ambiguities/conflicts in the reported research. Section 3.2 introduces ED and presents an appropriate PU signal model. The exact distributions of decision metric for deterministic and random PU signal models are derived in Section 3.3, while the Gaussian approximations to exact test statistic, and their validity conditions are discussed in Section 3.4. Finally, Section 3.5 discusses the performance enhancement of ED through cooperative detection.

3.1 Introduction

The decision metric for ED, in principle, is the energy content in the received signal at CR. However, there exists a noticeable ambiguity in defining the exact test statistic for ED in the literature. The classical work of Urkowitz [29], Digham et al. [122] and some recent publications like [30] and [123] belong to class of techniques that normalize energy in the received samples by noise variance to get the test statistic. Whereas, other authors like Zeng et al. [31] and Zhuan et al. [124] define the average energy in the received samples as the decision metric; i.e., they scale the energy in the received samples by the number of samples to make a decision on the presence/absence of primary signal which, in fact, becomes the measure of power in the received signal. On the other hand, authors like Sonnenchein and Fishman [125] consider unscaled version of energy content in the received samples as the test statistic. As a result of different scaling factors employed in test statistics, the probability of detection P_d and the probability of false alarm P_f are found to be different across various approaches yielding to a source of confusion for novice researchers in the field of spectrum sensing.

It is important to note that the classical results on ED, by Urkowitz [29], were developed for radar applications where the deterministic source signal is to be detected in the presence of white Gaussian noise. Many authors [30], [122], [123], and others used the results reported by Urkowitz under the assumption that the probability of detection can be considered as a conditional probability. However, it will be shown in this chapter that this is only possible when the unknown PU

signal comprises of equal energy constellation points as illustrated in Section 3.3.3.

Noticeably, most of the literature on ED [29], [31], [124], and [125] approximates the pdf of decision metric using Gaussian distribution under both the hypotheses. This approximation relies on the central limit theorem and is considered to be valid for large number of observed samples N_s. But how large N_s should be?, this question has not been properly addressed in the available literature and there are various numbers given by different authors in this regard. For example, Zeng et al. [31] used $N_s = 5000$ for Gaussian approximation. Urkowitz [29] proposed Gaussian approximation for $N_s > 250$ while Arshad et al. [32] argued that these approximations are valid for number of observed samples as little as $N_s = 10$. This indicates the lack of a clear approach for finding the minimum number of samples to achieve a desired detection performance at a given SNR.

Based on the above discussion, a general test statistic for ED based on an unscaled energy content of received samples is presented and the generic structure of corresponding threshold for the given spectrum reuse probability is derived. In this regard, various PU signal models are considered in the derivations of the exact distribution of ED test statistic and exact ROC curves are compared for these signal models. Furthermore, the validity of Gaussian approximations to exact distribution of ED test statistic under different scenarios is investigated.

3.2   System Model for Energy Detection

The block diagram of energy detector is depicted in Figure 3.1. The input band-
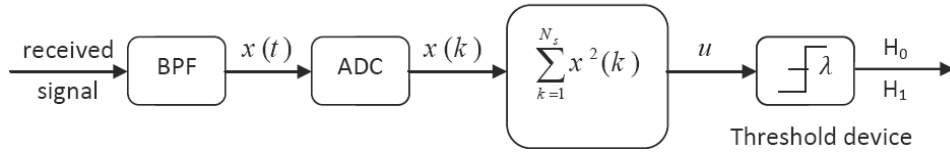
Figure 3.1: Block diagram of an energy detector (ED).

pass filter removes the out of band signals based on spectrum of interest, known to be centered around f_c and spanning over bandwidth W. The filtered received signal $x(t)$ is digitized by an analog to digital converter (ADC) and a simple squaring device followed by an accumulator gives the energy content in N_s samples of $x(k)$, which acts as the test statistic for ED as:

$$u = \sum_{k=1}^{N_s} x^2(k). \tag{3.1}$$

The decision metric, u, is then compared with a threshold, λ, to decide if the scanned band is vacant (H_0) or occupied (H_1).

It is important to point out that in classical literature [29],[122] etc., the energy detector measures the energy in the bandlimited (bandwidth=W Hz) received waveform $x(t)$ over sensing duration of T seconds and approximates this measure by the sum of squares of limited number of N_s received samples (see [29], p.524, Fig.1). However, in the proposed setting, the received signal is digitized by sampling at the Nyquist rate; i.e. $f_s = 2W$ samples/sec, where f_s is the sampling frequency which yields $N_s = 2WT$ samples for the observation window of T sec, after pre-filtering it with a band-pass filter of bandwidth W. The energy content

60

in N_s received samples serves as the test statistic as shown in Figure 3.1. This is in contrast to existing approach where the received signal waveform is reconstructed to find its energy.

The performance of ED is gaged with the probability of false alarm P_f and probability of detection P_d, which are given by:

$$P_f = P(\text{signal is detected } |H_0) = P(u > \lambda \,|H_0)$$
$$= \int_\lambda^\infty f(u|H_0)du, \tag{3.2}$$

$$P_d = P(\text{signal is detected } |H_1) = P(u > \lambda \,|H_1)$$
$$= \int_\lambda^\infty f(u|H_1)du, \tag{3.3}$$

where $f(u|H_i)$ represents the pdf of test statistic under hypothesis H_i with $i = 0, 1$. The exact and approximate distribution of test statistic are discussed in detail in Sections 3.3 and 3.4, respectively.

The fundamental detection objective is to maximize P_d while minimizing P_f. P_d vs P_f plot depicts *Receiver Operating Characteristics* and is considered as an important performance indicator. In practice, if a certain spectrum re-use probability of unused spectrum is targeted, P_f is fixed to a small value (e.g $\leq$ 5%) and P_d is maximized. This is referred to as constant false alarm rate (CFAR) detection principle [21] in which λ is calculated using (3.2). However, if the CRN is required to guarantee a given non-interference probability, P_d is fixed to a high

value (e.g. $\geq 95\%$) and P_f is minimized. This requirement is met by evaluating λ based on (3.3) and this approach is known as constant detection rate (CDR) principle. As evident from (3.2) and (3.3), the derivations of λ are very similar for CFAR and CDR, so the analytical results derived under the assumption of CFAR can be applied to CDR based detection with minor modifications and vice versa [21]. In this chapter, the analysis is based on CFAR and the results can be applied to CDR based detection with minor modifications.

3.3 Exact Test Statistic Distribution for ED

As indicated in Section 3.2, probability of false alarm and detection depend on the pdf of the test statistic under H_0 and H_1 respectively. Hence, accurate evaluation of P_f and P_d depend on the exact test statistic distribution. The following sections provide an insight into the derivation of exact expressions of P_f and P_d for various signal classes, and highlight some of the important hidden assumptions.

3.3.1 Exact P_f

Under H_0, $x(k) = n(k) \sim \mathcal{N}(0, \sigma_n^2)$ where, without loss of generality, $n(k)$ is assumed to be Gaussian with zero mean and σ_n^2 variance. The test statistic, u, is simply the sum of squares of N_s Gaussian random variables, each with zero mean and σ_n^2 variance. Hence, u, normalized with σ_n^2 is said to have a *central Chi-square*

distribution with N_s degrees of freedom:

$$H_0 : \quad \frac{1}{\sigma_n^2} u = \sum_{k=1}^{N_s} \left(\frac{1}{\sigma_n} n(k) \right)^2$$

$$= \sum_{k=1}^{N_s} (y(k))^2 \ \ where \ \ y(k) \sim \mathcal{N}(0,1). \tag{3.4}$$

$$\sim \chi_{N_s}^2. \tag{3.5}$$

Using (3.2), and the fact that $f(\frac{1}{\sigma_n^2}u|H_0){=}\chi_{N_s}^2$, the exact closed form expression of P_f can be obtained as:

$$P_f = P \left(\frac{1}{\sigma_n^2} u > \frac{1}{\sigma_n^2} \lambda | H_0 \right)$$

$$= \int_{\frac{\lambda}{\sigma_n^2}}^{\infty} f(\frac{1}{\sigma_n^2} u | H_0) du. \tag{3.6}$$

$$= Q_{\chi_{N_s}^2} \left(\frac{\lambda}{\sigma_n^2} \right), \tag{3.7}$$

which yields:

$$P_f = \frac{\Gamma(m, \frac{\lambda}{2\sigma_n^2})}{\Gamma(m)}. \tag{3.8}$$

We denote the right hand side of (3.8) as $F_m(\frac{\lambda}{2\sigma_n^2})$. This is a known result in ED based SS. It was obtained by Ghasemi and Sousa in [30], (for $\sigma_n^2 = 1$) and by Digham et al. in [122]. The only difference is that they defined the scaled ED test statistic as $u_{scl} = \frac{u}{\sigma_n^2}$.

3.3.2 General Structure of ED Threshold and Resolving the Energy Scaling Conflict

The ED threshold for constant false alarm constraint can be derived from (3.8) as:

$$\lambda = 2\sigma_n^2 F_m^{-1}(P_f), \tag{3.9}$$

which clearly indicates that the threshold depends on the noise variance, σ_n^2, the number of observed samples, N_s, and the targeted constant false alarm probability, P_f. It can be represented in a generic form as:

$$\lambda = \sigma_n^2 . f(N_s, P_f), \tag{3.10}$$

where f is a constant obtained as a function of N_s and P_f.

Therefore, in the general form, the test statistic given by (3.1) is compared to a threshold of the form indicated in (3.10). A careful look at these equations reveal that all prior reported ED algorithms are special cases of the general form of the energy metric, u, and threshold, $\sigma_n^2 . f(N_s, P_f)$. For example, Urkowitz [29], Ghasemi and Sousa [30], [123], and Digham et al. [122], suggested to compare $\frac{u}{\sigma_n^2}$ with f while Zeng et al. [31] and Zhuan et al. [124] proposed the comparison between $\frac{u}{N_s}$ and $\frac{\sigma_n^2 . f}{N_s}$ to identify holes in the scanned frequency spectrum.

3.3.3   Exact P_d

In a non-fading environment where the channel gain, h, is deterministic and can be considered as *unity* without loss of generality ($h = 1$), the received signal under H_1 is given by: $x(k) = s(k) + n(k)$ with, $n(k) \sim \mathcal{N}(0, \sigma_n^2)$. Thus, the test statistic, u, depends on the statistics of $s(k)$. In the following, various signal models for PU signal, $s(k)$, are discussed, and the underlying assumptions used in the derivation of exact closed form expression of P_d are highlighted.

Deterministic PU Signals

The most simple signals to be detected under AWGN environment belong to the class of unknown deterministic signals. This case was analyzed by Urkowitz [29], where it was shown that the assumption of unknown deterministic signal results in Gaussian received signal $x(k)$, similar to noise, with same variance σ_n^2 but with non-zero mean. Following the work of Urkowitz, exact closed-form expression for P_d was obtained by Digham et al. [122]. Most of the literature on ED based spectrum sensing refer to these fundamental works to identify the presence or absence of primary signal in the scanned frequency band. In general, PU signal contains information for its intended primary receiver, and hence, it is random in nature and cannot be treated as deterministic. However, as reported by Urkowitz [29], detection probability expression obtained for unknown deterministic signal is valid for random signal model provided; P_d is considered a conditional probability of detection where the condition is that the unknown signal to be detected (PU

signal in case of spectrum sensing) has a certain fixed amount of energy. This suggests that PU signal must not contain any information in its amplitude, which results in underlying assumption that PU signal must have deterministic, although unknown, energy. Only in that case, detection probability of PU signal is given by the classical results reported in [29], [122].

For example, if $s(k)$ belongs to an M-ary *Phase Shift Keying* (PSK) signalling, all PU signal points lie on a circle of radius, say A, and have equal power A^2. The symmetry of the constellation indicates that the detection probability of the system is equal to the detection probability when any one signal point is transmitted. This is similar to evaluating the detection probability by assuming unknown PU signal to be a deterministic signal with $s(k) = A$. It is noteworthy that for a deterministic PU signal of finite duration T with (unknown) constant amplitude A, A^2 represents the power of the PU signal point while TA^2 is the measure of total energy content, E_s, of the unknown signal $s(k)$.

Mathematically, for

$$s(k) \in \{A_i\} \ \text{ for } \ i = 1, 2, \cdots, M$$

$$\text{with} \quad |A_i| = A \ \ \forall \, i \quad \text{and} \quad \sum_{i=1}^{M} P(s(k) = A_i) = 1, \quad (3.11)$$

the detection probability based on the energy content of the received signal is

given by:

$$P_d = \sum_{i=1}^{M} P_d | \left(s(k) = A_i \right) \; P(s(k) = A_i) \tag{3.12}$$

$$= P_d | \left(s(k) = A \right). \tag{3.13}$$

$$(\because P_d | \left(s(k) = A_i \right) = P_d | \left(s(k) = A \right) \; \forall \; i)$$

Hence, this case simplifies into the detection of the unknown deterministic signals: $x(k) = A + n(k)$.

Under H_1, with $x(k) \sim \mathcal{N}(A, \sigma_n^2)$, the test statistic is simply the sum of squares of N_s Gaussian random variables, each with mean A and variance σ_n^2. Hence, u, normalized with σ_n^2 is said to have a *non-central Chi-square* distribution with N_s degrees of freedom:

$$H_1: \; \frac{1}{\sigma_n^2} u = \sum_{k=1}^{N_s} \left(\frac{1}{\sigma_n}(A + n(k)) \right)^2$$

$$= \sum_{k=1}^{N_s} (y(k))^2 : y(k) \sim \mathcal{N}\left(\frac{A}{\sigma_n}, 1 \right). \tag{3.14}$$

$$\sim \chi_{N_s}^2(\Omega) \; (deterministic \; s(k)). \tag{3.15}$$

and Ω is the non-centrality parameter given by:

$$\Omega = \sum_{k=1}^{N_s} \left(\frac{A}{\sigma_n} \right)^2 = \frac{N_s A^2}{\sigma_n^2}. \tag{3.16}$$

$$= N_s \gamma. \tag{3.17}$$

where $\gamma = \frac{A^2}{\sigma_n^2}$ is popularly known as the SNR.

It is important to point out here that some well known authors like Urkowitz [29], Ghasemi and Sousa [123], and also Digham et. al. [122], define SNR as $\gamma_1 = \frac{E_s}{N_0}$ and thus evaluate non-centrality parameter, given by (3.16) as, $\Omega_1 = \frac{N_s A^2}{\sigma_n^2} = \frac{2TWA^2}{2WN_0/2} = \frac{TA^2}{N_0/2} = \frac{2E_s}{N_0} = 2\gamma_1$.

Using (3.3) and the fact that $f(\frac{1}{\sigma_n^2} u | H_1) = \chi_{N_s}^2(\Omega)$, the exact closed-form expression of the detection probability for deterministic PU signal, P_{dd} can be obtained as:

$$P_{dd} = P\left(\frac{1}{\sigma_n^2} u > \frac{1}{\sigma_n^2} \lambda \,| H_1\right)$$

$$= \int_{\frac{\lambda}{\sigma_n^2}}^{\infty} f(\frac{1}{\sigma_n^2} u | H_1) du \tag{3.18}$$

$$= Q_{\chi_{N_s}^2(\Omega)}\left(\frac{\lambda}{\sigma_n^2}\right) \tag{3.19}$$

which yields:

$$P_{dd} = Q_m(\sqrt{\Omega}, \sqrt{\frac{\lambda}{\sigma_n^2}}) = Q_m(\sqrt{N_s \gamma}, \sqrt{\frac{\lambda}{\sigma_n^2}}), \tag{3.20}$$

where $m = N_s/2$ is the time-bandwidth product, assumed to be an integer number. This result was derived by Ghasemi and Sousa in [30], for $\sigma_n^2 = 1$. The only difference is that they defined the scaled ED test statistic as $u_{scl} = \frac{u}{\sigma_n^2}$. Similar results were shown by Digham et al. in [122], for $\sigma_n^2 = 1$ and defining SNR as $\gamma_1 = \frac{E_s}{N_0}$.

The key point to highlight here is the exact closed-form expression of P_{dd}, (3.20), reported extensively in the literature based on [29], [30], [122], [123] etc.,

caters only the cases in which the total detection probability can be considered as a conditional probability of detection which is true only for the PU signals comprising of equal energy constellation points. It is important to point out that this hidden assumption has never been pointed out in the literature though equal energy restriction on PU signal points is not always true in practice. Furthermore, if PU signal constellation points have different energy, the simplification of (3.12) to (3.13) does not remain valid, and hence, total detection probability needs to be evaluated according to (3.12). This means that the transmission probabilities of possible PU signal points would also become critical and need to be known *a priori* to evaluate the weighted summation encountered in (3.12).

Normally distributed PU signals

For the detection of unknown PU signals, many researches like Arshad et al. [32], Zhuan et al. [124] and Cabric et al. [126] argue that in the absence of any *a priori* knowledge about PU signal form, it is more appropriate to model the PU signal as an IID Gaussian random process with zero mean and variance σ_s^2; i.e., $s(k) \sim \mathcal{N}(0, \sigma_s^2)$. This case yields Gaussian received signal: $x(k) = s(k) + n(k)$ such that $x(k) \sim \mathcal{N}(0, \sigma_t^2)$ where σ_t^2 is the total variance of the received signal defined as:

$$\sigma_t^2 = \sigma_s^2 + \sigma_n^2 = \sigma_n^2(1 + \gamma_r), \quad \text{where} \quad \gamma_r = \frac{\sigma_s^2}{\sigma_n^2}. \tag{3.21}$$

Under H_1, with $x(k) \sim \mathcal{N}(0, \sigma_t^2)$, the detection probability (for *Normal* PU

signal) P_{dn} can be derived by replacing σ_n^2 by σ_t^2, H_0 by H_1 and P_f by P_{dn} in (3.4) and (3.8). The final closed-form expression is given by:

$$P_{dn} = \frac{\Gamma(m, \frac{\lambda}{2\sigma_t^2})}{\Gamma(m)} \triangleq F_m(\frac{\lambda}{2\sigma_t^2}).$$ (3.22)

PU signals with general Gaussian distribution

The above sections discussed the detection of unknown deterministic signals and Gaussian random signals (with zero DC level) in white Gaussian background noise. The most general assumption regarding the PU signal distribution is to allow the unknown signal to be composed of a deterministic component and a random component [127]. The PU signal then can be modeled as a Gaussian random process with the deterministic part corresponding to a non-zero mean A and a random part corresponding to a zero-mean Gaussian random process with variance σ_s^2. These assumptions lead to the *general Gaussian detection problem* with PU signal model as: $s(k) \sim \mathcal{N}(A, \sigma_s^2)$. This gives $x(k) \sim \mathcal{N}(A, \sigma_t^2)$ resulting in the normalized test statistic $(\frac{1}{\sigma_t^2}u)$ under H_1 to have a *non-central Chi-square* distribution with N_s degrees of freedom:

$$H_1: \ \frac{1}{\sigma_t^2}u = \sum_{k=1}^{N_s} \left(\frac{1}{\sigma_t}(s(k) + n(k))\right)^2$$

$$= \sum_{k=1}^{N_s} (y(k))^2 : y(k) \sim \mathcal{N}\left(\frac{A}{\sigma_t}, 1\right).$$ (3.23)

$$\sim \chi_{N_s}^2(\Omega_n) \ \left(s(k) \sim \mathcal{N}(A, \sigma_s^2)\right).$$ (3.24)

and Ω_n is the non-centrality parameter given by:

$$\Omega_n = \sum_{k=1}^{N_s} \left(\frac{A}{\sigma_t}\right)^2 = \frac{N_s A^2}{\sigma_t^2} = \frac{N_s A^2}{\sigma_n^2(1+\gamma_r)} = N_s \frac{\gamma}{1+\gamma_r}. \tag{3.25}$$

The resulting exact closed-form expression for detection probability (non-zero mean PU signal), denoted by P_{dn2}, is given by:

$$\begin{aligned}
P_{dn2} &= Q_{\chi_{N_s}^2(\Omega_n)}\left(\frac{\lambda}{\sigma_t^2}\right) \\
&= Q_m\left(\sqrt{\Omega_n}, \sqrt{\frac{\lambda}{\sigma_t^2}}\right) \\
&= Q_m\left(\sqrt{\frac{N_s\gamma}{1+\gamma_r}}, \sqrt{\frac{\lambda}{\sigma_n^2(1+\gamma_r)}}\right).
\end{aligned} \tag{3.26}$$

PU signals with non-Gaussian distribution / Normally distributed PU signals in non-Gaussian noise

The more generic class of random PU signals are with non-Gaussian distribution having arbitrary mean and variance. The extensive survey of the literature in this field reveals that the detection of non-Gaussian distributed PU signals in white Gaussian background noise has not been extensively addressed in the literature. This case is similar to the detection of Normally distributed PU signals perturbed by a non-Gaussian e.g. an impulsive noise. Signal detection over a non-Gaussian channel leads to a completely different analysis [128] and is beyond the scope of thesis.

3.3.4 Comparison of Exact Closed-Form Expressions for P_f and P_d
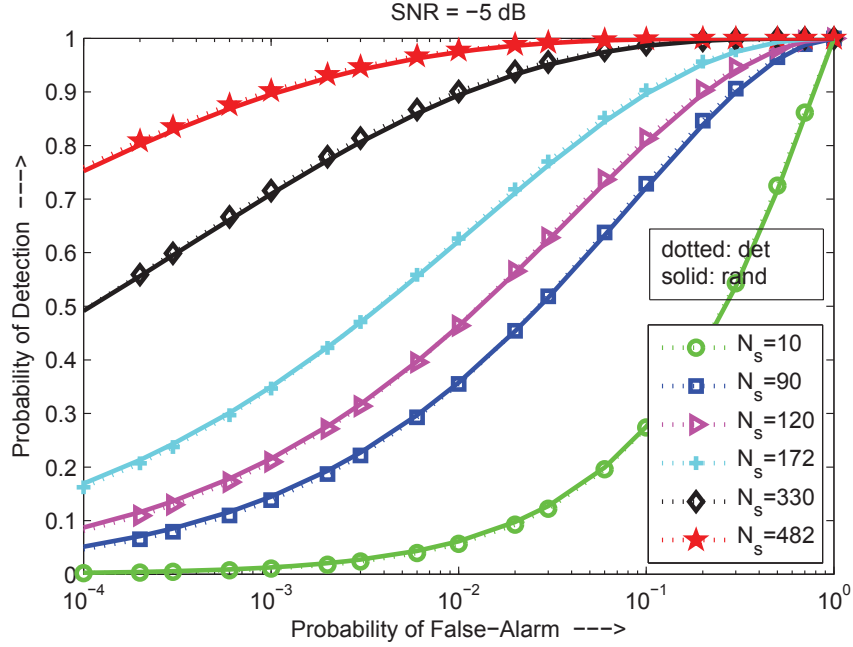
Figure 3.2: Exact ROC at -5 dB SNR for various N_s.

The exact closed-form expressions for P_f and P_d under AWGN are summarized in Table 3.1 for deterministic and random PU signal models. These probabilities are function of detection threshold, λ, which is determined by fixed P_f based on CFAR detection principle. Hence, the P_d, in general, depends on N_s, γ and target P_f. Figures 3.2-3.4 highlight the impact of underlying PU signal model on the detection performance of ED under low (-5 dB), moderate (0 dB) and high (5 dB) SNR conditions.

The comparison between deterministic and random PU signal model can be regarded as testing the similarity between *non-central* and *central* Chi-square distributed test statistics with N_s degrees of freedom and the non-centrality pa-
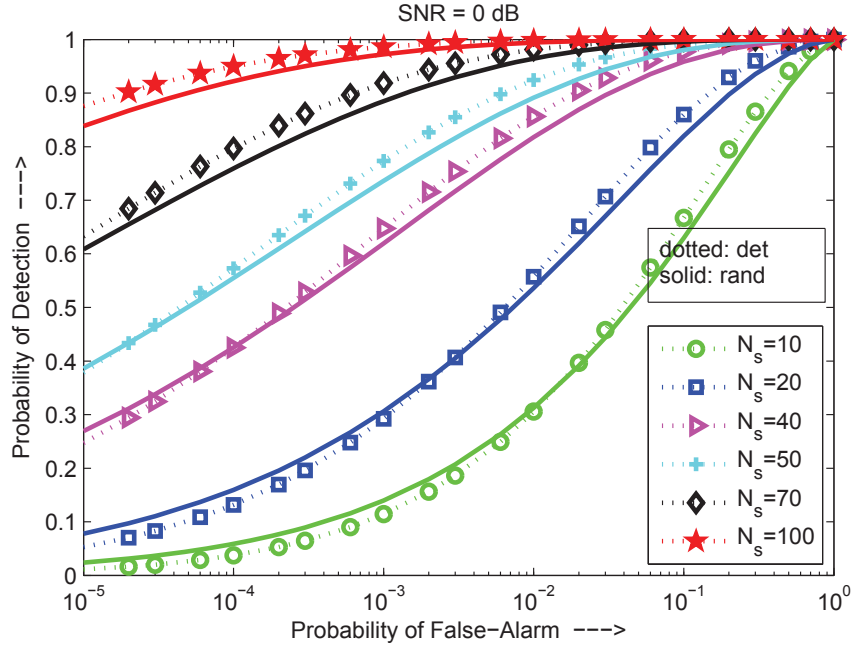
Figure 3.3: Exact ROC at 0 dB SNR for various N_s.

rameter, Ω, given by the product of N_s and γ. Figure 3.2 reveals that the nature (statistical characteristics) of PU signal does not play any significant role in determining the detection performance of ED when the observed PU signal is very weak; i.e., -5 dB SNR. This is because of the fact that under low SNR conditions (SNR<0 dB), received signal characteristics are pre-dominated by receiver noise which is assumed to be identical in both cases of deterministic and random PU signal. However, ROC curves for the two cases start diverging from each other when the received PU signal power becomes comparable to noise power as depicted in Figure 3.3 for 0 dB SNR. For SNR>0 dB, underlying assumption about the PU signal model becomes critical and lower bound on observed number of samples and minimum required SNR vary significantly for deterministic and random PU signals. This is verified through Figure 3.4, which shows that deterministic and

73
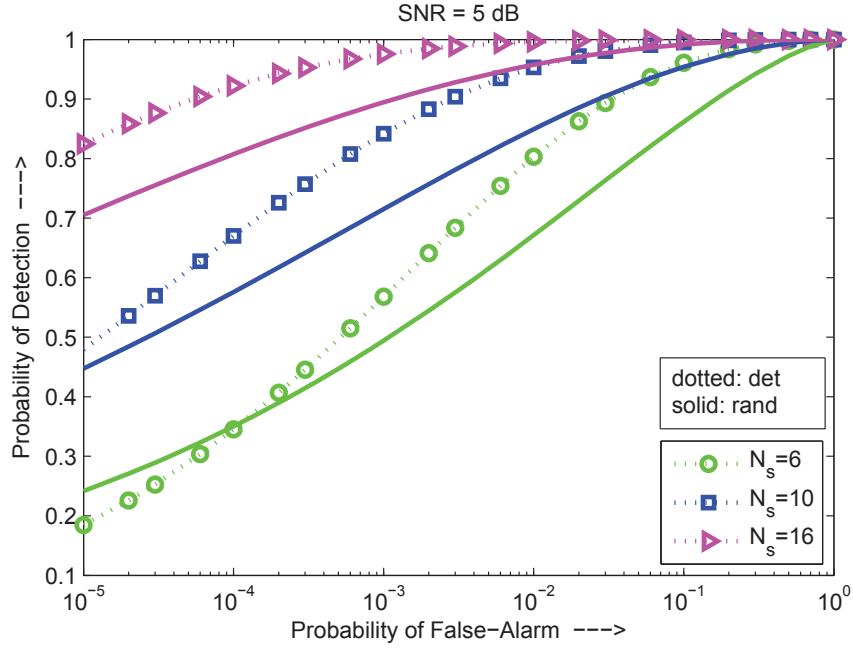
Figure 3.4: Exact ROC at 5 dB SNR for various N_s.

random PU signals behave in an entirely different manner to meet the given P_d and P_f requirements, even at a reasonable SNR of 5 dB. The role of SNR in determining the ED performance under different PU signal models is highlighted in Figure 3.5 by fixing the observed number of samples, N_s, to 10.

3.3.5 An Exact Lower Bound on N_s

An important result evident from Figures 3.2-3.4 is the inverse relationship between the required number of samples, N_s, and the quality of received signal in terms of SNR to meet given fixed P_f and target P_d. This relationship can be obtained by putting the value of λ from (3.9) into exact expression of P_d given by (3.20) for deterministic PU signal model or in (3.22) for random PU signal model. As the relationship between N_s and SNR is similar for deterministic and random
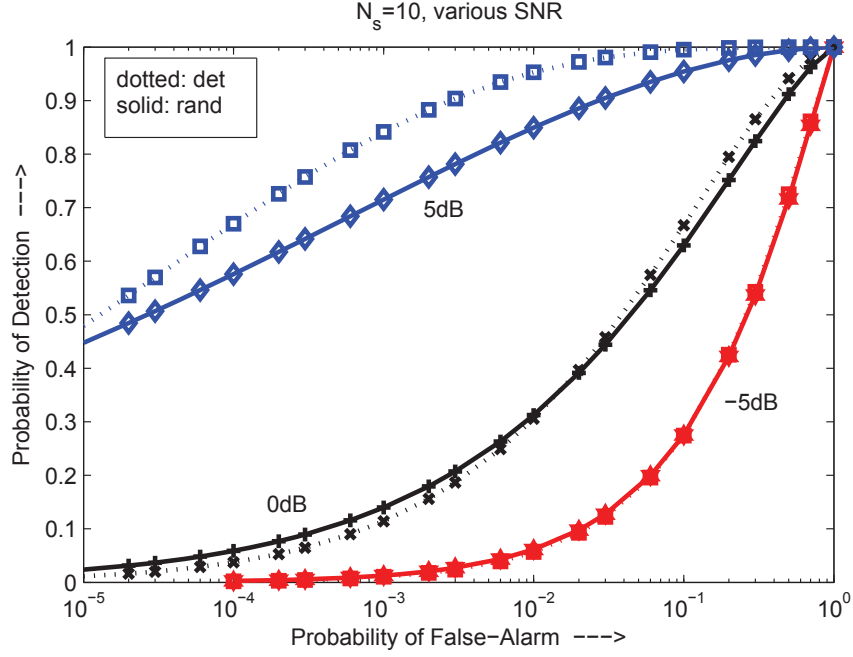
Figure 3.5: Exact ROC comparison for deterministic and random PU signal model for $N_s = 10$ at -5 dB, 0 dB and 5 dB SNR.

PU signal, the deterministic signal model is considered in further investigations. In this case, appropriate detection threshold to ensure given fixed P_f can be found from (3.7) as:

$$\lambda = \sigma_n^2 Q_{\chi_{N_s}^2}^{-1} \left(P_f \right). \tag{3.27}$$

If at the same time, a certain minimum P_d has to be maintained, then (3.19) should also yield the same λ:
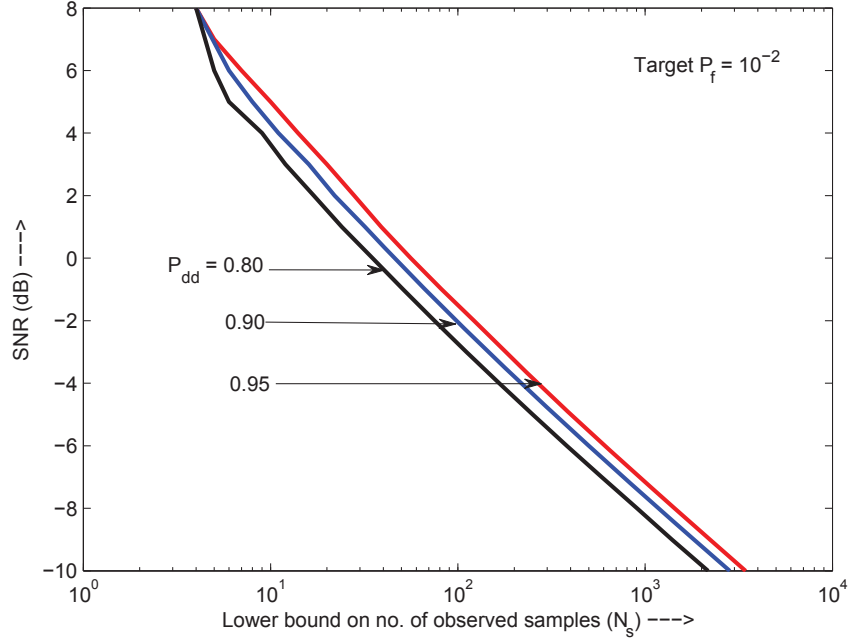
$$\lambda = \sigma_n^2 Q_{\chi_{N_s}^2 (N_s \gamma)}^{-1} \left(P_{dd} \right). \tag{3.28}$$

Figure 3.6: Exact lower bound on N_s and required SNR for $P_f = 10^{-2}$ for deterministic PU signal model.

Equating (3.27) and (3.28), we get

$$Q^{-1}_{\chi^2_{N_s}}(P_f) = Q^{-1}_{\chi^2_{N_s}(N_s\gamma)}(P_{dd}), \qquad (3.29)$$

which can be solved graphically to find a solution in the form of minimum required SNR and corresponding lower bound on N_s to guarantee desired P_f and P_d. Figure 3.6 shows the lower bound on N_s as a function of SNR for fixed P_f. A similar set of curves for fixed P_d is given in Figure 3.7. These figures clearly indicate that any targeted detection performance in terms of maximum P_d and minimum P_f is possible at as low SNR as desired by increasing the number of observed samples. However, it is noteworthy, that these results do not take into consideration any
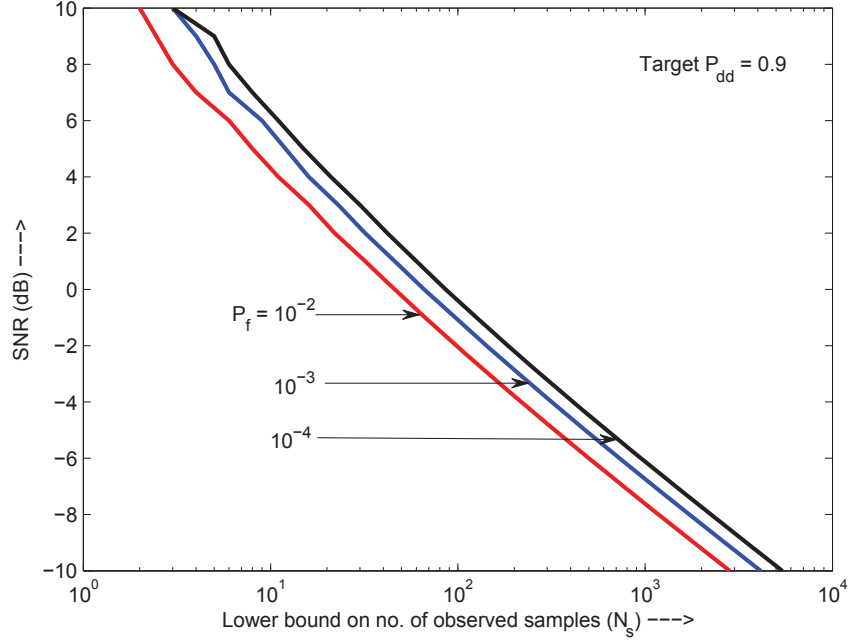
Figure 3.7: Exact lower bound on N_s and required SNR for $P_{dd} = 0.9$ for deterministic PU signal model.

uncertainties in the noise variance estimate and are valid only under non-fading channel conditions.

3.4 Approximate Test Statistic Distribution for ED

It was shown in Section 3.3 that the test statistic for ED follows Chi-square distribution with N_s degrees of freedom under either of conditions: noise alone, or signal plus noise. It is also well known that as the degrees of freedom (observed number of samples here, $N_s = 2m$) increase, the Chi-square distribution converges to Normal distribution, as dictated by *central limit theorem*. The following

sections shows the Gaussian approximations to the exact test statistic distributions which are considered to be valid for large time-bandwidth product, m, only. The main contribution in this regards is in terms of performance comparison between the exact and approximate expressions of P_d and P_f for different PU signal models under variety of SNR conditions to find the lower bound on number of samples N_s for the convergence of approximate to exact expressions. Specifically, we establish that the validity of Gaussian approximations is not only limited to spread-spectrum PU signal model as indicated in [125] or other similar cases like [31], and [124] where $m > 100$, rather, received SNR and desired upper limit on P_f also play critical roles in defining the practical lower bound on observed number of samples.

3.4.1 Approximate P_f

Under H_0 with $x(k) = n(k) : \mathcal{N}(0, \sigma_n^2)$, the test statistic can be analyzed as the sum of N_s statistically independent random variables. In this case, u, normalized with σ_n^2, as given by (3.4), is equivalent to:

$$H_0 : \quad \frac{1}{\sigma_n^2} u = \sum_{k=1}^{N_s} \left(\frac{1}{\sigma_n} n(k) \right)^2$$
$$= \sum_{k=1}^{N_s} z(k), \qquad (3.30)$$

where each random variable $z(k)$ in the sum has mean 1 and variance 2. Hence, the mean and variance of the sum is N_s and $2N_s$, respectively. Furthermore, $z(k)$

is known to have a smooth pdf given by *central Chi-square* distribution with 1 degree of freedom:

$$z(k) \sim \chi_1^2 = \frac{1}{\sqrt{2\pi x}} e^{-\frac{x}{2}} \qquad x \geq 0. \tag{3.31}$$

Therefore, for sufficiently large N_s, based on *central limit theorem*, the normalized test statistic may be well approximated by Gaussian distribution as:

$$H_0 : \quad \frac{1}{\sigma_n^2} u \sim \mathcal{N}(N_s, 2N_s). \tag{3.32}$$

Using (3.6), approximate expression for P_f is given by:

$$P_{f(app)} = Q\left(\frac{\frac{\lambda}{\sigma_n^2} - N_s}{\sqrt{2N_s}}\right) = Q\left(\frac{\lambda - \sigma_n^2 N_s}{\sigma_n^2 \sqrt{2N_s}}\right), \tag{3.33}$$

where $Q\left(\frac{\lambda - \sigma_n^2 N_s}{\sigma_n^2 \sqrt{2N_s}}\right)$ represents the right tail probability of a Gaussian random variable, $N(\sigma_n^2 N_s, \sigma_n^4 2N_s)$. The approximate closed-form expression of ED threshold for CFAR can be found from (3.33) as:

$$\lambda_{app} = \sigma_n^2 N_s \left(1 + \sqrt{\frac{2}{N_s}} Q^{-1}(P_f)\right). \tag{3.34}$$

As evident, approximate threshold follows the general structure of (3.10) with $f = N_s \times \left(1 + \sqrt{\frac{2}{N_s}} Q^{-1}(P_f)\right)$. Hence, for sufficiently large N_s, the general test statistic given by (3.1) may be compared with the threshold of the form indicated in (3.34) to identify any unused spectrum opportunity while ensuring given spectrum re-use

probability.

3.4.2   Approximate P_d

This section presents the Gaussian approximations to the exact test statistic distribution under H_1, and provides the approximate expressions of P_d for different signal models as discussed in Section 3.3.3.

Deterministic PU signals

For deterministic PU signal model, $x(k) \sim \mathcal{N}(A, \sigma_n^2)$ and the normalized test statistic, $\frac{1}{\sigma_n^2}u$ can be derived from (3.14) as the sum of N_s statistically independent random variables each with *non-central Chi-square* distribution having 1 degree of freedom and non-centrality parameter given by $\gamma = \frac{A^2}{\sigma_n^2}$ i.e.

$$H_1 : \quad \frac{1}{\sigma_n^2}u = \sum_{k=1}^{N_s} z(k). \qquad : z(k) \sim \chi_1^2(\gamma) \qquad (3.35)$$

The mean value of each variable in the sum is $1 + \gamma$ while its variance is given by $2(1 + 2\gamma)$. Thus, the mean and variance of the sum is $N_s(1 + \gamma)$ and $2N_s(1 + 2\gamma)$, respectively. Therefore, for sufficiently large N_s, based on *central limit theorem*, the normalized test statistic may be well approximated by Gaussian distribution as:

$$H_1 : \quad \frac{1}{\sigma_n^2}u \sim \mathcal{N}\left(N_s(1 + \gamma), 2N_s(1 + 2\gamma)\right). \qquad (3.36)$$

Hence, using (3.18), P_{dd} can be well approximated by the right tail probability of Gaussian random variable $\mathcal{N}\left(N_s(1+\gamma), 2N_s(1+2\gamma)\right)$ as:

$$P_{dd(app)} = Q\left(\frac{\frac{\lambda}{\sigma_n^2} - N_s(1+\gamma)}{\sqrt{2N_s(1+2\gamma)}}\right) = Q\left(\frac{\lambda - \sigma_n^2 N_s(1+\gamma)}{\sigma_n^2\sqrt{2N_s(1+2\gamma)}}\right) \tag{3.37}$$

Normally distributed PU signals

When PU signal is modeled as: $s(k) \sim \mathcal{N}(0, \sigma_s^2)$, the received signal is also zero mean Gaussian: $x(k) \sim \mathcal{N}(0, \sigma_t^2)$ and the test statistic, u, normalized with σ_t^2 is given by the sum of N_s statistically independent random variables. Each random variable, $z(k)$ follows *central Chi-square* distribution having 1 degree of freedom as:

$$H_1 : \frac{1}{\sigma_t^2}u = \sum_{k=1}^{N_s} z(k). \qquad : z(k) \sim \chi_1^2 \tag{3.38}$$

As $z(k)$ is known to have mean 1 and variance 2, the mean and variance of the sum is N_s and $2N_s$, respectively. Therefore, for sufficiently large N_s, based on *central limit theorem*, the normalized test statistic may be well approximated by Gaussian distribution as:

$$H_1 : \frac{1}{\sigma_t^2}u \sim \mathcal{N}(N_s, 2N_s). \tag{3.39}$$

Hence, P_{dn} can be well approximated by the right tail probability of Gaussian

random variable $\mathcal{N}(N_s, 2N_s)$ as:

$$P_{dn(app)} = Q\left(\frac{\frac{\lambda}{\sigma_t^2} - N_s}{\sqrt{2N_s}}\right) = Q\left(\frac{\lambda - \sigma_n^2 N_s(1 + \gamma_r)}{\sigma_n^2\sqrt{2N_s(1 + 2\gamma_r + \gamma_r^2)}}\right), \qquad (3.40)$$

where $\gamma_r = \frac{\sigma_s^2}{\sigma_n^2}$.

Comparison of (3.37) and (3.40) reveals that approximate detection probabilities of deterministic and zero mean random simplify to the same expression with the additional γ_r^2 in the denominator of (3.40) which becomes significant only for high SNR case, where N_s is usually not very large and the approximations do not remain meaningful. The other difference; i.e., $\gamma \triangleq \frac{A^2}{\sigma_n^2}$ and $\gamma_r \triangleq \frac{\sigma_s^2}{\sigma_n^2}$, is just notational, to differentiate the SNR while considering the deterministic and random PU signal model.

PU signals with general Gaussian distribution

For general Gaussian PU signal model with $s(k) \sim \mathcal{N}(A, \sigma_s^2)$ and $x(k) \sim \mathcal{N}(A, \sigma_t^2)$, the resulting normalized test statistic $(\frac{1}{\sigma_t^2}u)$ is given by the summation of N_s statistically independent random variables in which each random variable, $z(k)$ follows *non-central Chi-square* distribution having 1 degree of freedom and non-centrality parameter given by $\frac{\gamma}{1+\gamma_r}$; i.e.,

$$H_1: \quad \frac{1}{\sigma_t^2}u = \sum_{k=1}^{N_s} z(k) \qquad : z(k) \sim \chi_1^2\left(\frac{\gamma}{1 + \gamma_r}\right). \qquad (3.41)$$

Thus, the expression similar to deterministic case is obtained, except that γ is replaced by $\frac{\gamma}{1+\gamma_r}$. Therefore, similar to (3.36), the approximate normalized test statistic is given as:

$$H_1 : \ \frac{1}{\sigma_t^2} u \sim \mathcal{N}(N_s(1 + \frac{\gamma}{1 + \gamma_r}), 2N_s(1 + 2\frac{\gamma}{1 + \gamma_r})), \qquad (3.42)$$

while the resulting approximate expression of P_{dn2} is found to be:

$$P_{dn2(app)} = Q\left(\frac{\lambda - \sigma_n^2 N_s(1 + \frac{\gamma}{1+\gamma_r})}{\sigma_n^2 \sqrt{2N_s(1 + 2\frac{\gamma}{1+\gamma_r})}}\right). \qquad (3.43)$$

3.4.3 Validity Conditions for Gaussian Approximations

The results obtained for approximate closed-form expressions of P_f and P_d under AWGN are summarized and compared with exact expressions in Table 3.1 for different classes of PU signals.

As already pointed out in Section 3.3.4 for exact distribution of test statistics, PU signal model plays a significant role in determining ED performance for SNR$\geq$0 dB while for SNR$<$0 dB, both deterministic and random PU signals behave identically as evident from ROC shown in Figure 3.2. Following the same lines, it is straightforward to deduce similar behavior for Gaussian approximations of test statistics.

Typically, the exact test statistic for ED, which follows the Chi-square distribution with N_s degrees of freedom under both H_0 and H_1, is approximated by the Gaussian distribution based on *Central Limit Theorem*, and hence, the validity of

Table 3.1: Comparison of exact and approximate closed-form expressions for P_d and P_f.

Metric	Distribution	Exact closed-form expression	Approximate closed-form expression
P_f with $s(k)=0$	$n(k) \sim \mathcal{N}(0,\sigma_n^2)$	$P_f = Q_{\chi^2_{N_s}}\left(\frac{\lambda}{\sigma_n^2}\right)$ $=\frac{\Gamma(m,\frac{\lambda}{2\sigma_n^2})}{\Gamma(m)} \triangleq F_m\!\left(\frac{\lambda}{2\sigma_n^2}\right)$	$P_{f(app)} = Q\left(\frac{\lambda-\sigma_n^2 N_s}{\sigma_n^2\sqrt{2N_s}}\right)$
P_d with $n(k) \sim \mathcal{N}(0,\sigma_n^2)$	$s(k) \sim A$	$P_{dd} = Q_{\chi^2_{N_s}(\Omega)}\left(\frac{\lambda}{\sigma_n^2}\right)$ $=Q_m(\sqrt{N_s\gamma},\sqrt{\frac{\lambda}{\sigma_n^2}})$	$P_{dd(app)} =$ $Q\left(\frac{\lambda-\sigma_n^2 N_s(1+\gamma)}{\sigma_n^2\sqrt{2N_s(1+2\gamma)}}\right)$
	$s(k) \sim \mathcal{N}(0,\sigma_s^2)$	$P_{dn} = Q_{\chi^2_{N_s}}\left(\frac{\lambda}{\sigma_t^2}\right)$ $=\frac{\Gamma(m,\frac{\lambda}{2\sigma_n^2(1+\gamma)})}{\Gamma(m)}$	$P_{dn(app)} =$ $Q\left(\frac{\lambda-\sigma_n^2 N_s(1+\gamma_r)}{\sigma_n^2\sqrt{2N_s(1+2\gamma_r+\gamma_r^2)}}\right)$
	$s(k) \sim \mathcal{N}(A,\sigma_s^2)$	$P_{dn2} = Q_{\chi^2_{N_s}(\Omega_n)}\left(\frac{\lambda}{\sigma_t^2}\right)$ $=Q_m\left(\sqrt{\frac{N_s\gamma}{1+\gamma}}\,\sqrt{\frac{\lambda}{\sigma_n^2(1+\gamma)}}\right)$	$P_{dn2(app)} =$ $Q\left(\frac{\lambda-\sigma_n^2 N_s(1+\frac{\gamma}{1+\gamma_r})}{\sigma_n^2\sqrt{2N_s(1+2\frac{\gamma}{1+\gamma_r})}}\right)$

these Gaussian approximations is generally attributed to large N_s. This section focuses on random PU signal model and instead of focussing on only N_s, considers the SNR, as well as the targeted P_d for a given fixed P_f, to identify general conditions under which the ED test statistic can be approximated by a simple Gaussian.

Figures 3.8-3.10 compare the exact and approximate ROC curves for various values of N_s under different SNR conditions. These figures show that, in general, the exact and approximate curves converge for a larger value range of P_f when the number of observed samples, N_s, are increased. On the other hand, as lower P_f is targeted, the approximate curve starts diverging from the exact ROC. These observations point to the fact that the actual lower bound on N_s, for which the exact test statistic may be replaced by its Gaussian counter part, depends on the SNR and the target performance in terms of minimum required P_d and maximum
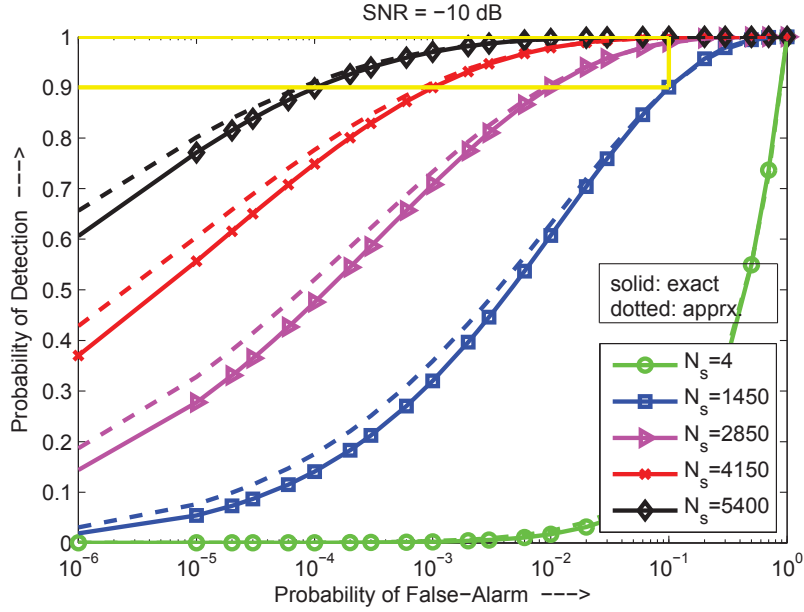
Figure 3.8: Comparison of exact and approximate ROC for various values of N_s at $-10\ dB\ SNR$.

allowed P_f. For $-10\ dB\ SNR$, Figure 3.8 shows that the approximate ROC does not diverge much from exact ROC even for P_f as low as 10^{-4} and for samples as few as 4. However, in order to simultaneously achieve $P_d > 90\%$ and $P_f < 10\%$, large number of samples are generally required under low SNR. For example, to achieve, $P_d > 90\%$ and $P_f < 10\%$, at $-10\ dB\ SNR$, minimum of 1450 samples are required as evident from Figure 3.8. Thus, for $SNR < 0\ dB$, when N_s is selected to guarantee typical sensing performance i.e. $P_d > 90\%$ and $P_f < 10\%$ (shown by a box in figure), approximate expressions for P_d and P_f, remain unconditionally valid with negligible error between probabilities evaluated using exact and approximate expressions.

For $SNR \geq 0\ dB$, the validity of approximate test statistic at a given SNR for fixed P_f becomes a function of both number of observed samples, N_s, and operative
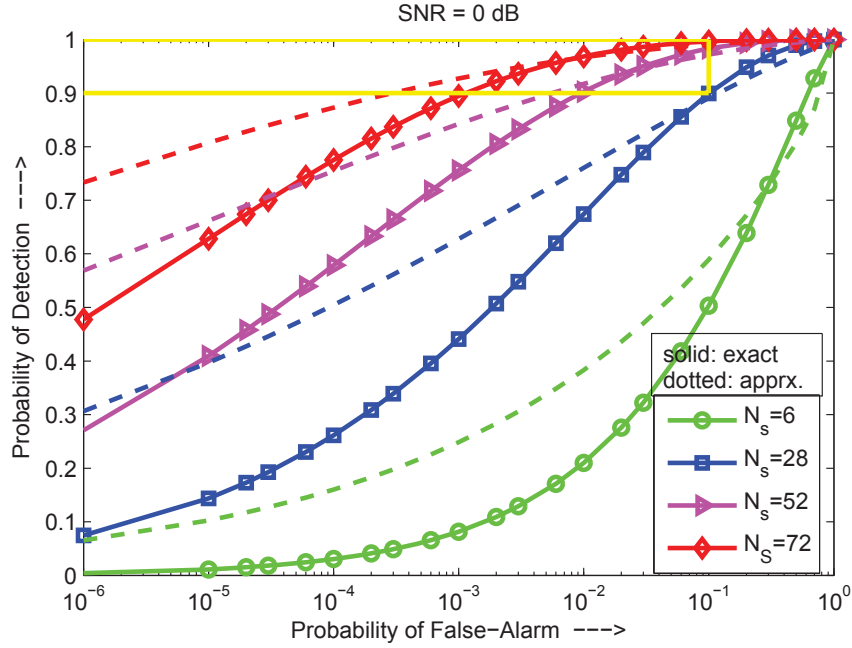
Figure 3.9: Comparison of exact and approximate ROC for various values of N_s at 0 dB SNR.

P_d range. In general, for a given SNR and N_s, approximate expression of P_d yields lower value than the exact probability of detection when the required P_f is higher than a certain value, called *cross-over* false alarm probability. *Cross-over* point represents the point of intersection of exact and approximate ROC curve and is identified by *cross-over* detection and false alarm probabilities, COP_d and COP_f respectively. For $P_f < COP_f$, approximate evaluation of P_d gives optimistic results where the approximate P_d is reported higher than the actual (exact) P_d. The *cross-over* detection and false alarm probabilities depend on the SNR and N_s. In general, for a fixed SNR, COP_f decreases while COP_d increases with increasing N_s. Similar behavior is observed by increasing SNR for fixed N_s. This is evident from Figure 3.9 and Figure 3.10 which compare the exact and approximate ROC for $N_s = 6, 28, 52, 72$ and $N_s = 4, 12, 20, 28$, which are the exact minimum number
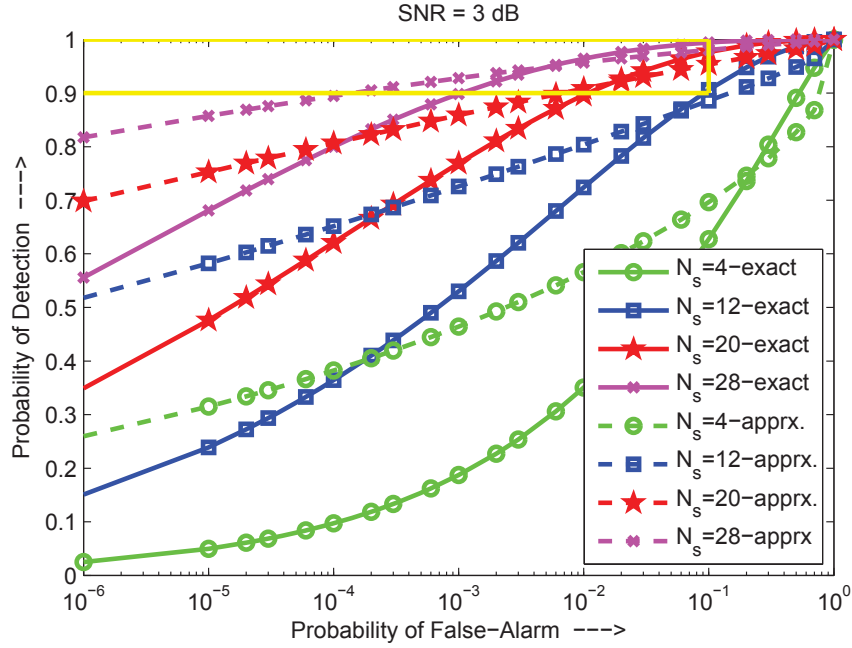
Figure 3.10: Comparison of exact and approximate ROC for various values of N_s at 3 dB SNR.

of samples that guarantee $P_d > 90\%$, for $P_f = 0.5, 0.1, 0.01, 0.001$, at SNR of 0 dB and 3 dB, respectively.

The validity range of Gaussian approximations is defined in terms of exact minimum and maximum probability of false alarm for which the absolute error (the difference between the exact P_d and its approximated value) remains less than 10^{-2} while maintaining $P_d > 90\%$. The results shown in Figure 3.9 and 3.10 are tabulated in terms of *Cross-over* probabilities and validity range of Gaussian approximations in Table 3.2.

The absolute approximation error in P_d is shown against the number of samples, N_s, in Figure 3.11 wherein the dips correspond to *cross-over* points. The optimal range of N_s, which offers negligible approximation error for given SNR and P_f, is also highlighted in this figure along with the corresponding P_d. The results

Table 3.2: *Cross-over* probabilities and validity range of Gaussian approximations for $P_d > 90\%$.

SNR (dB)	P_f	Min. N_s	COP_f	COP_d	Validity range			
					Min. P_f	P_d corresponding to Min. P_f	Max. P_f	P_d corresponding to Max. P_f
0	10^{-2}	52	2.1×10^{-2}	0.935	1.2×10^{-3}	0.912	6.0×10^{-2}	0.972
	10^{-3}	72	8.5×10^{-3}	0.964	3.4×10^{-3}	0.940	1.0×10^{-1}	0.995
3	10^{-2}	20	1.7×10^{-2}	0.919	1.1×10^{-2}	0.900	2.7×10^{-2}	0.938
	10^{-3}	28	5.3×10^{-3}	0.949	2.7×10^{-3}	0.931	1.2×10^{-2}	0.968

indicate that, similar to low SNR case, if we select N_s to guarantee $P_d > 90\%$ and $P_f < 10\%$, the approximation error always remains within tolerable limits ($< 10^{-2}$) even at high SNR. The Gaussian approximations only become invalid when we try to achieve very low P_f using very few samples at high SNR. However, since the detection probability also falls below acceptable limits in such scenarios, therefore, we may deduce that for all practical cases, Gaussian approximations remain valid.

The above discussion leads to the fact that the most critical thing to know is the lower bound on required number of samples, N_s, and SNR, γ, to meet given detection requirements in terms of P_d and P_f. The exact relationship between the required number of samples, N_s, and the quality of received signal in terms of SNR to meet given fixed P_f and target P_d was derived in Section 3.3.5. The following section makes use of approximate P_d and P_f expressions to derive closed-form
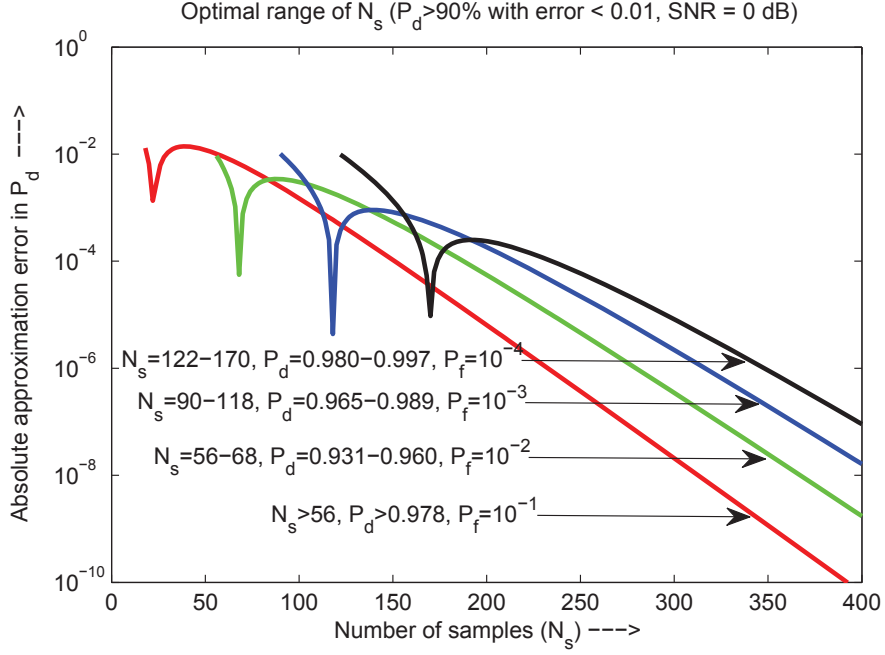
Figure 3.11: Optimal range of N_s targeting $P_d > 90\%$ with approximation error $< 10^{-2}$ for 0 dB SNR.

relationship between N_s and SNR.

3.4.4   An Approximate Lower Bound on N_s

The lower bound on N_s can be obtained by putting the value of λ from (3.34) into approximate expression of P_d given by (3.37) for deterministic PU signal model or in (3.40) for random PU signal model. The appropriate detection threshold to ensure given fixed P_f can be found from (3.34) as:

$$\lambda = \sigma_n^2 N_s \left(1 + \sqrt{\frac{2}{N_s}} Q^{-1}(P_f) \right).$$

(3.44)
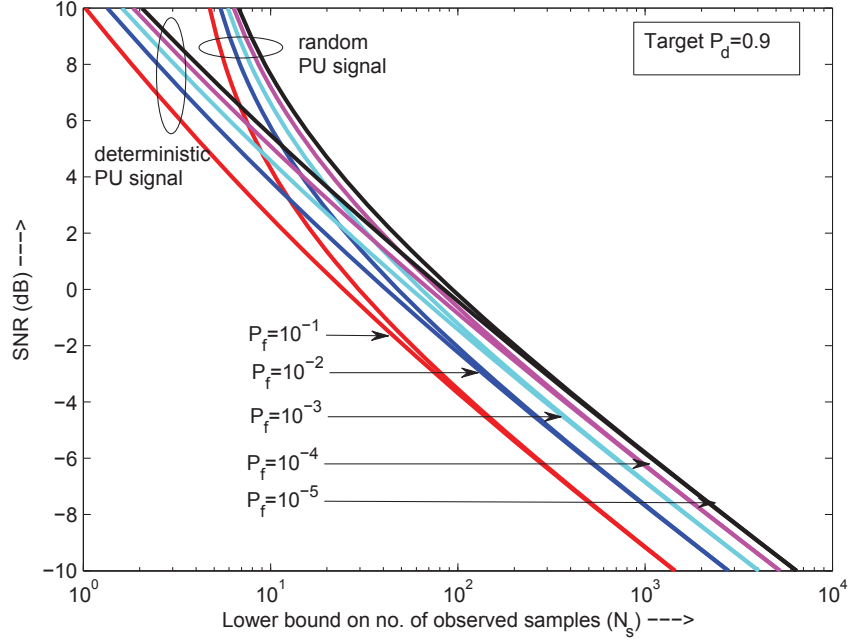
Figure 3.12: Comparison of approximate lower bound on N_s and required SNR for $P_d = 0.9$ for deterministic and random PU signal model.

If at the same time, we have to satisfy certain minimum P_d, then (3.37) should also yield the same λ:

$$\lambda = \sigma_n^2 N_s \left(1 + \gamma + \sqrt{\frac{2}{N_s}(1 + 2\gamma)} Q^{-1}(P_{dd}) \right).$$ (3.45)

Equating (3.44) and (3.45) and solving for N_s, we get

$$N_s = 2 \left(\frac{Q^{-1}(P_f) - \sqrt{1 + 2\gamma} Q^{-1}(P_{dd})}{\gamma} \right)^2.$$ (3.46)
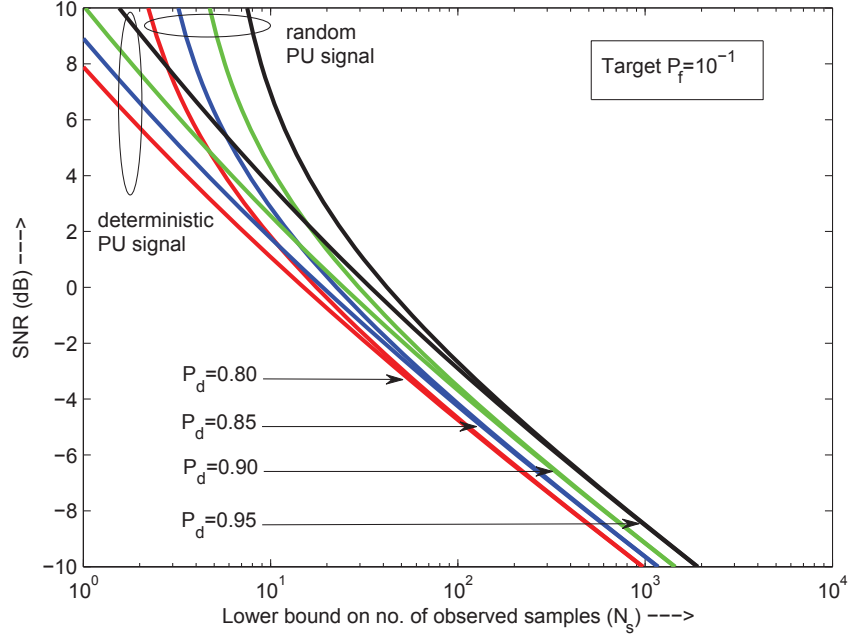
Figure 3.13: Comparison of approximate lower bound on N_s and required SNR for $P_f = 0.1$ for deterministic and random PU signal model.

Similarly, Equating (3.44) with λ obtained from (3.40), N_s for random PU signal model is given by:

$$N_s = 2 \left(\frac{Q^{-1}(P_f) - Q^{-1}(P_{dn})}{\gamma} - Q^{-1}(P_{dn}) \right)^2. \qquad (3.47)$$

The above equations show that number of samples, N_s, required to achieve the desired detection probabilities is proportional to SNR^{-2} and hence any targeted detection performance is possible at SNR as low as desired by increasing the number of observed samples. This is shown for both deterministic and random PU signal models in Figure 3.12 for target P_d of 90% and in Figure 3.13 for target $P_f = 10\%$. The two figures also indicate that deterministic and random PU signal

91

models converge for low SNR case or equivalently for large sample values while they differ in high SNR scenario. It is important to point out that these results do not take into consideration any uncertainties in the noise variance estimate and are valid only under non-fading channel conditions.

3.5   Energy Detection Based Cooperative SS

The analysis in this chapter assumes that the channel gain remains constant (non-fading environment) throughout the sensing duration. In practice, multipath fading and shadowing severely deteriorate the performance of spectrum sensing [76], [122]. However, the sensing reliability can always be improved by exploiting the multi user diversity in CRNs, through cooperative detection [20], [21]. This is evident from Figure 3.14, which shows the complementary ROC of ED under Rayleigh fading and Log-normal shadowing (with typically observed 6 dB spread, time-bandwidth product = 5, and average received SNR of 10 dB), and highlights sensing performance enhancement through cooperation, in a CRN with 10 CRs [123].

A comprehensive survey of cooperative spectrum sensing (CSS) schemes [112] identifies ED as the most popular sensing technique owing to its simplicity and non-coherent/blind nature. The significance of ED is also evident from the fact that most of the cooperative sensing techniques reported in recent literature [32], [129], [130] employ ED for local detection of primary transmissions. In cooperative detection, combining the local observations from spatially distributed CRs
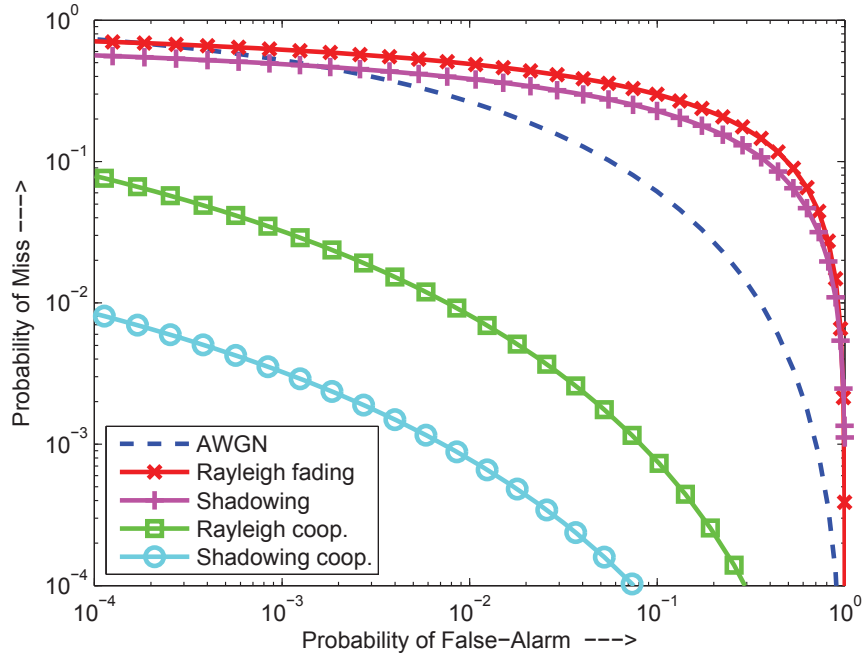
Figure 3.14: Performance degradation of ED under fading/shadowing and its mitigation through cooperation.

provides a more reliable spectrum awareness but requires additional processing (which takes time and consumes energy) of the sensing information to reach a unified global decision on PU activity. ED, being computationally very simple, proves to be a suitable building block of a cooperative detection framework as it offers significant *cooperative gain* with minimum *cooperation overhead*. This is evident from the Figure 3.15 which shows the complementary ROC curve of ED based CSS employing *decision fusion* and *data fusion*. For decision fusion, we reach a global decision by combining 1-bit local sensing results using OR-rule. In comparison, all the locally observed energies are added up equally (equal gain combining (EGC)), in the data fusion approach, to form the global test statistic which is then compared with global threshold. The performance comparison is

based on given constraint on false-alarm rate at 10 dB SNR for the time-bandwidth product of 5 for 20 cooperating CRs [131].
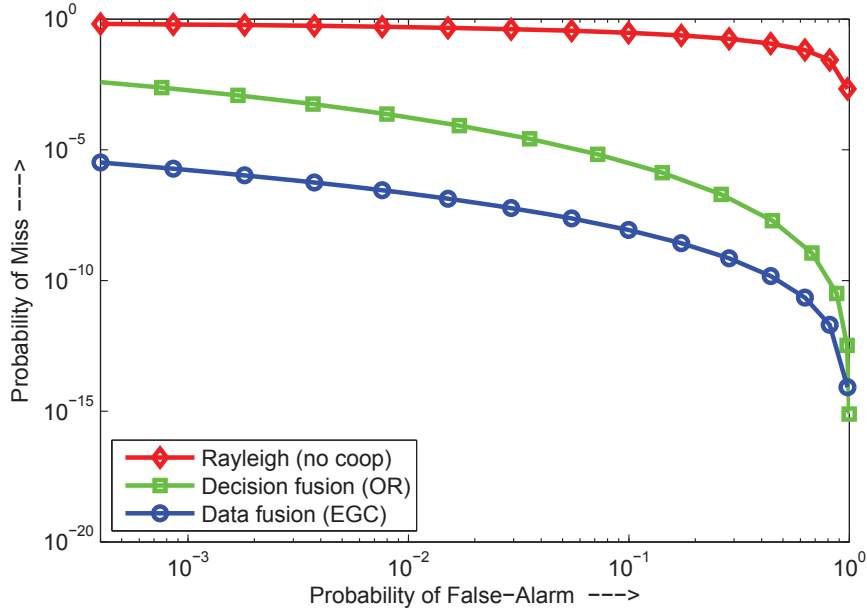
Figure 3.15: Sensing performance of ED based cooperative spectrum sensing using decision and data fusion.

Results in Figure 3.15 show that even 1-bit decision fusion (incurring minimum cooperation overhead in terms of control channel bandwidth) of ED based local sensing provides miss-detection rate below 0.00001 at $P_f = 0.1$ and it remains < 0.01 (detection rate $> 99\%$) even when P_f is decreased up to 0.0001. This indicates that the ED based CSS can yield high throughput efficient cognitive radio networks by significantly decreasing the average false alarm rate per CR for the given probability of detection constraint. The achievable average false alarm probability per CR for different number of cooperating CRs is shown in Figure 3.16. The figure compares the selfish and social welfare (altruistic) cooperation approaches by considering a game-theoretic cooperation model where targeted

94

probability of detection is set at 99% and cooperation overhead in terms of time spent in combining local sensing decisions is taken to be 0.001ms [53].
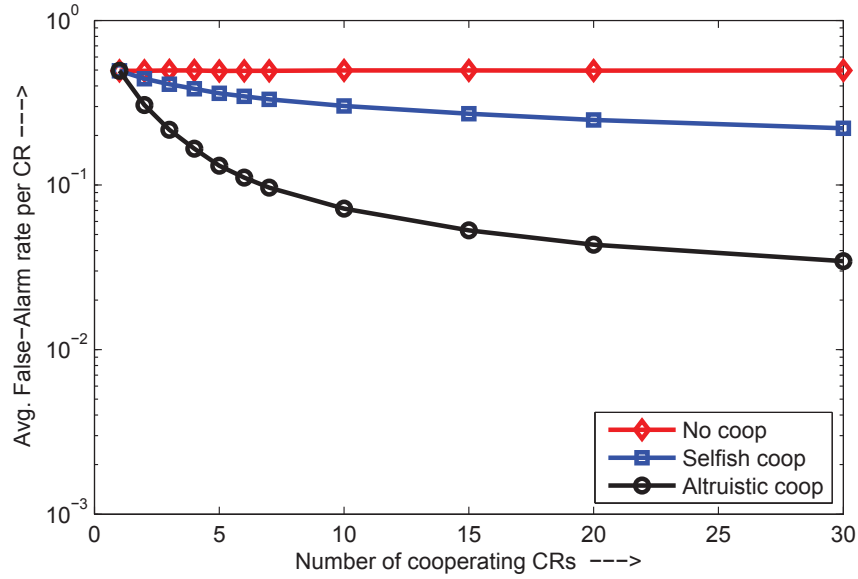
Figure 3.16: Average false-alarm rate per CR for different number of cooperating CRs in ED based CSS using selfish and altruistic cooperation.

All these factors characterize ED with less robustness and low accuracy/reliability, however, in spite of these disadvantages, ED remains the most common detection approach because of its low complexity, semi-blind nature and due to the fact that the performance degradation can be mitigated by the diversity gain obtained through cooperation among the CRs.

CHAPTER 4

THROUGHPUT-EFFICIENT SPECTRUM ACCESS IN CENTRALIZED CRNS

Although spectrum sensing plays a vital role in realizing throughput-efficient spectrum access in cognitive radio networks, after the FCC ruling [56] which obviated the SS requirement in CRNs, there has been a dire need to explore stand-alone efficient SA schemes where SUs do not solely rely on SS performance for their throughput improvement. In this regard, this chapter addresses the problem of efficient spectrum access in CRNs under the assumption that available spectrum opportunities are known a priori. A centralized cognitive radio network is considered and a game-theoretic approach is used to dynamically share the available spectrum resources among competing SUs. A throughput-efficient network partitioning problem is formulated as a coordinated CF game with externalities and

an efficient CF algorithm is proposed to reach a Nash-stable network partition with the objective of improving the network throughput. Furthermore, a closed form expression of the optimal bandwidth allocation for any given network partition is derived. Performance analysis shows that the proposed coalition formation algorithm with optimal bandwidth allocation provides a substantial gain in the network throughput over existing coalition formation techniques as well as the simple cases of singleton and grand structures.

The organization of this chapter is as follows: Section 4.1 introduces the existing work that uses coalitional game-theoretic framework for efficient spectrum access, and highlights the main contributions of the chapter. Section 5.2 introduces the network model and identifies the two avenues that have been explored to enhance the achievable throughput of cognitive radio networks. The optimal BW allocation for a given network partition is presented in Section 5.3 while the algorithmic details of CF process to reach a throughput-efficient Nash-stable network partition are discussed in Section 5.4. The convergence speed improvement of the proposed coordinated CF algorithm is achieved through two initialization algorithms proposed in Section 4.5. Performance analysis of the CF algorithms is provided in Section 4.6.

4.1 Introduction

Coalitional game-theoretic tools [66] have been explored for efficient spectrum access in cognitive radio networks from different viewpoints [54], [132]-[134]. How-

ever, the contribution of this chapter differs from the existing work in number of ways. First, most of these works do not consider the network throughput as the objective function. Furthermore, the role of externalities (effect of SUs outside the coalition) in CF process is often ignored. For instance, a generic rate allocation problem has been analyzed in [132] as a CF game in *characteristic form* (without considering the effect of externalities) with *transferable utility* which allows the coalition value (coalition sum-rate) to be arbitrarily apportioned among the coalition members. In contrast, this chapter aims at maximizing the secondary network throughput by forming disjoint coalitions such that the total available transmission BW is made available to each coalition, while this BW is *optimally* sub-divided into orthogonal bands within each coalition. Hence, the CF game is modeled in a *partition form* since the payoff (transmission rate) of each coalition member is affected by the interference from simultaneous transmissions of members of different coalitions over the same frequency band. Moreover, the proposed game has *non-transferable utility*, since the optimal BW allocation restricts the distribution of the coalition value among the coalition members.

The coalitional games in partition form were recently investigated in [54], and [133]. The authors in [54], have considered the joint spectrum sensing and access problems where the competing SUs shared the spectrum in chunks of pre-fixed/slotted BW (as defined by PU channels), while in [133], the available BW is proposed to be shared among competing SUs according to their channel gain ratios. Also in [134], the available spectrum for the secondary communications

98

is equally divided among the SUs. It is evident that these are not optimal BW allocation approaches from network rate perspective.

Furthermore, since distributed CF approaches suffer from prohibitively large information exchange [68] among the players proposing to form a coalition and sharing local channel state information (CSI), this problem is addressed here by considering a *coordinated* CF approach. The coordinated CF scheme devises a master controller node in the secondary network known as *secondary coordinator*. Since the objective is to optimize the overall network performance, the proposed CF algorithm is designed to be executed centrally at the SC, which would otherwise yield CF to be practically un-realizable specifically for time limited, power limited, and control channel BW limited networks.

The research contributions presented in this chapter are fundamentally different from the existing work from two perspectives: (1) In comparison to conventional approach where the available spectrum resources are shared in terms of channels of pre-fixed and equal BW, a continuous BW allocation among the coalition members is proposed and a closed form expression of rate optimal BW allocation is derived. (2) An efficient coordinated CF algorithm is developed for the secondary network throughput maximization by considering a CF game with externalities and NTU, and its convergence to a throughput-efficient Nash-stable network partition is analytically proved.

4.2 Network Model

A cognitive radio network with N secondary links is considered along with a centrally located secondary coordinator node that is assumed to have CSI between all the secondary transmitters and secondary receivers. The role of the SC node is only to manage the coalition formation and the BW allocation between the different secondary links. The total available BW for secondary access is considered to be W, and the channel between any of the secondary transmitters and any of the secondary receivers over this BW is assumed to follow a quasi-static flat fading model. A representative network model with a centrally located SC and randomly distributed ST-SR pairs in its coverage area, is illustrated in Figure 5.1.

The throughput-efficient network partitioning problem is addressed from two perspectives. First, frequency reuse of the available BW is proposed by partitioning the N links into a set of coalitions such that each coalition will be using the total available BW. Such partitioning would, on one hand, have the potential to increase the network rate because of reusing the BW, but would on the other hand cause interference between the different coalitions. Therefore, the choice of the partitioning structure would substantially affect the total achievable network rate, and hence this chapter develops a CF algorithm that can be used to reach the Nash-stable network partition. Second, since each coalition in the network partition will be using the total available bandwidth (W), the available BW is proposed to be optimally distributed among the coalition members based on the available CSI with the objective of maximizing the total network throughput. It
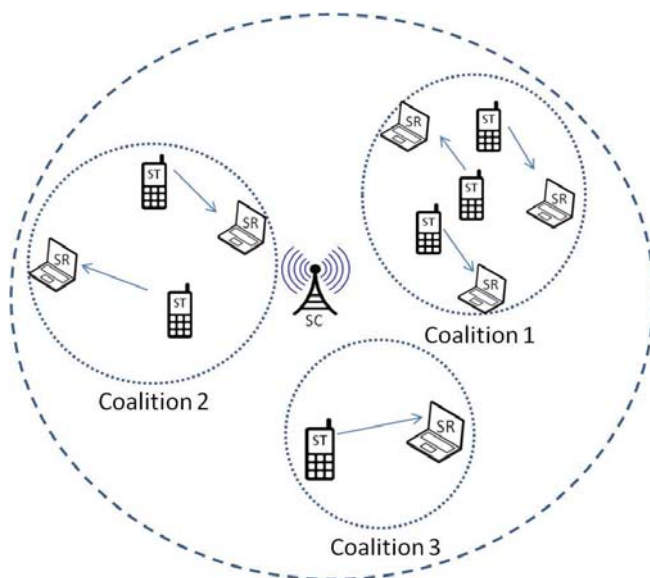
Figure 4.1: A representative centralized CRN model with SC and ST-SR pairs.

is important to highlight here that the two problems discussed above are coupled, which means that none of them can be solved without solving the other. This is because the coalitions can not be formed without evaluating the optimal rate of each coalition, and at the same time the optimal rate of each coalition depends on which players are inside this coalition and which ones are outside it. This renders the problem hard but interesting. First, the optimal BW allocation problem is solved for a given network partition, and then this optimal bandwidth allocation is exploited in the proposed coordinated CF algorithm.

4.3 Optimal Bandwidth Allocation

This section presents the optimal bandwidth allocation among the members of a coalition for a given network partition. Let the current network partition, at a certain time instant, be $\Pi = \{S_1, S_2, ..., S_{|\Pi|}\}$, where $|\Pi|$ is the number of disjoint

coalitions under network partition Π. In the system model under consideration, each of the $|\Pi|$ coalitions will use the total available bandwidth W. Consider Coalition $S_k \in \Pi$, with $|S_k|$ representing the number of members (links) in S_k. In the proposed terminology, m_i^k will refer to Member (Link) i of Coalition S_k while P_i^k will represent the transmission power of this member. Each member m_i^k of S_k will be allocated a fraction μ_i^k of the total bandwidth, where $\sum_{i=1}^{|S_k|} \mu_i^k = 1$. The total interference power affecting the bandwidth W being used by Coalition S_k is the sum of all received power from all members in all other coalitions. For simplicity of the analysis, the interference affecting the band $\mu_i^k W$ being used by Member m_i^k is evaluated as an average interference affecting this band which is a fraction μ_i^k of the total interference power affecting the total bandwidth at the receiver of Link m_i^k, i.e.,

$$\bar{I}_i^k = \mu_i^k \sum_{l \neq k} \sum_{j=1}^{|S_l|} P_j^l |h_{ji}^{lk}|^2$$

$$= \mu_i^k I_i^k \tag{4.1}$$

where h_{ji}^{lk} is the channel between the transmitter of Link j in Coalition S_l and the receiver of Link i in Coalition S_k, and hence the total rate of Coalition S_k can be written as

$$\mathcal{R}^{S_k} = \sum_{i=1}^{|S_k|} R_i^{S_k} = \sum_{i=1}^{|S_k|} \mu_i^k W \log\left(1 + \frac{P_i^k |h_{ii}^{kk}|^2}{\mu_i^k (N_0 W + I_i^k)}\right). \tag{4.2}$$

In order to maximize the rate achieved by this coalition, the problem can be formulated as

$$\max_{\mu_i^k} \sum_{i=1}^{|S_k|} \mu_i^k W \log(1 + \frac{P_i^k |h_{ii}^{kk}|^2}{\mu_i^k (N_0 W + I_i^k)}),$$

$$\text{subject to} \sum_{i=1}^{|S_k|} \mu_i^k = 1 \text{ and } 0 \le \mu_i^k \le 1. \quad (4.3)$$

Using the Perspective property [135], and the concavity of the log function, it can be shown that this problem is concave, and hence the globally optimal solution is guaranteed to exist. In the following, a closed form for the optimal solution is derived:

The objective function of (5.3) can be written as

$$W \sum_{i=1}^{|S_k|} \mu_i^k \log(1 + \frac{x_i^k}{\mu_i^k}), \quad (4.4)$$

where $x_i^k = \frac{P_i^k |h_{ii}^{kk}|^2}{N_0 W + I_i^k}$. Since the log function is concave, and since $\sum_{i=1}^{|S_k|} \mu_i^k = 1$ and $0 \le \mu_i^k \le 1$, then the objective function can be upper bounded by

$$W \sum_{i=1}^{|S_k|} \mu_i^k \log(1 + \frac{x_i^k}{\mu_i^k}) \leqslant W \log(1 + \sum_{i=1}^{|S_k|} \mu_i^k \frac{x_i^k}{\mu_i^k}),$$

$$= W \log(1 + \sum_{i=1}^{|S_k|} x_i^k). \quad (4.5)$$

It is evident that this upper bound can be achieved by choosing

$$\mu_{i,\text{opt}}^k = \frac{x_i^k}{\sum_{m=1}^{|S_k|} x_m^k}, \quad (4.6)$$

Hence, the closed form expression of optimal rate $R_{i,opt}^{S_k}$ for any $i \in S_k$ is given by:

$$R_{i,\text{opt}}^{S_k} = \mu_{i,\text{opt}}^k W \log \left(1 + \sum_{m=1}^{|S_k|} x_m^k \right). \tag{4.7}$$

4.4 Coordinated Coalition Formation

The closed form expressions of the rate optimal BW allocation among coalition members are derived, in the previous section, under the assumption that a network partition is known apriori. In this section, the problem of finding a Nash-stable partition is addressed by answering the key question: In order to maximize the network throughput, should a player act in a non-cooperative manner and utilize the total bandwidth W or make a coalition with other player(s) and share the available BW with them. It is important to highlight that a non-cooperative approach (*singleton* coalitions: coalitions consisting of one player only) offers a total bandwidth of W Hz to each player and provides maximum spectrum re-use in the network at the cost of high interference among the players. On the other hand, *grand* coalition avoids the interference by sharing the available BW among all players with no spectrum re-use. For the considered throughput maximization problem, a balance needs to be maintained between interference avoidance and spectrum re-use, and the optimal network partition might neither be singleton nor grand [68]. However, finding an optimal network partition was shown to be NP-complete [72], as the number of possible partitions (given by Bell number B_N [73]) grows exponentially with the number of communication links, N, in

the network. Hence, there is a need to develop algorithms to organize links into non-overlapping coalitions that are at least stable, if not optimal. Furthermore, since the objective is to improve the system performance in terms of the overall network rate, the stable partition search is assumed to be executed centrally at the SC node by playing a *coordinated coalition formation game.*

4.4.1 Game Formulation

A throughput-efficient Nash-stable network partition is found by playing a CF game in *partition form* with *non-transferable utility* (NTU).

In the proposed CF game, the N secondary links act as the players of the game constituting the set $\mathcal{N} = \{1, 2, ..., N\}$. For any coalition $S_k \subseteq \mathcal{N}$, $S_k \in \Pi$, $\mathcal{V}(S_k, \Pi)$ contains only a single vector $\mathbf{v}(S_k, \Pi) \in \mathbb{R}^{|S_k|}$ where each element $v_i \in \mathbf{v}(S_k, \Pi)$ represents the payoff of player $i \in S_k$ and is given by its respective rate $R^{S_k}_{i,opt}$ as:

$$\mathcal{V}(S_k, \Pi) = \left\{ \mathbf{v}(S_k, \Pi) \in \mathbb{R}^{|S_k|} \mid v_i(S_k, \Pi) = R^{S_k}_{i,opt} \right\} \tag{4.8}$$

where, $R^{S_k}_{i,\mathrm{opt}}$ is given by (5.6). Since the value of any coalition S_k cannot be arbitrarily divided among the coalition members, the proposed CF game has a non-transferable utility. Furthermore, the CF game is in partition form since the payoff of every player $i \in S_k$; $R^{S_k}_{i,opt}$, depends not only on the players in S_k but also on the players in $\mathcal{N} \backslash S_k$ which interfere with $i \in S_k$.

In the next subsection, we describe the proposed algorithm to reach a Nash-stable network partition.

4.4.2 CF Algorithm

Let the current network partition be $\Pi = \{S_1, S_2, ..., S_{|\Pi|}\}$, where $|\Pi|$ is the number of coalitions under network partition Π. The sum of total rates of all ($|\Pi|$) coalitions under the partition Π; i.e. $\Re^\Pi = \sum_{k=1}^{|\Pi|} \mathcal{R}^{S_k}$, where $\mathcal{R}^{S_k}$ is the total rate of Coalition S_k and is defined in (2), represents the network rate when partition Π is in place. Hence, the achievable throughput by the cognitive radio network strongly depends on how the secondary links are organized into coalitions.

The proposed CF algorithm is summarized in Table 4.1. The algorithm is initialized with a non-cooperative setup (exploiting full frequency re-use) where the initial network partition Π_{init} is composed of N singleton coalitions as: $\Pi_{init} = \{\{1\}, \{2\}, ..., \{N\}\}$ and $\Re^{\Pi_{init}}$ is calculated as the initial network rate. The algorithm consists of two phases and goes sequentially, in a round robin fashion, over all players $i \in \mathcal{N}$ to examine which *action*, a player can take to improve the total network rate. The *action space* of player i is defined as: $A_i = \{\text{stay}, \text{switch}\}, \ \forall \, i \in \mathcal{N}$. Hence, a player i can *stay* in its current coalition with associated partition Π or it may decide to *switch* to another coalition (which might even be an empty coalition ϕ, which means that a player may decide to leave and act as a *singleton*) leading to a new network partition $\acute{\Pi}$. In this way, the proposed switch operation updates the partition structure by either keeping the same number of coalitions in the network partition or increasing/decreasing the number of coalitions by only 1, and hence, provides a mechanism to make a transition from one network partition to another. Here, it is important to point

Table 4.1: Proposed CF algorithm designed for centralized CRN.

Algorithm: CF algorithm is executed centrally at SC node where, in each round, the algorithm goes sequentially over all players $i \in \mathcal{N}$.

Initialization:
Initial partition: $\Pi_{init} = \{\{1\}, \{2\}, ..., \{N\}\}$. Initial rate: $\Re^{\Pi_{init}}$.
The two phases of proposed CF algorithm:
    Phase 1: Starting from current partition Π (at the beginning of all time, $\Pi = \Pi_{init}$) and based on action space A_i of player i, the algorithm iterates over all players $i \in \mathcal{N}$ to find a set of all partitions $\mathcal{P}_\Pi$ reachable from Π via one switch operation by any of the players.
    Phase 2: $\Pi^* \in \mathcal{P}_\Pi$ giving the maximum network rate is identified and the transition $\Pi \to \Pi^*$ is made provided $\Re^{\Pi^*} > \Re^{\Pi}$.

The algorithm converges to a throughput-efficient, stable, final network partition Π_f, if, after iterating over all the players $i \in \mathcal{N}$, no transition is made; i.e. every player prefers to *stay* in its current coalition.

out that, unlike existing CF algorithms [54, 55], wherein a player $i \in S_k$ arbitrarily selects a coalition S_l to investigate the possibility of performing a switch operation and it switches to S_l if a pre-defined switch rule is satisfied, here, a two-phase centralized CF algorithm is proposed that examines all switch/stay possibilities of all the players, at each CF round, and then perform the *action* that would maximize the network throughput in this round. In **phase one**, at each CF round, all the *feasible partitions* $\mathcal{P}_\Pi$, which can be reached from Π via only one switch operation by any one player in the network, are evaluated in terms of achievable network rates. In **phase two**, the network partition $\Pi^* \in \mathcal{P}_\Pi$ giving the maximum network rate is identified and the transition from partition Π to the new partition Π^* is executed only if the network throughput achieved under partition Π^*; i.e., $\Re^{\Pi^*}$, is more than the current network rate $\Re^{\Pi}$, otherwise, the current network partition Π is maintained. Formally the *transition rule* is defined as:

    Definition 2: Given the network partition $\Pi = \{S_1, S_2, ..., S_p\}$ of $\mathcal{N}$, a player $i \in \mathcal{N}$ decides to *switch* from its current coalition $S_k \in \Pi$ to join another coalition

$S_l \in \Pi \cup \phi$ for $l \neq k$, hence forming $\Pi^* = \{\Pi \backslash \{S_k, S_l\}\} \cup \{S_k \backslash \{i\}\} \cup \{S_l \cup \{i\}\}$

where $\Pi^* \in \mathcal{P}_\Pi$, according to the following **switch/transition rule**:

$$\Pi \rightarrow \Pi^* \Longleftrightarrow \Re^{\Pi^*} > \Re^{\acute{\Pi}} \ \forall \ \acute{\Pi} \in \mathcal{P}_\Pi \text{ and } \acute{\Pi} \neq \Pi^* \tag{4.9}$$

Each round of the proposed CF algorithm concludes with a single (best possible) switch/stay operation.

Remark 1: The algorithm reaches a stable throughput-efficient network partition Π_f, if, after iterating over all the players $i \in \mathcal{N}$, no transition is made; i.e. each player prefers to stay in its current coalition.

Remark 2: The proposed CF algorithm is repeated periodically throughout the network operation to handle environmental changes such as mobility or joining/leaving of players.

4.4.3 Convergence and Throughput Efficiency of Final Network Partition

For any current network partition Π, the proposed switch rule ensures that in each round of the CF algorithm, the switch operation compares all possible partitions in $\mathcal{P}_\Pi$ and, if executed, always results in a new network partition $\Pi^* \in \mathcal{P}_\Pi$ with increased network throughput (see Equation 4.9). This guarantees oscillation avoidance, which means that the CF algorithm cannot go back to an already visited network partition. Furthermore, for a finite number of secondary links N, the number of possible partitions is also finite (given by Bell number B_N [73]), which

guarantees that the CF algorithm always converges to a stable throughput-efficient network partition Π_f after finite number of rounds/iterations. The throughput efficiency of this resulting network partition Π_f is evident from the fact that the network throughput is increased in each round of the CF algorithm after every switch operation. As a result, the proposed algorithm converges to a final network partition Π_f which offers the throughput that cannot be further increased by making transition to any partition that belongs to $\mathcal{P}_{\Pi_f}$, and hence partition Π_f is a *Nash-stable* partition.

4.5 Speed-Improved CF Algorithms With Initialization

This section presents an improvement over the proposed CF algorithm in terms of its convergence speed by introducing a heuristic approach for suitable initialization of the coordinated CF process. Since, the proposed CF algorithm is designed to be executed centrally at the SC, and since the convergence speed strongly depends on the initial network partition Π_{init}, the available CSI between all ST-SR pairs is proposed to be exploited at SC and two heuristic algorithms for CF initialization are presented: (1) Init-CF-1 and (2) Init-CF-2. In these two algorithms, instead of starting the CF process in a singleton state SS: $\Pi_{init} = \{\{1\}, \{2\}, ..., \{N\}\}$ or in a grand state GS: $\Pi_{init} = \{1, 2, ..., N\}$, the relative interference at the receiver of each link in the network, from all other links, is observed and the randomly

distributed links are arranged in such a way that the links with maximum interference between each other make a coalition. The two Init-CF algorithms are summarized in Table 4.2 and explained in following subsections.

4.5.1   Init-CF-1

The first initialization approach is based on the cumulative interference observed at the receiver of each communication link in the network. The signal to cumulative interference ratio (SCIR) is evaluated for all links and all those links in the network at which $SCIR < \lambda$, where λ represents an arbitrary threshold value of SCIR, are identified as *weak links*. The link offering maximum interference to a weak link is identified as a *dominant interfering link*. Finally, weak links are paired with dominant interfering links. In this way, each weak link, for which the cumulative interference power exceeds $1/\lambda$ times its received signal power, makes a coalition with the link offering it the maximum interference among all.

4.5.2   Init-CF-2

In the second variant of the initialization algorithm, termed as, Init-CF-2, *weak links* are defined on the basis of individual (rather than cumulative) interference observed at the receiver of each communication link in the network. A link is considered *weak*, if the observed interference (from any one link) at its receiver exceeds an arbitrary threshold value, κ. Finally, each weak link makes coalition with its *dominant interfering link*.

Table 4.2: Proposed initialization algorithms for centralized CF.

CF initialization: The coordinated CF process may be initialized with any of the two proposed Init-CF algorithms to accelerate the convergence of CF algorithm to a Nash-stable network partition.

The two proposed Init-CF algorithms:
    Init-CF-1:

1. Identify all *weak links*: $SCIR_i < \lambda$.

2. Pair *weak links* with their *dominant interfering links*.

3. A *weak link* that also happens to be a *dominant interfering link* for some other *weak link(s)*, may form a coalition with its *dominant interfering link* and with the *weak link(s)* that consider it as a *dominant interfering link*.

    Init-CF-2:

1. Identify all *weak links*: Interference from any single link $> \kappa$.

2. Pair *weak links* with their *dominant interfering links*.

3. A *weak link* that also happens to be a *dominant interfering link* for some other *weak link(s)*, may form a coalition with its *dominant interfering link* and with the *weak link(s)* that consider it as a *dominant interfering link*.

CF initialization is invoked at the beginning of the CF process and provides a suitable initial network partition, Π_{init} comprising of disjoint coalitions of interfering links based on the operating channel conditions.

Therefore, the two initialization algorithms differ in the definition of weak links. However, once a weak link is identified, it is paired with its dominant interfering link. It is important to point out here that the two initialization algorithms organize the randomly distributed links into disjoint coalitions; i.e. each link is a member of only one coalition. As a consequence, a weak link that also happens to be a dominant interfering link for some other weak links, may form a coalition with its dominant interfering link and with the weak links that consider it as a dominant interfering link. For example, if link 1, 2 and 4 are identified as weak links in the network of 5 links, with link 1 experiencing maximum interference from link 3, link 2 experiencing maximum interference from

111

link 4 and link 4 experiencing maximum interference from link 5, the emerging initial network partition is $\Pi_{init} = \{\{1,3\}, \{2,4,5\}\}$, where links 2, 4 and 5 make a single coalition since link 5 gives high interference to link 4 and link 4 gives high interference to link 2, while, link 2 does not interfere with link 4 or link 5, and link 4 does not interfere with link 5.

Appropriate values for λ and κ, can be found through simulation for given number of links and operating average direct link SNR. The achievable improvement in the convergence speed of the proposed CF algorithms with initialization (measured in terms of the number of CF rounds required to reach a final Nash-stable throughput efficient network partition) is evaluated in Section 4.6.4 for different values of λ and κ.

4.6   Performance Analysis

This section analyzes the performance of the proposed centralized CF algorithm by comparing the average network rate (bits/sec) with two benchmark network partitions: (1) Non-cooperative solution comprising of all singleton coalitions and (2) Fully cooperative solution resulting in a single grand coalition. The total available bandwidth W for the secondary access is taken to be 5 MHz. All the channels are assumed to follow a quasi-static Rayleigh flat fading model, and hence the received signal power, interference power and signal to noise ratio (SNR) are exponentially distributed, and the results are averaged over $100,000$ channel realizations. The transmit power P_i and noise power spectral density

112

(N_0) are normalized to 1, and their effects are included in the channel coefficients. The mean of the interference power among the neighboring links is assumed to be uniformly distributed between $0\ dB$ and $10\ dB$, while relatively lower interference, with means uniformly distributed between $-10\ dB$ and $-5\ dB$, is assumed to be originating from far away links.

4.6.1 Average Network Throughput Comparison With Slotted BW Allocation and Distributed CF Approaches
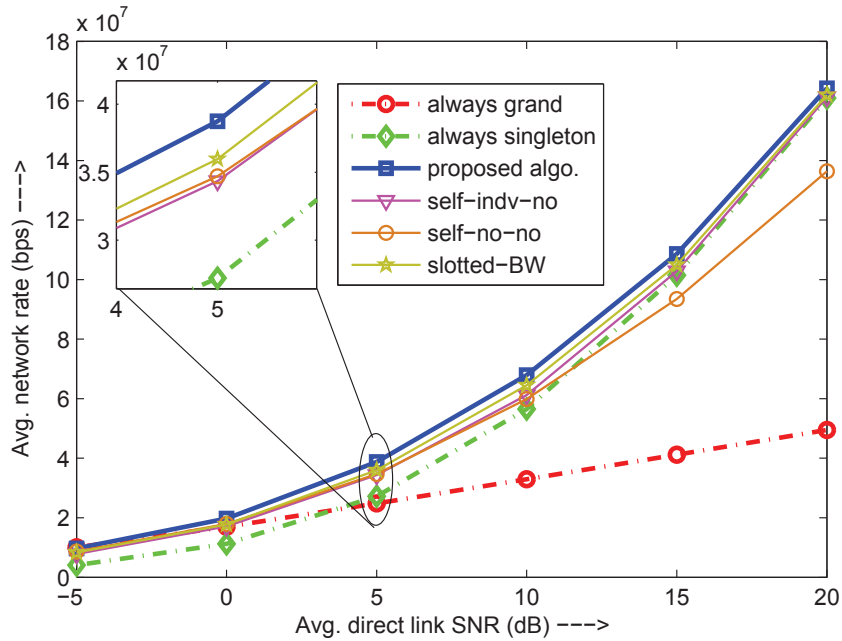
Figure 4.2: Average network rate comparison with conventional distributed CF with optimal BW and centralized CF with slotted BW allocation for 10 links.

Figure 4.2 highlights the average network throughput improvement offered by the proposed CF algorithm with optimal BW allocation over the cases of always singleton/grand in addition to two schemes popularly used in literature: (1)

when the spectrum is shared among competing players in the form of channels of pre-fixed BW (*slotted* channels) [53], and (2) when CF is based on the selfish preferences of players [54], [55]. It is worth noting that all the previous works [53], [54], and [55] consider the joint optimization of sensing time and secondary transmission rate, and hence their results cannot be compared directly to ours. However, Figure 4.2 shows the average network throughput improvement offered by the proposed CF algorithm over *slotted* BW allocation and over selfish CF approaches applied to our network model. The two selfish CF algorithms compared are: (1) *self-no-no* as proposed in [55] where the switch rule can be viewed as a *selfish* decision made by a player to move from its current coalition to a new coalition, regardless of the effect of its move on other players and (2) *self-indv-no* as given in [54] where a player decides to switch to a new coalition if it can strictly improve its own rate, without decreasing the rate of any member of the new coalition.

The simulation results indicate that at very low/high average direct link SNR values, the proposed CF algorithm converges to grand/singleton structure, respectively, while for moderate SNR values ($0\ dB < SNR < 15\ dB$), it provides substantial network rate gain over always singleton/grand structure. For example, at $SNR = 5\ dB$, the proposed CF algorithm offers 42.5% more network rate as compared to always singleton/grand structure. Furthermore, at $SNR = 5\ dB$, the proposed CF algorithm provides 15% throughput improvement when compared with selfish CF algorithms (*self-no-no* and *self-indv-no*) with optimal BW

allocation and 10.5% throughput improvement over using *slotted* BW allocation in the proposed CF algorithm.

4.6.2 Effect of Number of Links on Average Network Throughput
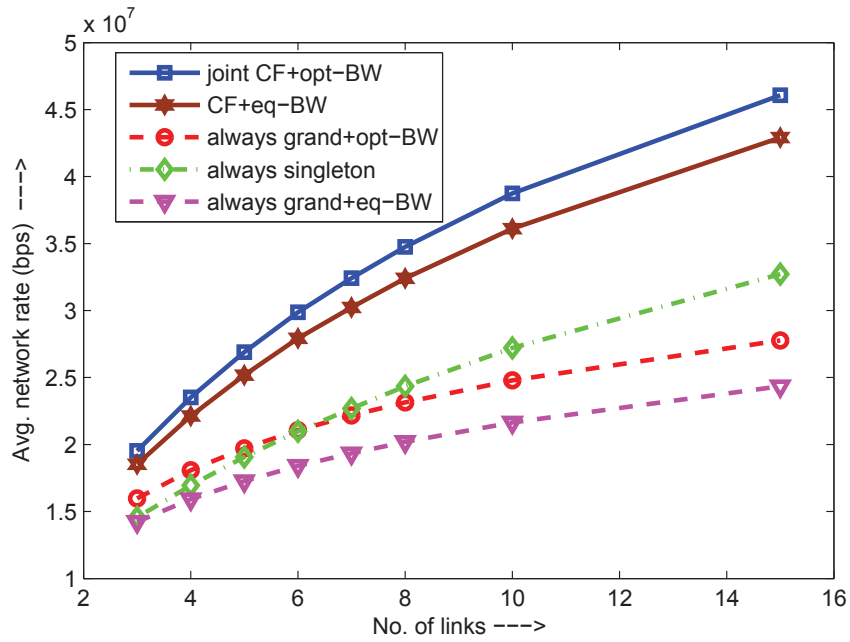
Figure 4.3: Average network rate improvement by using joint CF + BW allocation algorithm for different network sizes with average direct link SNR = 5 *dB*.

Figure 4.3 shows the effect of increasing the network size on the achievable network throughput gains at an average direct link $SNR = 5\ dB$. These results indicate that the gain in the average network throughput, offered by the proposed algorithm, increases as the network size increases. Furthermore, Figure 4.3 quantifies separately the gains achieved by the proposed CF algorithm and by the optimal BW allocation. Our results show that for $N = 10$ links, the proposed CF algorithm with equal BW allocation offers 32.8% more average network through-

put, as compared to always singleton case, which is further increased by 9.7%, reaching up to 42.5% when the optimal bandwidth allocation is employed.

4.6.3 Average Coalition Size and Number of Coalitions
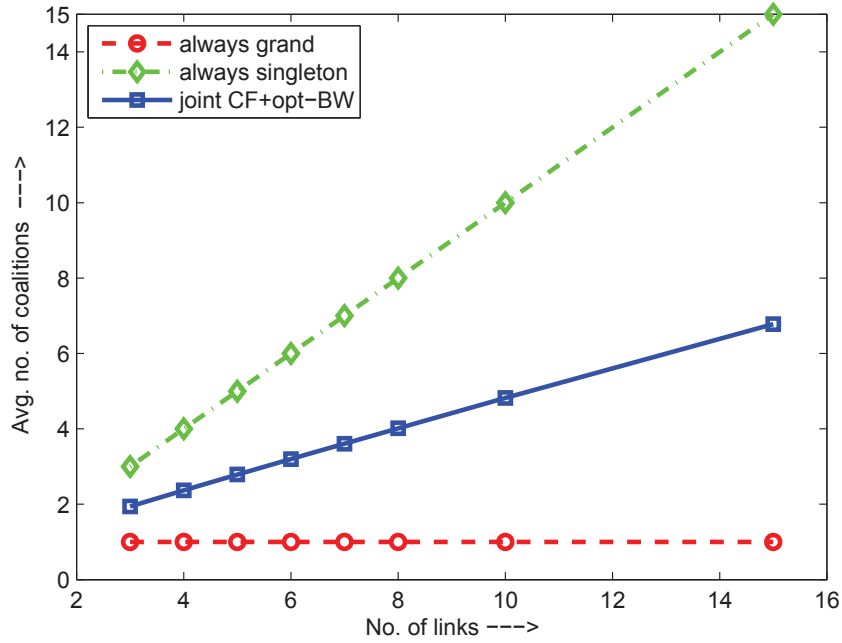
Figure 4.4: Average number of coalitions for different network sizes with average direct link SNR $=$ 5 dB.

In comparison to grand/singleton coalitions which always result in a fixed known number of coalitions in the final coalition structure (grand: 1 coalition, singleton: N coalitions for N links) regardless of the observed SNR over the direct link, the proposed CF algorithm gives the Nash-stable final coalition structure which strongly depends on the average direct link SNR. In general it can be observed that for N links, the number of coalitions in the final coalition structure monotonically increases with the average direct link SNR starting from 1, i.e., grand coalition, at very low SNR to N, i.e., singleton, at very high SNR.

The final coalition structure which emerges from the proposed joint CF and optimal BW allocation algorithm is analyzed in terms of average number of coalitions in Figure 4.4. Focusing on moderate operating SNR, the final coalition structure is analyzed for different network sizes with average direct link $SNR = 5\ dB$ and it is found out that the average coalition size is 2 in the emerged stable coalition structure or equivalently it comprises of approximately $N/2$ coalitions, on average, as shown in Figure 4.4.

4.6.4 Convergence Speed Improvement and Computational Complexity Reduction Via CF Initialization

The proposed CF algorithm exploits the computational capabilities of the SC to converge to a final Nash-stable network partition. The convergence speed strongly depends on the initial network partition Π_{init} and average direct link SNR. The coordinated CF process may be initialized with any of the two proposed Init-CF algorithms to accelerate the convergence of CF algorithm to a Nash-stable network partition.

For a network size of $N = 10$ links, and for different interference thresholds, Figure 4.5 depicts the convergence speed when the coordinated CF process is augmented with the proposed initialization algorithms (Init-CF-1 and Init-CF-2). It also shows the convergence speed improvement over the CF algorithm initialized in a conventional singleton/grand state. The convergence speed is evaluated in terms of required number of CF rounds to reach a Nash-stable partition. It can
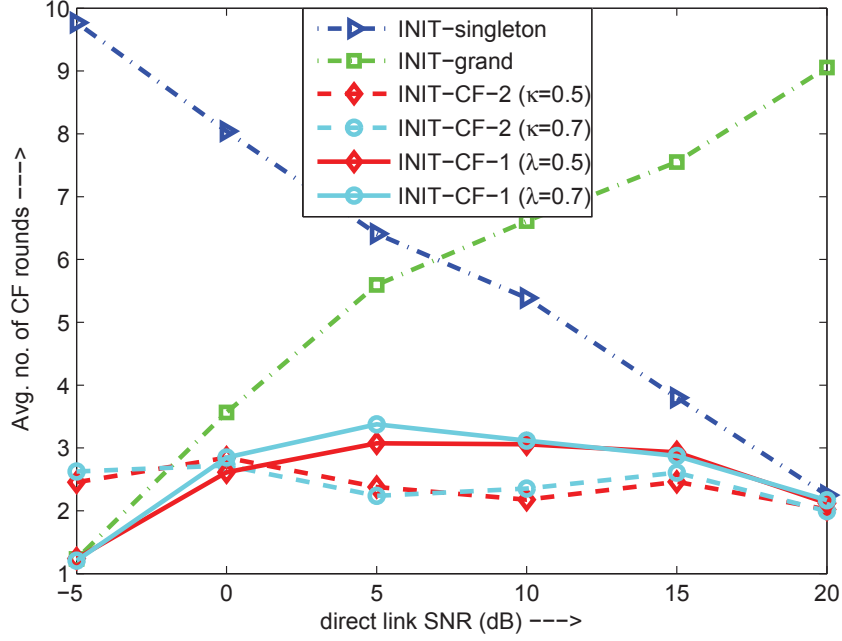
Figure 4.5: Average number of CF rounds before reaching a Nash-stable partition.

be seen from Figure 4.5 that for very low direct link SNRs, most of the links experience high interference and hence prefer to organize in a grand coalition. On the other hand, as the average direct link SNR is increased (relative to the interference), it is expected that the links would tend to operate as singleton. As a result, CF algorithm converges very fast to a Nash-stable partition when started from a grand state at low direct link SNR, while convergence speed decrease drastically with increasing direct link SNR. However, if the CF process is initialized in a singleton state, the CF algorithm takes a long time to converge at a low direct link SNR, while it converges very fast at a high direct link SNR. In comparison, the proposed CF initialization algorithms offer fast convergence over the wide operative range of direct link SNR.

Figure 4.6 shows the computational complexity of the proposed CF algorithm
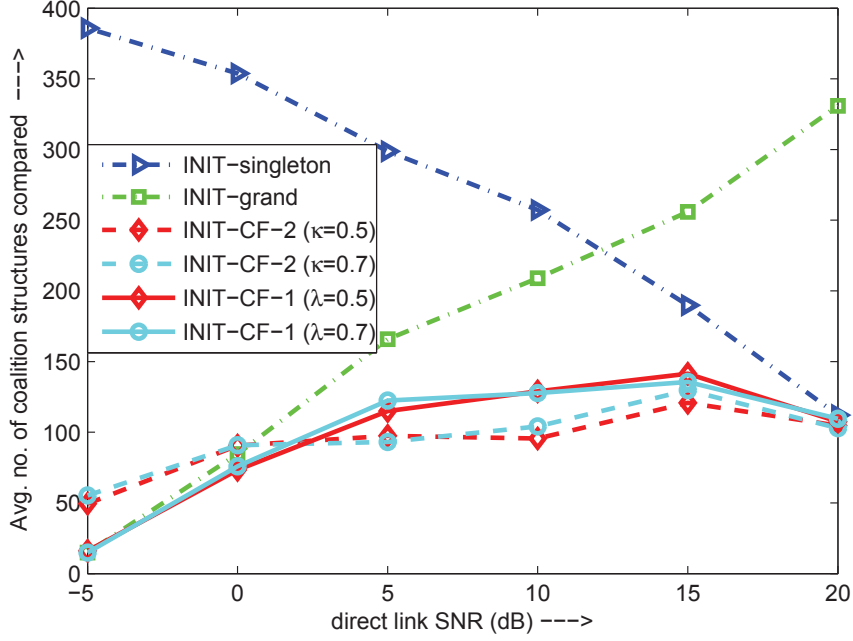
Figure 4.6: Average number of network rate comparisons made to reach a Nash-stable partition.

in terms of total network rate comparisons, made before converging to a Nash-stable network partition, for the grand/singleton start case, and highlights the reduction in the required number of comparisons when the CF process is augmented with the proposed initialization algorithms (Init-CF-1 and Init-CF-2). In a given CF round, the maximum number of rate comparisons is $N(N-1)/2$ which occurs when the current network partition comprises of all singleton coalitions. This results in a worst case complexity of $\mathcal{O}(N^2)$, which becomes smaller as coalitions start to form. On the other hand, the minimum rate comparisons are N which occurs when the current partition is a grand coalition leading to the best case complexity of $\mathcal{O}(N)$. Therefore, the complexity in terms of rate comparisons made during a CF round lie between the two extremes, with the worst case complexity becoming smaller However, as coalitions start to form, this complexity

119

becomes smaller. This is evident from Figure 4.6 which shows that algorithm complexity, in terms of number of network rate comparisons, is proportional to the number of CF rounds, where the average number of rate comparisons per CF round varies between $[10, 40]$.

Figure 4.5 and Figure 4.6 show that both Init-CF-1 and Init-CF-2 initialization schemes offers improved convergence speed (in comparison to grand/singleton start) regardless of the operating SNR, and their performance is not affected much by the choice of interference threshold, provided the threshold is kept > 0.5. In particular, Init-CF-1 offers better convergence speed (reduced rate comparisons) at low direct link SNR (< 0 dB) in comparison to Init-CF-2, while Init-CF-2 outperforms Init-CF-1 when the direct link SNR is > 0 dB.

THROUGHPUT-EFFICIENT SPECTRUM ACCESS IN DISTRIBUTED CRNS

This chapter extends the problem of joint coalition formation and bandwidth allocation, analyzed in Chapter 4, to distributed cognitive radio networks. An ad hoc cognitive radio network is considered, in which SUs may cooperate to increase their individual rate, leading to *selfish cooperation*, or they may cooperate to maximize the group sum-rate, which is called *altruistic cooperation*. Similar to Chapter 4, the concept of frequency reuse and optimal BW allocation is applied, and the throughput-efficient distributed network partitioning problem is modeled as a CF game in a *partition form* with *non-transferable utility* (NTU). Variety of CF rules are proposed and the convergence/stability properties of the proposed CF algorithm under different CF rules, are studied.

The chapter organization is as follows: Section 5.1 introduces the existing work on distributed CF and highlights the main contributions of the chapter. Section 5.2 presents the network model. The optimal BW allocation for a given network partition is presented in Section 5.3, while the proposed distributed CF algorithm and the different proposed CF rules are discussed in Section 5.4. Probabilistic analysis of the proposed CF algorithm is presented in Section 5.5, and some key simulation results are provided in Section 5.6.

5.1 Introduction

The throughput-efficient spectrum access problem in distributed cognitive networks has been recently investigated in [54] and [133], using coalitional game-theoretic tools. The authors in [54] consider the joint optimization of sensing and access, where a player switches to a new coalition if it can improve its payoff, without decreasing the payoff of any member of the new coalition. Furthermore, the competing SUs share the spectrum in chunks of pre-fixed/slotted BW (as defined by PU channels). In [133], coalition members share the available BW according to their channel gain ratios, and the transition from one coalition structure to other, occurs only through the merging of two existing coalitions.

In comparison to existing work where the available spectrum resources are shared in terms of channels of pre-fixed or equal BW, this chapter considers a continuous BW allocation among the coalition members and provides a closed form expression of rate-optimal BW allocation. Furthermore, in comparison to

existing CF algorithms based on restricted movements of distributed SUs, an efficient distributed CF algorithm is developed through which *individually rational* (targeting to improve their own rate) SUs are self-organized based on individual/group rate improvement. Variety of CF rules are designed based on whether SUs consider the effect of their movement, from present (old) coalition to another (new) coalition, on other SUs in the network, and if they seek approvals from the new and/or old coalition, whether these approvals are individual or group approvals. For the CF rules that may lead to cycles in the CF process, the history condition is introduced in the CF algorithm to guarantee Nash-stability, and three different exit procedures are described when a CF cycle is inevitable. Furthermore, the probabilistic analysis of the stability of grand coalition structure (GCS) and singleton coalition structure (SCS) is performed to show the effectiveness of the proposed algorithm by evaluating a lower bound on the probability that a general network partition (other than GCS/SCS) is stable.

5.2   Network Model

An adhoc cognitive radio network with N distributed secondary links (secondary transmitter-receiver (ST-SR) pairs) is considered. It is assumed that the total available BW for secondary access is W Hz, and the channel between any of the secondary transmitters and any of the secondary receivers over this BW follows a quasi-static flat fading model. A representative network model is illustrated in Fig. 5.1.
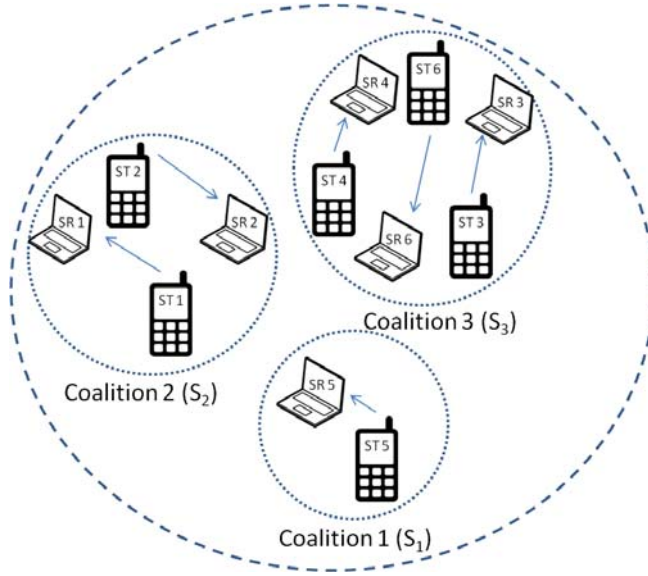
Figure 5.1: A representative network model with 6 secondary links.

Similar to Chapter 4, the throughput-efficient distributed network partitioning problem is addressed from two perspective; i.e., (1) frequency reuse of the available BW among non-overlapping coalitions, and (2) optimal BW allocation among the coalition members. Fig. 5.1 shows a snapshot of a network partition Π resulting from the proposed CF algorithm with $N = 6$ distributed secondary links arranged in $|\Pi| = 3$ coalitions. Each link is identified by a unique global index i, $i \in \{1, 2, \cdots, N\}$, while each coalition S_l, $l \in \{1, 2, \cdots, |\Pi|\}$, has a representative member, designated as *coalition head* H^l, which is responsible for optimally allocating the total available BW among the members of S_l and coordinating with the links proposing to join S_l. Any member of Coalition S_l can act as coalition head. However, without loss of generality, a coalition member, with largest global index, i is selected to act as H^l. The motivation behind the selection convention of H^l is discussed in Section 5.4.3.

The following section revisits the BW allocation problem, with a slight variation in notations in comparison to Chapter 4, and presents the closed form expression of the optimal BW allocation for a given coalition structure.

5.3 Optimal Bandwidth Allocation

Let the network partition at a certain time instant be: $\Pi = \{S_1, S_2, \cdots, S_{|\Pi|}\}$, with $|\Pi|$ disjoint coalitions, such that each of the $|\Pi|$ coalitions will use the total available bandwidth W. Consider Coalition $S_k \in \Pi$, with $|S_k|$ representing the number of members (links) in S_k. The Member (Link) i of Coalition S_k is referred to as m_i^k, while P_i^k represents the transmission power of this member. Each member m_i^k of S_k will be allocated a fraction $\mu_i^{S_k}$ of the total bandwidth, where $\sum_{i=1}^{|S_k|} \mu_i^{S_k} = 1$. The total interference power affecting the bandwidth W being used by Coalition S_k is the sum of all received power from all members in all other coalitions. For simplicity of the analysis, the interference affecting the band $\mu_i^{S_k} W$ being used by Member m_i^k is approximated as the average interference affecting this band which is a fraction $\mu_i^{S_k}$ of the total interference power affecting the total bandwidth at the receiver of Link m_i^k; i.e.,

$$
\begin{aligned}
\bar{I}_i^{S_k} &= \mu_i^{S_k} \sum_{l=1, l \neq k}^{l=|\Pi|} \sum_{j=1}^{|S_l|} P_j^l |h_{ji}^{lk}|^2 \\
&= \mu_i^{S_k} \sum_{l=1, l \neq k}^{l=|\Pi|} I_i^{S_k, S_l} = \mu_i^{S_k} I_i^{S_k}.
\end{aligned}
\tag{5.1}
$$

where, h_{ji}^{lk} represents the channel between the transmitter of Link j in Coalition S_l and the receiver of Link i in Coalition S_k. $I_i^{S_k,S_l} = \sum_{j=1}^{|S_l|} P_j^l |h_{ji}^{lk}|^2$ is the interference experienced by the receiver of Link i in Coalition S_k from all players in Coalition S_l, and $I_i^{S_k} = \sum_{l=1,l\neq k}^{l=|\Pi|} I_i^{S_k,S_l}$ represents the total interference from all other coalitions in the network affecting the total bandwidth W. The total rate of Coalition S_k under Partition Π can be written as:

$$\mathcal{R}^{S_k,\Pi} = \sum_{i=1}^{|S_k|} R_i^{S_k,\Pi} = \sum_{i=1}^{|S_k|} \mu_i^{S_k} W \log\left(1 + \frac{P_i^k |h_{ii}^{kk}|^2}{\mu_i^{S_k}(N_0 W + I_i^{S_k})}\right). \tag{5.2}$$

In order to maximize the rate achieved by this coalition, the problem can be formulated as

$$\max_{\mu_i^{S_k}} \sum_{i=1}^{|S_k|} \mu_i^{S_k} W \log(1 + \frac{P_i^k |h_{ii}^{kk}|^2}{\mu_i^{S_k}(N_0 W + I_i^{S_k})}),$$
$$\text{subject to} \sum_{i=1}^{|S_k|} \mu_i^{S_k} = 1 \text{ and } 0 \leq \mu_i^{S_k} \leq 1. \tag{5.3}$$

Similar to Chapter 4, the objective function of (5.3) can be written as:

$$W \sum_{i=1}^{|S_k|} \mu_i^{S_k} \log(1 + \frac{x_i^k}{\mu_i^{S_k}}), \tag{5.4}$$

where $x_i^k = \frac{P_i^k |h_{ii}^{kk}|^2}{N_0 W + I_i^{S_k}}$, which can be upper bounded by choosing

$$\mu_{i,\text{opt}}^{S_k} = \frac{x_i^k}{\sum_{m=1}^{|S_k|} x_m^k}. \tag{5.5}$$

126

Hence, the closed form expression of optimal rate $R_{i,\text{opt}}^{S_k,\Pi}$, for any $i \in S_k$, is given by:

$$R_{i,\text{opt}}^{S_k,\Pi} = \mu_{i,\text{opt}}^{S_k} W \log \left(1 + \sum_{m=1}^{|S_k|} x_m^k \right). \tag{5.6}$$

5.4 Distributed Coalition Formation

The closed form expression of the rate-optimal BW allocation among coalition members, is derived in the previous section, under the assumption that a *network partition* is known apriori. In this section, the problem of finding an appropriate network partition in ad hoc cognitive radio networks, is addressed, wherein individual CRs interact with each other (without relying on a centralized entity, as in Chapter 4) to achieve their goals (rate improvement, in our case), by playing a *distributed coalition formation game.*

5.4.1 Preliminaries and Game Formulation

Utility and Value Functions

For the proposed joint coalition formation and bandwidth allocation problem, the payoff $\phi_i(S_k, \Pi)$ of player $i \in S_k$, $S_k \in \Pi$ is the rate achieved by player $i \in S_k$ when the total available BW is optimally shared by the members of coalition S_k, defined as:

$$\phi_i(S_k, \Pi) = R_{i,\text{opt}}^{S_k,\Pi}, \tag{5.7}$$

where $R_{i,\text{opt}}^{S_k,\Pi}$ is given by (5.6). Therefore, the value function $\mathcal{V}(S_k, \Pi)$ is defined as a mapping given by a vector $\mathbf{v}(S_k, \Pi) \in \mathbb{R}^{|S_k|}$, where each element $v_i \in \mathbf{v}(S_k, \Pi)$ represents the payoff (rate) of player $i \in S_k$; i.e.,

$$\mathcal{V}(S_k, \Pi) = \left\{ \mathbf{v}(S_k, \Pi) \in \mathbb{R}^{|S_k|} \mid v_i(S_k, \Pi) = \phi_i(S_k, \Pi) = R_{i,\text{opt}}^{S_k,\Pi} \right\}. \qquad (5.8)$$

Outcome of the Game

The *outcome* of the game is given by the pair $(\mathbf{x}, \Pi)$, where $\mathbf{x} \in \mathbb{R}^{\mathcal{N}}$ represents the payoff vector of all players in the network under partition Π.

Pareto Dominance and Core

The *outcome* $O = (\mathbf{x}, \Pi_x)$ *Pareto dominates* the outcome $O' = (\mathbf{y}, \Pi_y)$ if O is as good as O' for every player $i \in \mathcal{N}$ and there is at least one agent j who strictly prefers the outcome O. Mathematically, O Pareto dominates O' when $x_i \geq y_i \ \forall \ i \in \mathcal{N}$ and for at least one player $j \in \mathcal{N}$, $x_j > y_j$. This is equivalently said as O' is Pareto dominated by O.

The outcome is *Pareto optimal* if it is not *Pareto dominated* by any other outcome. The set of all undominated outcomes is called the *core*.

Game Formulation

Proceeding on similar lines to Chapter 4, the joint BW allocation and CF problem is modeled as a CF game in *partition form* with *non-transferable utility* (NTU) [66].

The following sections set up the building blocks to devise a distributed algorithm that allows the secondary links to self-organize into throughput-efficient coalition structure.

5.4.2 Building Blocks of the Proposed CF Algorithm

Action Space

The *action space* A_i of player $i \in \mathcal{N}$ defines the possible set of *actions* that a player $i \in \mathcal{N}$ can take to move from its current coalition to any other coalition in the network. In the proposed formulation, a CF algorithm is derived based on the movements of one player at a time, for which the *action space* of player i is defined as: $A_i = \{\text{stay}, \text{switch}\}$, $\forall\, i \in \mathcal{N}$. Thus, a player i *stays* in its current coalition with associated partition Π or *switches* to another coalition (which might even be an *empty* coalition ϕ; i.e., a player may decide to *split* from its current coalition and act alone non-cooperatively as a *singleton*) leading to a new network partition $\acute{\Pi}$. It is important to point out that the proposed switch operation updates the current network partition by either keeping the same number of coalitions in the network partition or increase/decrease the number of coalitions by only one. An action is taken by the player based on the preference relation, which is defined next.

Preference Relation

In CF games, player $i \in \mathcal{N}$ compares being the member of different coalitions, under their respective partitions, based on a *preference relation* [68] defined as:

Definition 1: For any player $i \in \mathcal{N}$, a preference relation $\succeq_i$ is defined as a complete, reflexive and transitive binary relation over the set of all possible (coalition,partition) pairs that player i can be a member of; i.e., the set $\{(S_k, \Pi) | S_k \subseteq \mathcal{N}, S_k \in \Pi, \Pi \in \mathcal{P}\}$.

Based on the above definition, for any player $i \in \mathcal{N}$, given two coalitions and their respective partitions, $S_1 \in \Pi$ and $S_2 \in \acute{\Pi}$, that player i can be a member, the notation $(S_1, \Pi) \succeq_i (S_2, \acute{\Pi})$ indicates that Player i prefers to be a member of Coalition S_1 under Partition Π over Coalition S_2 under $\acute{\Pi}$, or at least, player i prefers both pairs equally. Furthermore, $(S_1, \Pi) \succ_i (S_2, \acute{\Pi})$, indicates that player i *strictly* prefers S_1 under Partition Π over S_2 under Partition $\acute{\Pi}$. For every application, a preference relation $\succ_i$ can be evaluated in a different way to allow the players to quantify their preferences based on their observations, leading to different CF rules. In the following, a generalized CF rule is presented, while further details on the evaluation of preferences are discussed in Section 5.4.4.

Generalized CF Rule

A CF rule quantifies the individual preferences of distributed players over different coalitions. Before defining a generalized framework of the different CF rules, it is important to investigate how the achievable utility per player will change if the

preference relation considers the effect of the switching action on other players as well. This requires acquiring the *approval* from the players whose utilities are affected by the proposed switching action.

Remark 1: In the proposed joint BW allocation and CF game in partition form, since the utility of player in a coalition depends on the players outside its coalition but not on how these players are organized (as evident from (5.1) and (5.7)), therefore when a player switches, only the payoff of players in the *old coalition* and *new coalition* are updated.

In the light of above discussion, a variety of CF rules can be derived by defining the following generalized triplet:

$$CFRule \triangleq (selfish, approval(new), approval(old)) \equiv (s, a_n, a_o). \quad (5.9)$$

The first parameter *selfish*, s, emphasizes the *individual rationality* of the player. The other two parameters: approval from new and old coalition: $a_n, a_o \in \{no, indv, altru\}$ indicates the three possible approval alternatives: (1) (no): approval not required (2) ($indv$): individual approval is required from each player in the new/old coalition and (3) ($altru$): altruistic approval is required from the coalition as a whole which is granted based on the sum-rate achieved by the new/old coalition, and hence, it can be viewed as a much relaxed form of approval. A variety of CF rules can be derived based on CF rule triplet (5.9). Different classes of CF rules, along with their properties are discussed in Section 5.4.4.

In general, a player $i \in \mathcal{N}$ decides to leave its current Coalition $S_k \in \Pi$ and

join another Coalition $S_l \in \Pi \cup \{\phi\}$, $l \neq k$ and hence making a transition from Π to $\acute{\Pi} = \{\Pi \backslash \{S_k, S_l\}\} \cup \{S_k \backslash \{i\}, S_l \cup \{i\}\}$, if and only if $(S_l \cup \{i\}, \acute{\Pi}) \succ_{i,(s,a_n,a_o)}$ (S_k, Π), where $\succ_{i,(s,a_n,a_o)}$ indicates a strict preference relation that is based on the underlying CF rule specified by the triplet (s, a_n, a_o).

For the practical implementation of different CF rules, which may require an approval from new/old coalition, the CF process is proposed to be coordinated through a representative member of a coalition, termed as *coalition head*, that is defined next.

Coalition Head

For any coalition $S_l \in \Pi$, $\Pi = \{S_1, S_2, \cdots, S_{|\Pi|}\}$, the coalition member with the largest global index i is designated as the coalition head (H^l). A coalition head is characterized by following distinctive features: (1) A coalition head H^l is aware of all the members of its coalition S_l by acting as a *gateway* for its coalition. This means that every member of S_l who decides to leave S_l, informs H^l and every player who proposes to *switch* from its current coalition to $S_l \in \Pi$, seeks an approval from H^l, if required by the underlying CF rule. (2) A coalition head H^l optimally allocates the total available BW among its coalition members and calculate the current rate $R_m^{S_l,\Pi}$ for all of its members $m = 1, 2, \cdots, |S_l|$. This is accomplished by letting all the members of coalition S_l share the information of the direct link channel gain, h_{mm}^{ll}, and the average interference experienced by each one of them, with H_l. In this way H^l approves/disapproves the *switching* proposal made to it, based on the underlying CF rule. (3) Finally, coalition heads

are responsible for identifying the end of CF process according to the proposed
CF algorithm.

5.4.3 Proposed CF Algorithm and the Implementation Protocol

This sections presents the proposed CF algorithm and present a detailed protocol
to practically implement the distributed CF process according to the proposed
algorithm.

Coalition Formation Algorithm

The proposed distributed CF algorithm is summarized in Figure 5.2. Under the
assumption that each player in the network is aware of the average external in-
terference it experiences through measurements fed back from its receiver over a
control channel, such as cognitive pilot channel (CPC) [136], CF algorithm can
be initialized either in a singleton structure, with the initial network partition:
$\Pi_0 = \{\{1\}, \{2\}, \cdots, \{N\}\})$ or in a grand coalition: $\Pi_0 = \mathcal{N} = \{1, 2, \cdots, N\}$.
The CF algorithm is proposed to be initialized in a grand coalition based on the
rationale that the random locations of SUs in ad hoc CRNs usually result in high
interference among the communication links, and a network partition comprised of
large size coalitions (coalitions with large number of players) are highly probable
to emerge as a final stable network partition Π_f.

The proposed CF algorithm is invoked by distributed players in the ascending
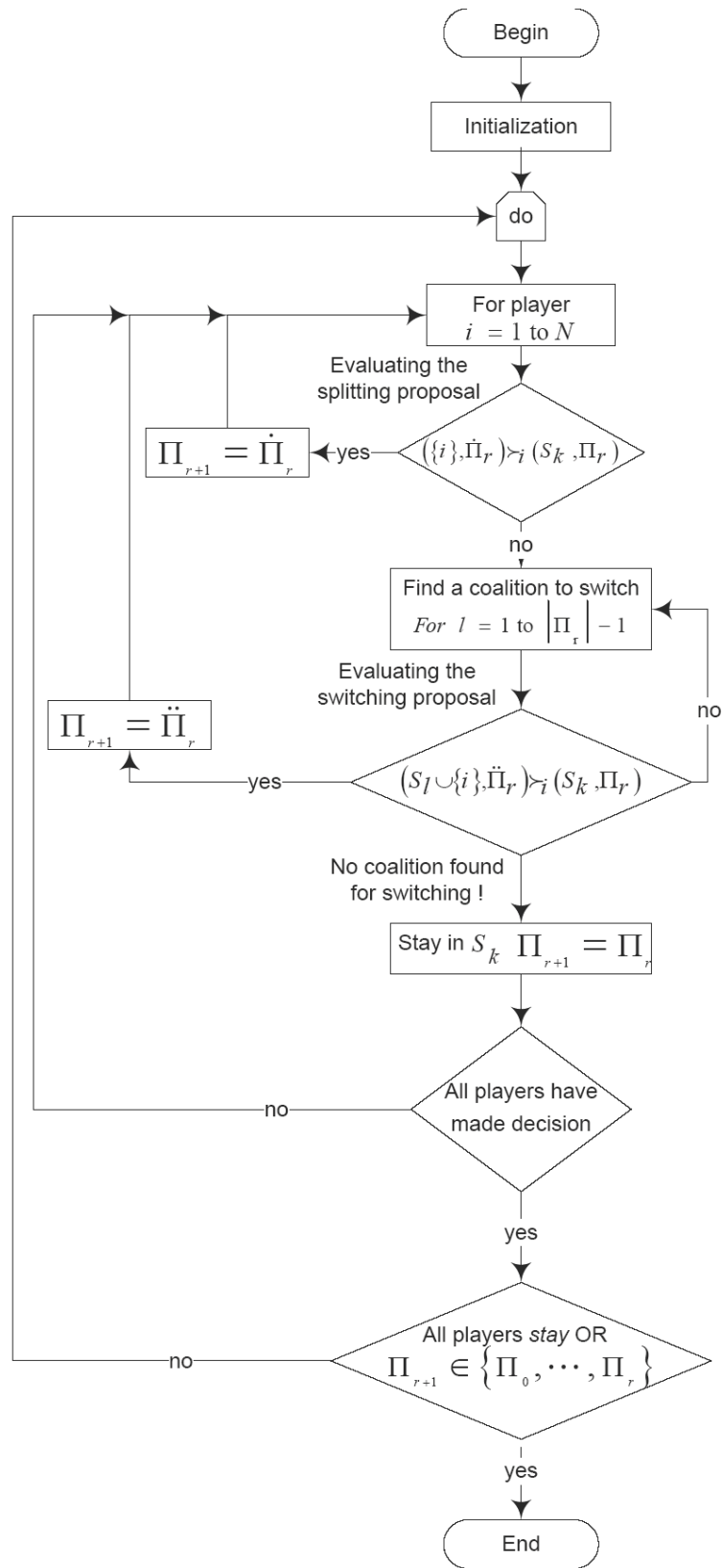
Figure 5.2: Flow chart of the proposed distributed CF algorithm for the CF round: $r + 1$.

order of their global index i. The algorithm completes one *CF round* when all the N players in the network have taken action (*stay* or *switch*) based on the underlying CF rule. Hence, one CF round consists of N *iterations*, where at each iteration, only one player can move from its current coalition to a new coalition. In this way, a CF round offers a sequence of network partition transitions as:

$$\Pi_{r-1,N} \to \Pi_{r,1} \to \Pi_{r,2} \to \cdots \to \Pi_{r,N}, \tag{5.10}$$

where $\Pi_{r,i}$ represents the partition formed after Player i takes *action* in its turn during CF Round r, and hence, $\Pi_{r,N}$ indicates the network partition at the end of CF Round r.

In each partition transition, the player is assumed to be *opportunistic*; i.e., a player i *switches* to the first coalition; $S_l \in \Pi \cup \{\phi\}$, which it finds to be satisfying the underlying CF rule, while first checking $S_l = \phi$ followed by all the coalitions $S_l \in \Pi$, $\forall \, l = 1, 2, \cdots, |\Pi|$, and $l \neq k$, in a round-robin fashion. Hence, the CF algorithm completes its iteration for player $i \in \mathcal{N}$ when it finds a suitable coalition; $S_l \in \Pi \cup \{\phi\}$, to *switch* to, or when after checking all *switching* possibilities, it *prefers* to *stay* in its current coalition; $S_k \in \Pi$.

After iterating over all the players in the network, one round of the proposed CF algorithm concludes. The algorithm keeps on iterating over all the players in the network until all players decide to *stay* in their current coalition; i.e., $\Pi_{r,i} = \Pi_{r-1,N}$, $\forall \, i \in \mathcal{N}$ (which indicates that the algorithm has *converged* to a final *stable* network partition Π_f), or the CF process leads to a *cycle* (*non-*

135

convergent state), in which case the distributed players at the end of certain CF round r, are self-organized into an already witnessed network partition at the end of some previous CF round $r - s$; i.e., $\Pi_{r,N} = \Pi_{r-s,N}$, $s = \{1, 2, \cdots r\}$, where $\Pi_{0,N} = \Pi_0$ specifies the initial network partition. For the practical implementation of the proposed distributed CF algorithm and to determine the convergent/non-convergent final state of the algorithm with minimum computation and memory overhead, the following CF protocol is proposed:

Coalition Formation Protocol

The coalition formation process starts from an initial network partition Π_0, known to all players in the network such that each player $i \in \mathcal{N}$ is aware of all the *coalitions heads* in Π_0. During a CF Round r, Player $i \in \mathcal{N}$ takes an appropriate action $a_i \in A_i$ in Iteration i according to the underlying CF rule. The player informs other players about its action by broadcasting an *action code* through which each player in the network is informed of the resulting network partition $\Pi_{r,i}$ and all the coalition heads therein. The action codes are pre-fixed bit sequences, that represent the index of the new coalition for *switch*, or all zeros for *stay*. Since, a player can *switch* to any one of the maximum $N - 1$ non-empty coalitions or it may *prefer* to *stay* in its current coalition, it is clear that $log(N)$ bits are sufficient to encode the action of any player. It is important to point out here that each player in the network needs to keep track of the current network partition and the coalition heads therein in order to take an action on its turn. Furthermore, the Player with the highest global index; i.e., $i = N$, also maintains a *stay-counter*

which indicates the number of players that prefer to *stay* in their current coalition during a CF round. The *stay-counter* is reset at the beginning of each CF round, and incremented by one, whenever a player decides to *stay* in its current coalition (indicated by its action code consisting of all zeros).

In general, a *Switching* action is taken based on the underlying CF rule, following a pre-defined 3-step protocol:

Step 1: Making the switching request: A player $i \in S_k$, $S_k \in \Pi$ sends a *switch-to request* to the head H^l of a coalition $S_l \in \Pi \cup \{\phi\}$, $l \neq k$ by sharing its link-specific information over a dedicated control channel. For $S_l = \phi$, Player i itself acts as the head of the proposed new singleton Coalition $\{i\}$, and hence, no information exchange is required. For the proposed non-singleton new coalition, the shared information includes: (a) the direct channel gain h_{ii}^{ll} ($= h_{ii}^{kk}$), (b) the increased interference $I_i^{\{i\}}$ ($= I_i^{S_k} + I_i^{\{i\},S_k \setminus \{i\}}$) experienced by player $i \in \mathcal{N}$ resulting from leaving its current coalition S_k and considering it will become singleton, and (c) its current rate $R_i^{S_k,\Pi}$.

If the underlying CF rule requires the approval from old coalition, Player i sends a *switch-from request* to its current coalition head H^k by indicating its global index i.

Step 2: Switching request evaluation: Having received the *switch-to request* along with the required information from player $i \in S_k$, $S_k \in \Pi$, coalition head H^l evaluates the switching proposal by analyzing the proposed new coalition $\grave{S}_l = S_l \cup \{i\}$ under the proposed new network partition $\ddot{\Pi} =$

$\left\{ S_1, S_2, \cdots, S_k \backslash \{i\}, \cdots, S_l \cup \{i\}, \cdots, S_{|\Pi|} \right\}$. In this regard, H^l first updates the interference experiences by Player $i \in \grave{S}_l$ as $I_i^{\grave{S}_l} = I_i^{\{i\}} - I_i^{\grave{S}_l, S_l}$ and by all other players as $I_j^{\grave{S}_l} = I_j^{S_l} - I_j^{\grave{S}_l, \{i\}} \ \forall \ j \in S_l$. These interferences are then used to determine the optimal BW fraction $\mu_j^{\grave{S}_l}$ and ultimately the rate $R_{j,opt}^{\grave{S}_l, \ddot{\Pi}}$ for all the members $j \in \grave{S}_l$, as required by the underlying CF rule. H^l approves/disapproves the *switch-to request* based on the individual preference of player i, and if required, taking into consideration the effect of proposed switch action on the members of S_l according to the underlying CF rule.

The *switch-from request* is handled by the head H^k of old Coalition S_k by analyzing the effect of proposed switch action on the members of $\acute{S}_k = S_k \backslash \{i\}$. In this regard, H^k, evaluates the increased interference $I_j^{\acute{S}_k} = I_j^{S_k} + I_j^{\{S_k, \{i\}\}} \ \forall \ j \in \acute{S}_k$ and used it determine the optimal BW fraction $\mu_j^{(\acute{S}_k)}$ and ultimately the rate $R_{j,opt}^{\acute{S}_k, \ddot{\Pi}} \ \forall \ j \in \acute{S}_k$. H^k approves/disapproves the *switch-from request* based on the effect of proposed switch action on the members of $\acute{S}_k$ according to the underlying CF rule.

Step 3: Indicating the switching decision: Player $i \in \mathcal{N}$ decides to switch from its current Coalition $S_k \in \Pi$ to Coalition $S_l \in \Pi \cup \{\phi\}$, $l \neq k$ based on the approval from H^l (and H^k, if required by the underlying CF rule). If the player $i \in \mathcal{N}$ switches, its entry is removed from the member list maintained by the head H^k of its previous coalition S_k, added to the list maintained by H^l and both the coalition heads update the rates of each of their coalition members under partition $\Pi_{r,i} = \left\{ S_1, S_2, \cdots, S_k \backslash \{i\}, \cdots, S_l \cup \{i\}, \cdots, S_{|\Pi|} \right\}$. In this case, Player i

broadcasts the action code indicating the index of Coalition S_l, and the algorithm completes its CF-iteration for Player $i \in \mathcal{N}$. The CF algorithm proceeds with the next player in the network, following the same 3-step protocol. On the other hand, if the switching action is not approved by the head(s), the above protocol is repeated for the same Player i until it finds a suitable coalition $S_l \in \Pi$ to *switch* to, or after checking all coalitions $S_l \in \Pi \cup \{\phi\}$, $l \neq k$, it prefers to *stay* in its current coalition $S_k \in \Pi$, in which case, Player i broadcasts the action code consisting of all zeros, and the Player $i = N$ responds by incrementing the locally maintained *stay-counter* by one.

At the end of CF round r; i.e., after iterating over all the players in the network, all players are aware of the current network partition $\Pi_{r,N}$ in addition the Player $i = N$ knowing (from *stay-counter*) the number of players that decide to stay in their coalition during the CF round r. If the *stay-counter* reads N, this indicates the end of CF game in a stable outcome where all the players prefer to stay in their coalition, converging to a final network partition $\Pi_f = \Pi_{r,N}$. However, if all the players do not stay in their coalition, this means that either the CF process has not converged so far or there might be a *cycle* in CF game. To identify a CF cycle, a *round-level partition history set*; $\mathcal{P}_{r^-} = \{\Pi_{0,N}, \Pi_{1,N}, \cdots, \Pi_{r-1,N}\}$, containing all the network partitions before CF round r, is maintained locally by the heads of all the coalitions, in the evolved network partition, at the end of each CF round. In the beginning of the CF process, each coalition head saves Π_0 in its *round-level partition history set*. At the end of CF round r, all the coalition heads in $\Pi_{r,N}$

check if $\Pi_{r,N} \in \mathcal{P}_{r-}$. The case $\Pi_{r,N} \notin \mathcal{P}_{r-}$ implies that $\Pi_{r,N}$ is not an already witnessed network partition and hence the CF game continues to the next round with each coalition head saving $\Pi_{r,N}$ in its *round-level partition history set*. On the other hand, if all the coalition heads find $\Pi_{r,N} \in \mathcal{P}_{r-}$, the game ends in a CF cycle. Section 5.4.5 presents the proposed solutions for dealing with CF cycles.

The convergence of the proposed distributed CF algorithm strongly depends on the underlying CF rule. The following section presents prominent CF rules by providing various evaluation criteria for the individual preferences of distributed players in an ad hoc cognitive radio network.

5.4.4 Proposed Coalition Formation Rules and the Convergence Properties

This sections presents different classes of CF rules based on the generalized CF rule triplet (5.9) and study the convergence properties of the proposed CF algorithm build on these rules.

Proposed CF rules

The proposed CF rule triplet (s, a_n, a_o) leads to three classes of CF rules: (1) Selfish class consisting of a single CF rule; (s,no,no), in which switching is decided solely by the switching player based on its own utility improvement, (2) Selfish with new coalition approval; $(s,indv,no)$ and $(s,altru,no)$, which requires not only the utility improvement of the switching player but also seeks an approval (*indi-*

vidual or *altruistic*) from the new coalition to take the proposed switching action, and (3) Selfish with approval from both the new and old coalition. CF rules in this class are most restrictive in the sense that switching takes place not only when the moving player improves its own utility but also when it is *welcomed* (*individually* or *altruistically*) by the new coalition as well as when it is *allowed* (*individually* or *altruistically*) by the old coalition. In this class, two CF rules are analyzed: (*s,indv,indv*) and (*s,altru,altru*) based on the rationale that it is more realistic to seek approval in the same form *indv,indv* or *altru,altru*, from the new and old coalition.

Remark 2: All the network partitions reachable from a certain partition under restrictive CF rules e.g. rules based on individual approval(s) are also accessible under relaxed CF rules e.g. rules based on altruistic approval(s). Similarly, since (s, a_n, a_o) based CF rules are more restrictive than (s, a_n, no) CF rules which are more restrictive than (s, no, no) rules, therefore, all the network partitions reachable under (s, a_n, a_o) CF rules are also reachable under (s, a_n, no) and (s, no, no) based CF algorithms. Also, all partitions reachable under (s, a_n, no) CF rules are also accessible under (s, no, no) based rules.

The proposed CF rules along with the definitions of underlying preference relation are illustrated in Table 5.1.

Convergence Properties of CF algorithm based on Proposed CF Rules

In the following, the convergence properties of the proposed CF algorithm are presented by analyzing the underlying CF rules according to their classes.

Table 5.1: Proposed CF rules and corresponding definitions of preference relation $(S_l \cup \{i\}, \acute{\Pi}) \succ_{i,(s,a_n,a_o)} (S_k, \Pi)$.

No.	CF rule	Preference relation
1	(s, no, no)	$R_i^{S_l \cup \{i\}, \acute{\Pi}} > R_i^{S_k, \Pi}$
2	$(s, indv, no)$	$R_i^{S_l \cup \{i\}, \acute{\Pi}} > R_i^{S_k, \Pi}$ AND $R_j^{S_l \cup \{i\}, \acute{\Pi}} \geq R_j^{S_l, \Pi}, \ \forall j \in S_l$
3	$(s, altru, no)$	$R_i^{S_l \cup \{i\}, \acute{\Pi}} > R_i^{S_k, \Pi}$ AND $\sum_{j \in S_l} R_j^{S_l \cup \{i\}, \acute{\Pi}} \geq \sum_{j \in S_l} R_j^{S_l, \Pi}$
4	$(s, indv, indv)$	$R_i^{S_l \cup \{i\}, \acute{\Pi}} > R_i^{S_k, \Pi}$ AND $R_j^{S_l \cup \{i\}, \acute{\Pi}} \geq R_j^{S_l, \Pi}, \ \forall j \in S_l$ AND $R_j^{S_k \setminus \{i\}, \acute{\Pi}} \geq R_j^{S_k, \Pi}, \ \forall j \in S_k, j \neq i$
5	$(s, altru, altru)$	$R_i^{S_l \cup \{i\}, \acute{\Pi}} > R_i^{S_k, \Pi}$ AND $\sum_{j \in S_l} R_j^{S_l \cup \{i\}, \acute{\Pi}} \geq \sum_{j \in S_l} R_j^{S_l, \Pi}$ AND $\sum_{j \in S_k, j \neq i} R_j^{S_k \setminus \{i\}, \acute{\Pi}} \geq \sum_{j \in S_k, j \neq i} R_j^{S_k, \Pi}$

Theorem 1: Starting from any initial network partition Π_0, the CF algorithm based on $(s, indv, indv)$, and $(s, altru, altru)$ rules always *converges* to a final network partition, Π_f, which is *stable* and *throughput efficient*.

Proof. Given any initial starting partition Π_0 and considering the CF algorithm based on $(s, indv, indv)$, and $(s, altru, altru)$ rules, the CF process consists of a sequence of network partition transitions:

$$\Pi_0 \to \Pi_{1,N} \to \cdots \to \Pi_{r,N} \to \cdots , \tag{5.11}$$

where $\Pi_{r,N}$ represents the partition formed at the end of CF Round r such that during this round, at least one player $i \in \mathcal{N}$ *switches* from its current coalition to a new coalition. Based on the definition of $(s,indv,indv)$ and $(s,altru,altru)$ CF rules (as given in Table 5.1), the switching action does not allow the distributed players to organize in a partition (in *round-level partition history set*) offering lower network rate as compared to the current network rate. As a result, $(s,indv,indv)$ and $(s,altru,altru)$ CF rules always result in a new network partition with improved

142

network throughput. Since, the number of partitions of a set is *finite* (given by Bell number [68]), therefore the sequence of network partition transitions in (5.11) terminates after finite number of CF rounds. Hence, the proposed CF algorithms in this class always converge to a final network partition Π_f.

Furthermore, both (*selfish,indv,indv*) and (*selfish,altru,altru*) rules provide a transition from Π to $\acute{\Pi}$ such that the new network partition $\acute{\Pi}$ always offers improved network throughput; i.e., $\sum_k^{|\acute{\Pi}|} \mathcal{R}^{S_k,\acute{\Pi}} > \sum_k^{|\Pi|} \mathcal{R}^{S_k,\Pi}$. Hence, the proposed CF algorithm based on these rules always yield a *network-throughput efficient* final partition. ▍

It is important to point out here that the CF algorithm based on (*s,indv,indv*) and (*s,altru,altru*) rules leads to *contractual individual stability* [137], which is the most restrictive form of stability in CF games.

Remark 3: The algorithms based on CF rules in which the switching action does not guarantee a new network partition with improved network throughput (or any other network metric), may lead to a *cycle*, since a player $i \in \mathcal{N}$ may find incentive to revisit a coalition in its *coalition history set* (set of all coalitions, that player i was a member of in the past but did not remain as its member because it, or some other coalition member, left the coalition) such that all the players get organized in an already encountered network partition at the end of some previous CF round.

Corollary 1: Starting from any initial network partition Π_0, the CF algorithm based on $(s, indv, no)$, and $(s, altru, no)$ rules is susceptible to end in a CF cycle.

The length of such a cycle is ≥ 3.

Illustration: Consider a CF game with three players and the initial network partition $\Pi_0 = \{\{1\}, \{2\}, \{3\}\}$ with the payoff vector $\mathbf{x}^{(0)} = [10, 20, 30]$. Furthermore, three possible network partitions are considered; $\Pi_1 = \{S_1, S_2\} = \{\{1, 2\}, \{3\}\}$, $\Pi_2 = \{S_1, S_2\} = \{\{1\}, \{2, 3\}\}$, and $\Pi_3 = \{S_1, S_2\} = \{\{2\}, \{1, 3\}\}$, with the payoff vectors $\mathbf{x}^{(1)} = [12, 21, 30]$, $\mathbf{x}^{(2)} = [10, 22, 31]$, and $\mathbf{x}^{(3)} = [11, 20, 32]$. For the considered game, the following preference relations exist:

$$(S_2, \Pi_2) \succ_{2,(s,indv,no)} (S_1, \Pi_1)$$

$$(S_2, \Pi_3) \succ_{3,(s,indv,no)} (S_2, \Pi_2) \qquad (5.12)$$

$$(S_1, \Pi_1) \succ_{1,(s,indv,no)} (S_2, \Pi_3)$$

It is conceivable that a CF cycle: $\Pi_1 \rightarrow \Pi_2 \rightarrow \Pi_3 \rightarrow \Pi_1$ of length 3 exists in this game. Furthermore, the existence of CF cycle is shown for *individual* approval from the new coalition which implicitly proves (see Remark 2) the existence of cycle for CF algorithms based on *altruistic* approval from the new coalition.

For the CF algorithm based on $(s, indv, no)$ rule, the final network partition Π_f is said to be *individual stable* (IS) [137], if the distributed players converge to Π_f such that no player prefers to leave its coalition. However, the stability of CF algorithm based on $(s, indv, no)$, and $(s, altru, no)$ rules cannot be guaranteed.

Corollary 2: Starting from any initial network partition Π_0, the CF algorithm based on (s, no, no) rule is vulnerable to a CF cycle, with the length of cycle as small as 2.

Illustration: Consider a CF game with two players and the initial network partition $\Pi_0 = \{S_1, S_2\} = \{\{1\}, \{2\}\}$ with the payoff vector $\mathbf{x}^{(0)} = [10, 20]$. Furthermore, consider a possible transition to the network partition; $\Pi_1 = S_1 = \{1, 2\}$, with the payoff vector $\mathbf{x}^{(1)} = [11, 19]$. For the considered game, the following preference relations exist:

$$(S_1, \Pi_1) \succ_{1,(s,no,no)} (S_1, \Pi_0)$$
$$(S_2, \Pi_0) \succ_{2,(s,no,no)} (S_1, \Pi_1)$$

(5.13)

It is conceivable that a CF cycle: $\Pi_0 \to \Pi_1 \to \Pi_0$ exists in this game with length 2.

For the CF algorithm based on (s, no, no) rule, the final network partition Π_f is said to be *Nash stable* (NS) [137], if the distributed players converge to Π_f such that no player prefers to leave its coalition. However, the stability of CF algorithm based on (s, no, no) rule cannot be guaranteed.

Based on the above discussion, CF rules that do not consider the effect of the movement of switching player, on both new and old coalition, are vulnerable to a *cycle* in the CF process which leads to *unstability*. The following section presents two solutions to deal with CF cycle.

5.4.5   Dealing With CF Cycle

A *CF cycle* indicates the *non-convergent* behavior of CF process in the sense that, instead of a single final network partition Π_f, it offers *multiple operating*

points in the form of a collection of network partitions Π_{cycle}. For example, when $\Pi_{r,N} = \Pi_{r-2,N}$, a CF cycle with length $2N$ is observed, indicated as:

$$\Pi_{cycle} = \left\{ \Pi_{r-2,N}, \Pi_{r-1,1}, \Pi_{r-1,2}, \cdots, \Pi_{r-1,N}, \Pi_{r,1}, \Pi_{r,2}, \cdots \Pi_{r,N} = \Pi_{r-2,N} \right\}.$$

(5.14)

Typically, the existence of a CF cycle is attributed to the *unstability* of CF algorithm. The conventional approach to avoid cycles in the CF process is to modify the CF rules. In the following, such modifications are discussed in the proposed CF rules, to guarantee stability. Furthermore, the case in which no variations are possible in the proposed rules is considered, and different exit procedures from possible cycles are described by defining how to select Π_f from Π_{cycle} or how to operate over multiple points in Π_{cycle} if a CF cycle is inevitable.

Avoiding Cycles in the CF Process

Remark 3 identifies the visit to *coalition history set* $h(i)$ by at least one player $i \in \mathcal{N}$ as the necessary condition for the occurrence of CF cycle. Therefore, cycles can be avoided in the proposed coalition formation algorithm by incorporating the history condition [54], [55] in the generalized CF rule (given under Section 5.4.2). History condition implies that a player $i \in \mathcal{N}$ under network partition Π can only propose to switch from its current Coalition $S_k \in \Pi$ to another coalition $S_l \in \Pi \cup \{\phi\}$, $l \neq k$ provided $S_l \notin h(i)$. This can be accomplished by maintaining coalition history set at each player $i \in \mathcal{N}$, which must be updated whenever a

player switches from its current coalition to another coalition.

It is important to point out here that some prior works such as [138] restrict the action space of players from *merge-split* to *merge-only* to avoid cycles in the CF process. However, it is arguable that using a history condition or restricting the action space of players, achieves stability at the cost of limited freedom of players in the network, and such approaches are not justified specially when players may find incentive to revisit a coalition in their coalition history set or prefer to switch from their current coalitions but are not allowed to. Therefore, it is interesting to analyze the behavior of players when no *stability-forcing* condition is imposed in the CF rules and discuss different exit procedures when the CF process leads to a cycle.

Exiting from Cycles in the CF Process

In the following, two fundamental approaches to deal with CF cycles are presented: (1) operate over multiple network partitions through time-sharing or (2) select an appropriate operating point from the pool of multiple network partitions given by the CF algorithm.

The number of partitions in a CF cycle is an integer multiple of N, say kN. If τ represents the total available transmission time, after which the CF process is invoked again to incorporate any change in the network conditions, it is proposed to divide τ in kN equal duration transmission slots during which the network operates over kN network partitions. The main rationale behind operating over multiple network partitions through time-sharing is to provide *fair* chance to each

147

player in the network to transmit when its preferred network partition is in place. This can be accomplished based on a predetermined time-sharing policy while the duration of each time slot can be readily calculated as $\tau/(kN)$. However, it is important to point out here that network partition after each iteration, $\Pi_{r,i}$, must be stored in the *iteration-level partition history set* to be maintained by all the players in the network, in order to know the multiple operating points when the CF process leads to a cycle. Furthermore, in order to operate over multiple network partitions, coalition heads in these partitions must save the optimal BW allocation for their members so that all the coalitions operate at maximum rate during their allocated time slot.

In comparison to operating over multiple network partitions, an appropriate operating point may be selected from Π_{cycle} to exit from the CF cycle. This would relieve the players, from saving/maintaining *iteration-level partition history set*, and the coalition heads, from saving the optimal BW allocation for its members under all network partitions in Π_{cycle}. However, an appropriate network partition can only be found after comparing all partitions in Π_{cycle} which requires all players to save their individual payoff (transmission rate) under all network partitions in Π_{cycle}. Any randomly chosen player can take the responsibility to acquire the individual payoffs of all players under all network partitions and making the comparisons to identify an appropriate network partition. Furthermore, once the appropriate network partition is selected, coalition heads in this partition would have to optimally allocate the BW to their members to maximize their coalition

sum-rate. The appropriate network partition may be selected to be any *Pareto optimal* (not *Pareto dominated* by another network partition in Π_{cycle}) partition from Π_{cycle}. It is important to highlight here that from network's perspective, the best partition would be the one which offers maximum throughput among Π_{cycle}. However, the results of Section 5.6 show that the gain in average payoff is not significant by operating over a throughput-efficient network partition or any other randomly selected partition in Π_{cycle}. Based on these observations, it is recommended to operate over the first network partition in Π_{cycle}; i.e., exiting the CF cycle with $\Pi_{r,N}$, similar to the case when all players converge to $\Pi_f = \Pi_{r,N}$, since this would require no computational overhead to any player in the network while achieving the average payoff per player comparable to throughput-efficient operating point.

5.5 Probabilistic Analysis of Coalition Formation

This section presents the probabilistic analysis of the stability of grand coalition and singleton structure. These probabilities will be used to evaluate a lower bound on the probability that a network partition, obtained through the proposed CF algorithm, that is neither GCS nor SCS, is stable. The probabilistic analysis shown in the following subsections considers the (*selfish,no,no*) CF rule. However, similar lines of derivations can be adopted for other CF rules.

5.5.1 Probability That GCS Is Stable

Consider a network with N links operating in a grand coalition; i.e., $\Pi_0 = \mathcal{N} = \{1, 2, ..., N\}$. This GCS would be stable if each player in the network prefers to stay in GCS. Mathematically, this requires that no player $i \in \mathcal{N}$ is capable of improving its rate by *splitting* from GCS to act as a singleton Coalition $\{i\} \in \dot{\Pi}_0$, $\dot{\Pi}_0 = \{\{i\}, \mathcal{N}\backslash\{i\}\}$; i.e.,

$$P(\text{GCS is stable}) = P\left(R_i^{\{i\},\dot{\Pi}_0} < R_i^{\mathcal{N},\Pi_0}\right) \quad \forall \, i \in \mathcal{N}, \tag{5.15}$$

where the two rate equations to compare are given by:

$$
\begin{aligned}
R_i^{\{i\},\dot{\Pi}_0} &= 1 \times W \log\left(1 + \frac{P_i|h_{ii}|^2}{1 \times (N_0 W + \sum_{j=1, j\neq i}^{N} P_j|h_{ji}|^2)}\right), \\
R_i^{\mathcal{N},\Pi_0} &= \frac{1}{N} \times W \log\left(1 + \frac{P_i|h_{ii}|^2}{\frac{1}{N} \times (N_0 W + 0)}\right).
\end{aligned}
\tag{5.16}
$$

It is important to point out here that for simplicity of the analysis, equal BW allocation ($\mu_i^{S_k} = \frac{1}{|S_k|}$) among coalition members is considered here, while the total available bandwidth (W) is re-used by each coalition in the existing network partition.

These rate equations can be expressed in terms of random variables (RVs) by taking into consideration that all channels follow a quasi-static Rayleigh flat fading model and the transmitted power P_i is normalized to 1, while the channel coefficients are normalized by noise power $N_0 W$. Therefore, the rate equations

can be expressed in a simplified form as:

$$R_i^{\{i\},\dot{\Pi}_0} = W \log \left(1 + \frac{X_i}{1 + Y_i^{\{i\}}} \right),$$

$$R_i^{\mathcal{N},\Pi_0} = \frac{1}{N} W \log \left(1 + N X_i \right),$$

(5.17)

where, $X_i \sim \alpha_i \exp(-\alpha_i x_i)$ is an exponentially distributed random variable, with $1/\alpha_i$ representing the mean direct link SNR for player $i \in \mathcal{N}$ and $Y_i^{\{i\}}$ is the total interference observed at the receiver of link $i \in \{i\}$ given by $\sum_{j=1, j \neq i}^{N} Y_{ji}$ with $Y_{ji} \sim \beta_{ji} \exp(-\beta_{ji} y_{ji})$, where $1/\beta_{ji}$ represents the mean SNR observed at the receiver of link i due to the interference caused from link $j \in \mathcal{N}, j \neq i$.

Since, all players decide, independently from each other, to stay/split from GCS, the probability that GCS is stable can be evaluated as the product, over all players $i \in \mathcal{N}$, of the probability that a player i prefers to stay in GCS, which can be obtained from (5.15) and (5.17). This can be written as:

$$P(\text{GCS is stable}) = \prod_{i=1}^{N} P(\text{player } i \text{ stays in GCS})$$

$$= \prod_{i=1}^{N} P \left((1 + \frac{X_i}{1 + Y_i^{\{i\}}}) < (1 + N X_i)^{\frac{1}{N}} \right).$$

(5.18)

Probability that a player i prefers to stay in GCS can be further simplified by using the total probability theorem [139] and exploiting the statistical independence between the RVs X_i and $Y_i^{\{i\}}$ as:

$P(\text{player } i \text{ stays in GCS})$

$$= \int_{-\infty}^{\infty} P\left(\left(\left(1 + \frac{X_i}{1 + Y_i^{\{i\}}}\right) < (1 + NX_i)^{\frac{1}{N}}\right) \mid X_i = x_i\right) f_{X_i}(x_i) dx_i \qquad (5.19)$$

$$= \int_0^{\infty} \left(1 - F_{Y_i^{\{i\}}}\left(\frac{x_i}{(1 + Nx_i)^{\frac{1}{N}} - 1} - 1\right)\right) \alpha_i \exp(-\alpha_i x_i) dx_i,$$

where $F_{Y_i^{\{i\}}}(y_i) = \int_0^{y_i} f_{Y_i^{\{i\}}}(\xi) d\xi$ is the probability distribution function of the sum of exponentials, $Y_i^{\{i\}} = \sum_{j=1, j \neq i}^{N-1} Y_{ji}$. This distribution function for the general case of distinct $\beta_{ji} \; \forall \; i, j$ can be evaluated (see Appendix) to yield:

$$F_{Y_i^{\{i\}}}(y_i) = \left(\prod_{j=1, j \neq i}^{N} \beta_{ji}\right) \left(\sum_{j=1, j \neq i}^{N} \frac{1 - exp(-\beta_{ji} y_i)}{\beta_{ji} \prod_{l=1, l \neq i, j}^{N} (\beta_{li} - \beta_{ji})}\right), \qquad (5.20)$$

and for the simple case of IID interferers where, $\beta_{ji} = \beta \; \forall \; i, j$ as:

$$F_{Y_i^{\{i\}}}(y_i) = 1 - \frac{\Gamma(N - 1, \beta y_i)}{\Gamma(N - 1)}. \qquad (5.21)$$

Using these distribution functions, (5.18), and (5.19), the probability that GCS is stable, for the most general case of different $\alpha_i, \; \forall \; i \in \mathcal{N}$ and different $\beta_{ji}, \; \forall \; i, j \in$

$\mathcal{N}$, is given by:

$$P(\text{GCS is stable}) = \prod_{i=1}^{N} \int_{0}^{\infty} \left(1 - \left(\prod_{j=1,j\neq i}^{N} \beta_{ji} \right) \right.$$

$$\left. \times \left(\sum_{j=1,j\neq i}^{N} \frac{1 - exp\left(-\beta_{ji}\left(\frac{x_i}{(1+Nx_i)^{\frac{1}{N}}-1} - 1 \right) \right)}{\beta_{ji} \prod_{l=1,l\neq i,j}^{N} (\beta_{li} - \beta_{ji})} \right) \right) \alpha_i \exp(-\alpha_i x_i) dx_i.$$

$$(5.22)$$

while, if $\alpha_i = \alpha$, $\forall\, i \in \mathcal{N}$ and $\beta_{ji} = \beta$, $\forall\, i,j \in \mathcal{N}$ is considered, the probability that GCS is stable can be evaluated as:

$$P(\text{GCS is stable}) = \left[\int_{0}^{\infty} \left(\frac{\Gamma\left(N-1, \beta\left(\frac{x}{(1+Nx)^{\frac{1}{N}}-1} - 1 \right) \right)}{\Gamma(N-1)} \right) \alpha \exp(-\alpha x) dx \right]^{N}.$$

$$(5.23)$$

5.5.2 Probability That SCS Is Stable

Proceeding on similar lines to Section 5.5.1, a network of N links is considered to be partitioned in N singleton coalitions; i.e., $\Pi_1 = \{S_1, S_2, ..., S_N\}$, with $S_i = \{i\}$. The network partition Π_1, comprising of all SCs, would be stable if each player in the network prefers to stay singleton. Mathematically, this requires that no player $i \in S_i, S_i \in \Pi_1$ is capable of improving its rate by *merging* with any other coalition $S_k \in \Pi_1, k \neq i$ to make a new coalition $S_{(ik)} = S_i \cup S_k = \{i, k\} \in \ddot{\Pi}_1$

where $\ddot{\Pi}_1 = \left\{ \bar{S}_{(ik)}, \{i,k\} \right\}, \bar{S}_{(ik)} = \Pi_1 \backslash \{i\} \backslash \{k\}$; i.e.,

$$P(\text{SCS is stable under } (s,no,no) \text{ CF rule}) = P\left(R_i^{\{i,k\},\ddot{\Pi}_1} < R_i^{\{i\},\Pi_1} \right) \quad \forall \; i,k \in \mathcal{N}. \tag{5.24}$$

It is important to point out here that the above probability that SCS is stable is based on the (s,no,no) CF rule. The other CF rules can also be analyzed by considering additional rate improvements. For example, the probability that SCS is stable for $(s,indv,no)$ CF rule would be given by:

$$P(\text{SCS is stable under } (s,indv,no) \text{ CF rule})$$
$$= 1 - \left[P\left(R_i^{\{i,k\},\ddot{\Pi}_1} > R_i^{\{i\},\Pi_1} \right), \; P\left(R_k^{\{i,k\},\ddot{\Pi}_1} < R_k^{\{k\},\Pi_1} \right) \right] \; \forall \; i,k \in \mathcal{N}. \tag{5.25}$$

For the sake of illustration, in the following, the evaluation of probability of all SCs being stable is demonstrated based on (s,no,no) CF rule as given by (5.24) by considering equal BW allocation among coalition members while the total available bandwidth (W) is re-used by each coalition in the existing network partition. Similar to Section 5.5.1, equal BW allocation among the coalition members is assumed. Therefore, the two rate equations to compare are given by:

$$R_i^{\{i,k\},\ddot{\Pi}_1} = 0.5 \times W \log \left(1 + \frac{P_i |h_{ii}|^2}{0.5 \times (N_0 W + \sum_{j=1,j\neq i,k}^N P_j |h_{ji}|^2)} \right),$$

$$R_i^{\{i\},\Pi_1} = 1 \times W \log \left(1 + \frac{P_i |h_{ii}|^2}{1 \times (N_0 W + \sum_{j=1,j\neq i}^N P_j |h_{ji}|^2)} \right). \tag{5.26}$$

Most importantly, since the rate of a player $i \in S, S \in \Pi$ does not depend on how the other players $j \in \Pi \backslash S$ are organized outside the coalition S, it is obvious that the rate of Player i being singleton would not depend on whether each of the remaining $\mathcal{N} \backslash i$ players make a singleton coalition, leading to network partition Π_1, or all the remaining players make a single coalition, leading to network partition $\dot{\Pi}_0$. Hence, $R_i^{\{i\},\Pi_1}$ would be same as $R_i^{\{i\},\dot{\Pi}_0}$, which is also evident from (5.16) and (5.26). Therefore, the rate equations needed to calculate the probability that SCS is stable can be expressed using the same RVs X_i and $Y_i^{\{i\}}$, used in Section 5.5.1, along with an additional RV $Y_i^{\{i,k\}} = \sum_{j=1,j\neq i,k}^N Y_{ji}$ which can be derived from $Y_i^{\{i\}}$ as: $Y_i^{\{i,k\}} = Y_i^{\{i\}} - Y_{ki}$. These rate equations can be expressed in a simplified form as:

$$R_i^{\{i,k\},\ddot{\Pi}_1} = 0.5 W \log \left(1 + \frac{2X_i}{1 + Y_i^{\{i,k\}}} \right),$$

$$R_i^{\{i\},\Pi_1} = W \log \left(1 + \frac{X_i}{1 + Y_i^{\{i\}}} \right). \tag{5.27}$$

Based on the statistical independence of individual players' decisions to stay as singleton or merge with another player, the probability that SCS is stable can be evaluated as the product, over all players $i \in \mathcal{N}$, of the probability that a

player i prefers to stay as SC, which can be obtained from (5.24) and (5.27). This can be written as:

$$P(\text{SCS is stable}) = \prod_{i=1}^{N} P(\text{player } i \text{ stays as SC}) = \prod_{i=1}^{N} \prod_{k=1, k \neq i}^{N} P\left(R_i^{\{i,k\}, \ddot{\Pi}_1} < R_i^{\{i\}, \Pi_1}\right)$$

$$= \prod_{i=1}^{N} \prod_{k=1, k \neq i}^{N} P\left((1 + \frac{2X_i}{1 + Y_i^{\{i,k\}}})^{0.5} < (1 + \frac{X_i}{1 + Y_i^{\{i,k\}} + Y_{ki}})\right).$$

(5.28)

Probability that a player i prefers to stay as SC can be further simplified by using the total probability theorem [139] and exploiting the statistical independence between the RVs X_i and $Y_i^{\{i,k\}}$ as:

$P(\text{player } i \text{ stays as SC})$

$$= \int_{-\infty}^{\infty} \int_{-\infty}^{\infty} P\left(\left(\left(1 + \frac{2X_i}{1 + Y_i^{\{i,k\}}}\right)^{0.5} < \left(1 + \frac{X_i}{1 + Y_i^{\{i,k\}} + Y_{ki}}\right)\right)\right.$$

$$\left. \mid X_i = x_i, Y_i^{\{i,k\}} = \acute{y}_i\right) f_{X_i}(x_i) f_{Y_i^{\{i,k\}}}(\acute{y}_i) dx_i d\acute{y}_i$$

$$= \int_{\acute{y}_i=0}^{\infty} \int_{x_i=0}^{\infty} \left(F_{Y_{ki}}\left(\frac{x_i}{(1 + \frac{2x_i}{1+\acute{y}_i})^{0.5} - 1} - 1 - \acute{y}_i\right)\right) f_{X_i}(x_i) f_{Y_i^{\{i,k\}}}(\acute{y}_i) dx_i d\acute{y}_i,$$

(5.29)

where (1) $F_{Y_{ki}}(y_{ki}) = \int_0^{y_{ki}} f_{Y_{ki}}(\xi) d\xi$ is the probability distribution function of an exponential RV $Y_{ki} \sim \beta_{ki} \exp(-\beta_{ki} y_{ki})$ where $1/\beta_{ki}$ represents the mean SNR observed at the receiver of link i due to the interference caused from link $k \in \mathcal{N}, k \neq i$. (2) $X_i \sim \alpha_i \exp(-\alpha_i x_i)$ is an exponentially distributed random

156

variable with $1/\alpha_i$ representing the mean direct link SNR for player $i \in \mathcal{N}$, and (3) $Y_i^{\{i,k\}}$ is the total interference observed at the receiver of link $i \in \{i, k\}$ given by $\sum_{j=1, j\neq i,k}^{N} Y_{ji}$ with $Y_{ji} \sim \beta_{ji} \exp(-\beta_{ji} y_{ji})$ where $1/\beta_{ji}$ represents the mean SNR observed at the receiver of link i due to the interference caused from link $j \in \mathcal{N}, j \neq i, k$. For the general case of distinct $\beta_{ji} \; \forall \; i, j$, the probability density function can be evaluate (see Appendix) as:

$$f_{Y_i^{\{i,k\}}}(\acute{y}_i) = \left(\prod_{j=1, j\neq i,k}^{N} \beta_{ji} \right) \left(\sum_{j=1, j\neq i,k}^{N} \frac{\exp(-\beta_{ji}\acute{y}_i)}{\prod_{l=1, l\neq i,j,k}^{N} (\beta_{li} - \beta_{ji})} \right), \qquad (5.30)$$

while for the simple case of IID interferers where, $\beta_{ji} = \beta \; \forall \; i, j$, the probability density function is given by:

$$f_{Y_i^{\{i,k\}}}(\acute{y}_i) = \frac{\beta^{N-2}}{\Gamma(N-2)} (\acute{y}_i)^{N-3} \exp(-\beta\acute{y}_i). \qquad (5.31)$$

Using these distribution, density functions, (5.28), and (5.29), the probability that SCS is stable, for the most general case of different $\alpha_i, \; \forall \; i \in \mathcal{N}$ and different $\beta_{ji}, \; \forall \; i, j \in \mathcal{N}$, is given by:

$P(\text{SCS is stable})$

$$= \prod_{i=1}^{N} \prod_{k=1, k\neq i}^{N} \int_{\acute{y}_i=0}^{\infty} \int_{x_i=0}^{\infty} \left(1 - \exp\left(\beta_{ki} \left(\frac{x_i}{(1 + \frac{2x_i}{1+\acute{y}_i})^{0.5} - 1} - 1 - \acute{y}_i \right) \right) \right)$$

$$\times \; \alpha_i \exp(-\alpha_i x_i) \left(\prod_{j=1, j\neq i,k}^{N} \beta_{ji} \right) \left(\sum_{j=1, j\neq i,k}^{N} \frac{\exp(-\beta_{ji}\acute{y}_i)}{\prod_{l=1, l\neq i,j,k}^{N} (\beta_{li} - \beta_{ji})} \right) dx_i d\acute{y}_i,$$

$$(5.32)$$

while, if $\alpha_i = \alpha \ \forall \ i \in \mathcal{N}$ and $\beta_{ji} = \beta, \ \forall \ i, j \in \mathcal{N}$ is considered, the probability that SCS is stable is given by:

$$
P(\text{SCS is stable}) = \left[\int_{\acute{y}_i=0}^{\infty} \int_{x_i=0}^{\infty} \left(1 - \exp\left(\beta \left(\frac{x_i}{(1 + \frac{2x_i}{1+\acute{y}_i})^{0.5} - 1} - 1 - \acute{y}_i \right) \right) \right) \right.
$$
$$
\left. \times \ \alpha \exp(-\alpha x_i) \ \left(\frac{\beta^{N-2}}{\Gamma(N-2)} (\acute{y}_i)^{N-3} \exp\left(-\beta \acute{y}_i \right) \right) dx_i d\acute{y}_i \right]^{N(N-1)}.
$$

$$(5.33)$$

5.5.3 Probability That a General Network Partition Is Stable

The probabilities of GCS and SCS being stable can be used to derive a lower bound on the probability that a network partition (other than GCS and SCS), is stable. The probability that a network partition other than GCS/SCS is stable, is reflective of the effectiveness of the proposed CF algorithms over a wide operating range of direct link SNR; ($[0, 20]$ dB) when the average interfering link SNR; $U[-10, 0]$ dB. Mathematically, the probability of a general network partition (other than GCS/SCS) being stable, is given by:

$$
P(\text{partition (other than GCS/SCS) is stable}) > 1 - P(\text{GCS is stable}) - P(\text{SCS is stable}).
$$

$$(5.34)$$

For the most general case of different $\alpha_i \ \forall \ i \in \mathcal{N}$ and different $\beta_{ji}, \ \forall \ i, j \in \mathcal{N}$,

this probability can be obtained using, (5.22), (5.32), and (5.34) to yield:

P(partition (other than GCS/SCS) is stable)

$$
> 1 - \left(\prod_{i=1}^{N} \int_{0}^{\infty} \left(1 - \left(\prod_{j=1, j \neq i}^{N} \beta_{ji} \right) \left(\sum_{j=1, j \neq i}^{N} \frac{1 - exp\left(-\beta_{ji}\left(\frac{x_i}{(1+Nx_i)^{\frac{1}{N}} - 1} - 1 \right) \right)}{\beta_{ji} \prod_{l=1, l \neq i,j}^{N} (\beta_{li} - \beta_{ji})} \right) \right) \right.
$$
$$
\left. \times \; \alpha_i \exp(-\alpha_i x_i) dx_i \right)
$$
$$
- \left(\prod_{i=1}^{N} \prod_{k=1, k \neq i}^{N} \int_{\acute{y}_i=0}^{\infty} \int_{x_i=0}^{\infty} \left(1 - \exp\left(\beta_i \left(\frac{x_i}{(1 + \frac{2x_i}{1+\acute{y}_i})^{0.5} - 1} - 1 - \acute{y}_i \right) \right) \right) \right.
$$
$$
\left. \times \; \alpha_i \exp(-\alpha_i x_i) \left(\prod_{j=1, j \neq i,k}^{N} \beta_{ji} \right) \left(\sum_{j=1, j \neq i,k}^{N} \frac{\exp(-\beta_{ji}\acute{y}_i)}{\prod_{l=1, l \neq i,j,k}^{N-1} (\beta_{li} - \beta_{ji})} \right) dx_i d\acute{y}_i \right).
$$
$$(5.35)$$

Similarly, considering $\alpha_i = \alpha$, $\forall \, i \in \mathcal{N}$ and $\beta_{ji} = \beta$, $\forall \, i, j \in \mathcal{N}$, the probability of a general network partition being stable is found using (5.23), (5.33), and (5.34) to yield:

P(partition (other than GCS/SCS) is stable)

$$
> 1 - \left[\int_{0}^{\infty} \left(\frac{\Gamma\left(N - 1, \beta\left(\frac{x}{(1+Nx)^{\frac{1}{N}} - 1} - 1 \right) \right)}{\Gamma(N-1)} \right) \alpha \exp(-\alpha x) dx \right]^{N}
$$
$$
- \left[\int_{\acute{y}_i=0}^{\infty} \int_{x_i=0}^{\infty} \left(1 - \exp\left(\beta\left(\frac{x_i}{(1 + \frac{2x_i}{1+\acute{y}_i})^{0.5} - 1} - 1 - \acute{y}_i \right) \right) \right) \right.
$$
$$
\left. \times \; \alpha \exp(-\alpha x_i) \left(\frac{\beta^{N-2}}{\Gamma(N-2)} (\acute{y}_i)^{N-3} \exp(-\beta \acute{y}_i) \right) dx_i d\acute{y}_i \right]^{N(N-1)}.
$$
$$(5.36)$$

5.6 Performance Evaluation

This section presents the performance evaluation of the proposed CF algorithm by examining the average payoff (rate in Mbps) per link and analyzing the effect of

different proposed CF rules on the algorithm convergence properties. It is assumed that each player is aware of the average interference from every other player in the network. Furthermore, it is assumed that the total available bandwidth W for the secondary access is 5 MHz. All the channels are assumed to follow a quasi-static Rayleigh flat fading model, and hence the received signal power, interference power and signal to noise ratio (SNR) are exponentially distributed. Simulation results are averaged over $100,000$ channel realizations. The transmit power P_i and noise power spectral density (N_0) are normalized to 1, and their effects are included in the channel coefficients. The network performance is analyzed for $N = 10$ randomly distributed links over a wide range of average direct link SNR with the mean of the interference power among the links to be uniformly distributed between -10 dB and 0 dB.

5.6.1   Average Payoff Per Link Under Different CF Rules

Figs. 5.3 and 5.4 show the average payoff (rate in Mbps) per link offered by the proposed CF algorithm with optimal BW allocation under different CF rules, when the CF process is initialized in a singleton structure (SCS) and grand coalition (GCS), respectively. The achievable rate is compared with three benchmark cases: (1) CF based on the sum-rate maximizing CF rule, which is called *global altruistic* rule, where, a player switches from its current coalition to a new coalition to improve the overall network throughput, irrespective of the effect of its movement on its individual rate, (2) always GCS/SCS, and (3) CF with equal BW allocation.
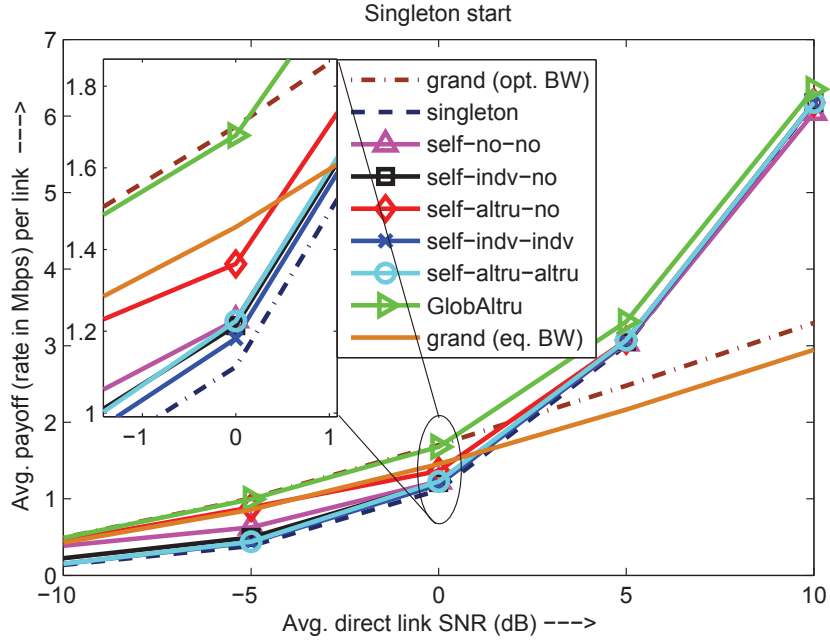
Figure 5.3: Average payoff per link: Singleton start.

Simulation results indicate that, in general, average payoff per link increases with increasing the average direct link SNR, however, the initial network partition plays an important role in determining the achievable payoff, specially at low SNR. The upper limit on the achievable payoff is depicted through global altruistic CF rule, which indicates that at low SNR ($SNR \leq 0\ dB$), average payoff per link is maximum in a GCS, while at high SNR ($SNR \geq 3\ dB$), SCS offers much better average payoff per link in comparison to GCS. Fig. 5.3 shows that starting from SCS, all the proposed CF rules offer almost the same average payoff per link at high average direct link SNR. The average payoff per link is approximately the same as in SCS, reaching up to 92% of the maximum achievable value (given by global altruistic rule) at 5 dB, and increasing further with the SNR. However, at low SNR, different CF rules offer different average payoff per link, which is normally

161
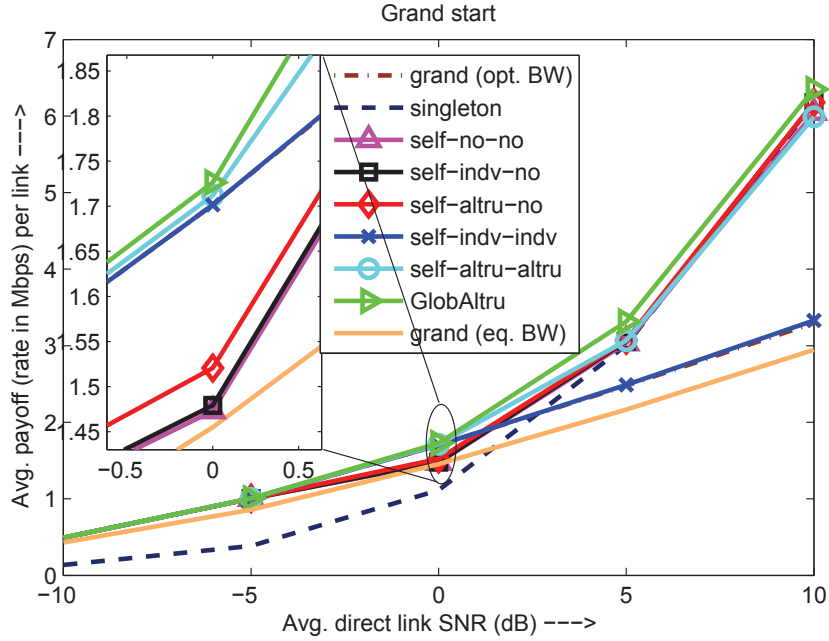
Figure 5.4: Average payoff per link: Grand start.

much lower than the achievable maximum payoff. This indicates that, starting from SCS, the distributed players do not reach the rate-maximizing GCS under any of the CF rules. In fact, (*self,altru,no*) performs best among all proposed CF rules in low SNR regime by providing 89% of the maximum achievable average payoff per link at $SNR = -5 \ dB$, but the payoff drops to 81% of the maximum achievable value at $SNR = 0 \ dB$.

Fig. 5.4 compares the performance of different CF rules when the CF algorithm is initialized in a GCS. In this case, all the proposed CF rules offer the maximum average payoff per link for $SNR \leq -5 \ dB$, which reflects that over this SNR range, all the players stay in GCS. For $-5 \ dB < SNR \leq 0 \ dB$, (*self,indv,indv*) and (*self,altru,altru*) rules maintain the maximum payoff per link while the payoff provided by all other CF rules drops as the SNR increases from

$-5\ dB$ to $0\ dB$, getting to 88% of the maximum achievable average payoff per link at $SNR = 0\ dB$. This indicates that the distributed players prefer to remain in GCS under (*self,indv,indv*) and (*self,altru,altru*) rules while they leave the GCS in case of other CF rules, when the average direct link SNR exceeds $-5\ dB$. In fact, under (*self,indv,indv*) rule, the players do not leave their initial coalition (GCS) at all, and hence, for $SNR > 0\ dB$), this rule offers much degraded average payoff per link as compared to other rules. It is also interesting to note that over moderate SNR range; i.e., $0\ dB < SNR < 5\ dB$, the average payoff per link under (*self,altru,altru*) rule decreases from 100% of the maximum achievable value at $0\ dB$ to 92% of the maximum achievable value at $5\ dB$, while the average payoff per link provided by all other rules (except (*self,indv,indv*) rule) increases from 88% of the maximum achievable value at $0\ dB$ to 92% of the maximum achievable value at $5\ dB$. Comparison of Figs. 5.3 and 5.4 reveal that at high SNR ($SNR > 5\ dB$), all CF rules (except (*self,indv,indv*)) offer almost same average payoff per link, no matter whether the CF algorithm is initialized in a GCS or SCS.

Furthermore, simulations results show that all CF rules offer more average payoff per link using optimal BW allocation as compared to equal BW allocation among the coalition members. The performance gain is depicted in Figs. 5.3 and 5.4 by comparing average payoff per link in GCS under optimal and equal BW allocation. The results indicate that optimal BW allocation provides 12% more average payoff per link as compared to equal BW allocation at the moderate SNR

value of 0 dB, where all CF rules offers approximately the same payoff.

Since, initialization of the proposed CF algorithm in GCS offers better average payoff per link over a wide SNR range, as compared to initialization in SCS, the following results assume GCS initialization, unless stated otherwise.

5.6.2 Effectiveness of the Proposed CF Algorithm
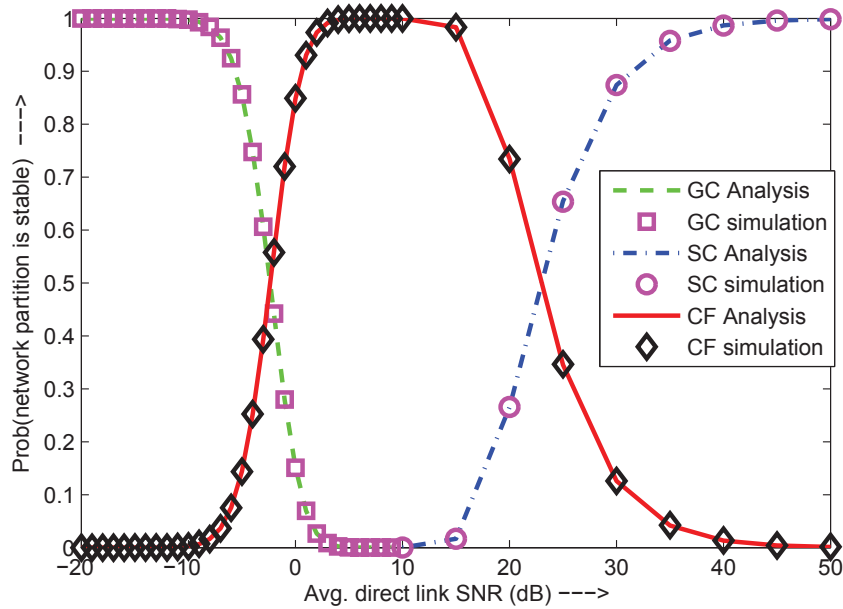
Figure 5.5: Useful average direct link SNR range of the proposed CF algorithm based on (*self,no,no*) rule.

Fig. 5.5 shows the probability of GCS and SCS being stable and use these probabilities to evaluate a lower bound on the probability that a general network partition, other than GCS and SCS, is stable against a wide range of average direct link SNR. Simulation results indicate that, in general, GCS is stable at low SNR while SCS is stable at high SNR. However, over a moderate operating SNR, both GCS and SCS do not remain stable and a general network partition emerges

with the probability > 0.5 over the wide SNR range from $-2.5\ dB$ to $23\ dB$ which shows the effectiveness of proposed CF algorithm for moderate operating SNR.

5.6.3   Final Network Partition Characteristics
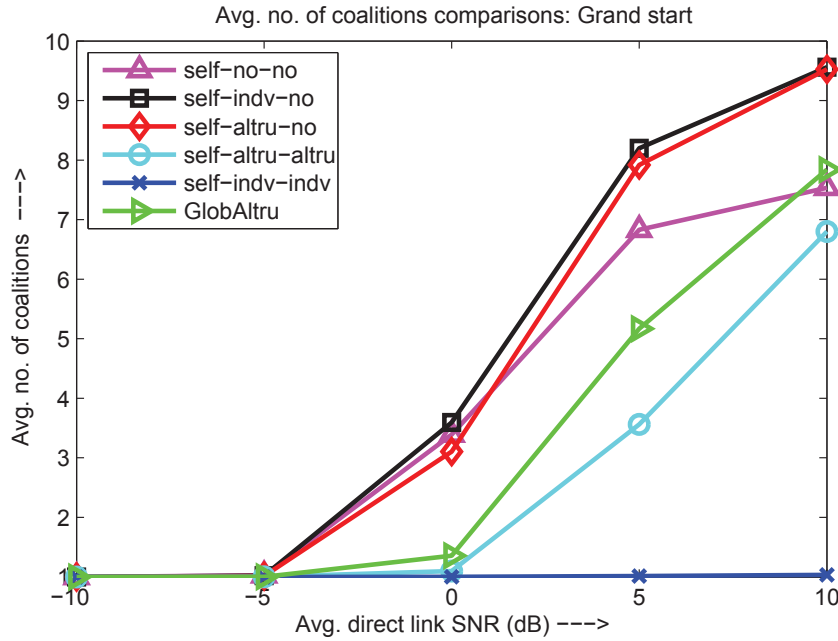
Figure 5.6: Final network partition characteristics: Number of coalitions.

The characteristics of the final network partition resulting from the proposed CF rules are investigated in terms of average number of coalitions and average maximum coalition size in Figs. 5.6 and 5.7, respectively. Simulation results indicate that at low SNR ($SNR \leq -5\ dB$), distributed players prefer to make a grand coalition while the average number of coalitions in the final network partition increases with the SNR for all CF rules with the exception of (*self,indv,indv*) rule, under which the players are never allowed to leave their initial (grand) coalition. Fig. 5.7 shows that at high SNR ($SNR = 10\ dB$), (*self,indv,no*) and (*self,altru,no*)
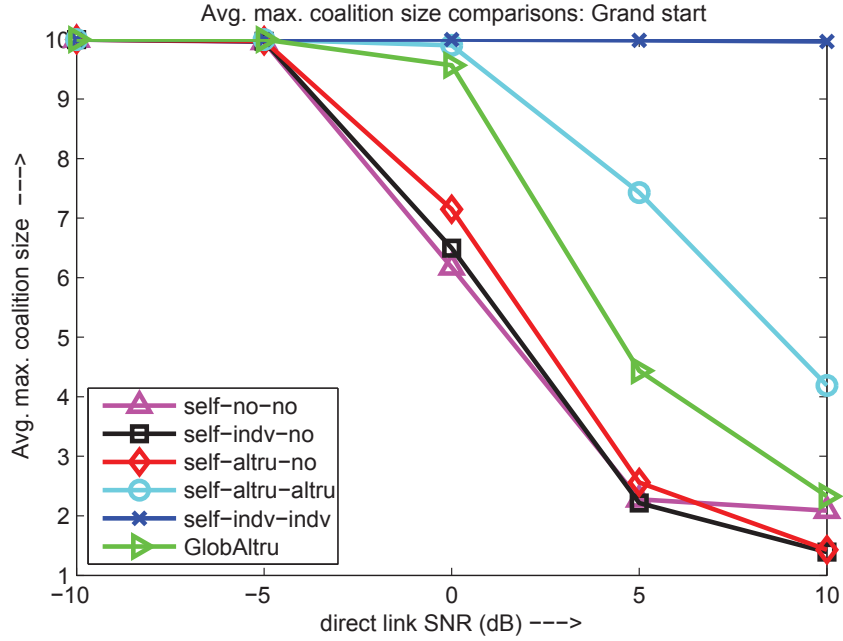
Figure 5.7: Final network partition characteristics: Maximum coalitions size.

rules approach SCS, with average maximum coalition size slightly greater than 1. However, the results show that at $SNR = 10\ dB$, the throughput-efficient structure (given by global altruistic CF rule) consists of maximum coalition size of 2, while (*self,altru,altru*) rule gives average maximum coalition size of 4.

5.6.4 Fairness

Fig. 5.8 shows the average variance among the payoffs of distributed players under different CF rules. In general, variance among the payoffs increases with increasing the SNR. This can be explained by observing that the proposed CF algorithm offers fair distribution of payoffs among players when the final network partition consists of coalitions of large sizes which emerge at low SNR, while large variance among the payoffs is observed at high SNR, as the distributed players prefer to
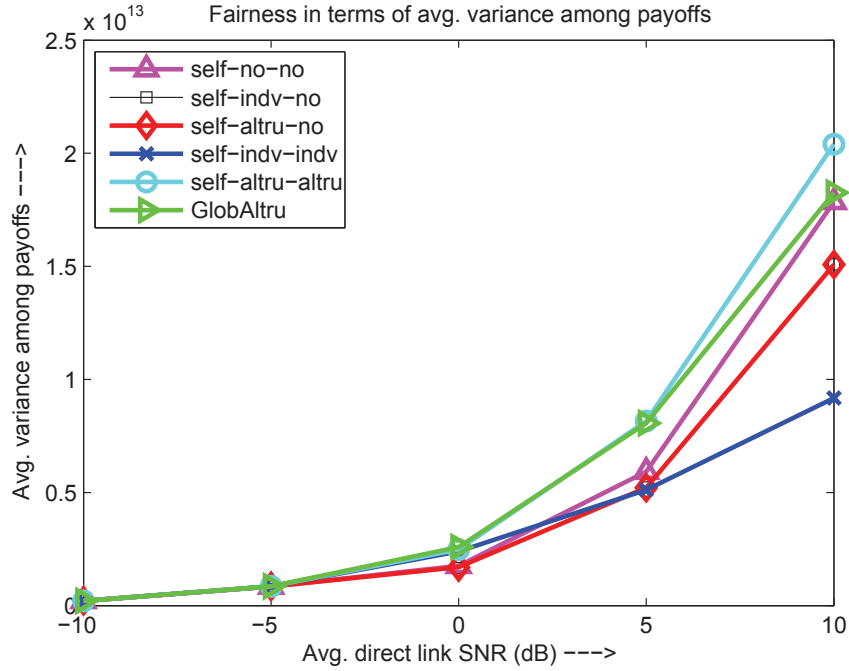
Figure 5.8: Fairness comparison among different CF rules.

operate in small coalitions. It is important to point out here that in comparison to proposed CF rules, global altruistic CF rule results in large variance among the payoffs of distributed players to achieve maximum network rate, over the entire SNR range. This indicates that the network-rate maximizing, global altruistic CF rule, sacrifices the fairness for the rate, while the proposed CF rules maintain a balance between network rate and fairness.

5.6.5 Computational Complexity

The computational complexity of the proposed CF algorithm under different CF rules is depicted in Fig. 5.9 in terms of average number of CF proposals evaluated per link before exiting the CF process. It is evident that at low SNR, CF algorithm initialized in GCS evaluates small number of CF proposals to reach the final
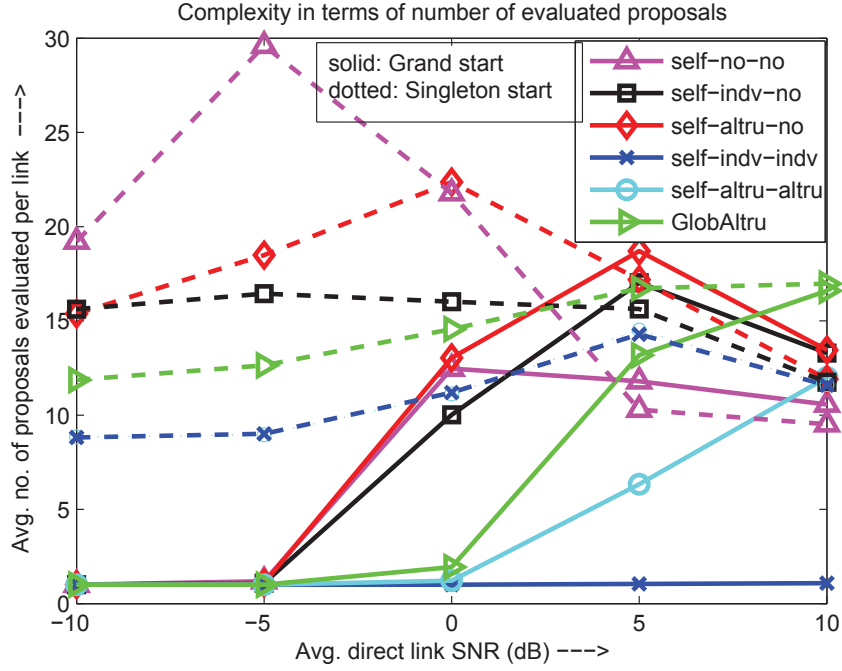
Figure 5.9: Computational complexity.

network partition while at high SNR, SCS initialization results in small number of proposal evaluations per link. However, independent of the algorithm initialization, (*self,altru,no*) rule is computationally most expensive while (*self,indv,indv*) and (*self,altru,altru*) rules evaluate minimum number of proposals per link to reach the final network partition, over wide SNR range.

5.6.6 Stability

The convergence properties of proposed CF rules under grand/singleton start of the CF algorithm are highlighted in Fig. 5.10 in terms of the percentage of stable points among total operating points given by the CF algorithm. Simulation results show that CF algorithm based on global altruistic, (*self,indv,indv*) and (*self,altru,altru*) rules always converge to a stable final network partition. CF
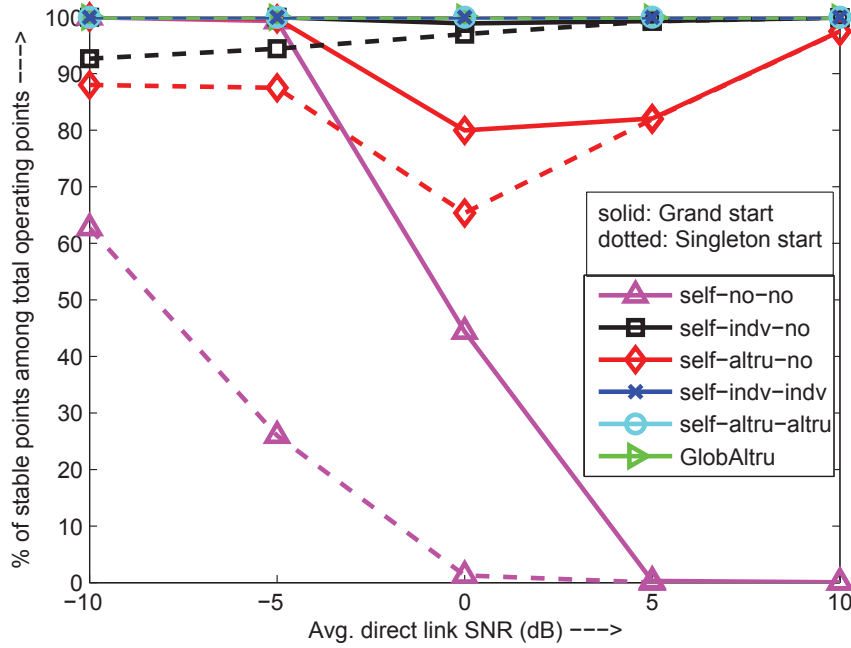
Figure 5.10: Stability.

algorithm based on (*self,indv,no*) rule converges to a stable operating point at $SNR > 5\ dB$, while at low SNR values, more than 93% of the operating points given by CF algorithm are stable when the algorithm is started in a singleton structure, while this percentage increases to 99% in case of grand start. In fact, for $SNR < -5\ dB$, CF algorithm started in a grand coalition converges for all the proposed CF rules since the distributed players do not leave the GCS, however, CF algorithm based on (*self,altru,no*) and (*self,no,no*) rules diverge as SNR increases from $-5\ dB$. With singleton start, CF algorithm based on (*self,altru,no*) and (*self,no,no*) rules do not converge to a stable final network partition for the whole SNR range.

5.6.7 Operating Over Single/Multiple Operating Points
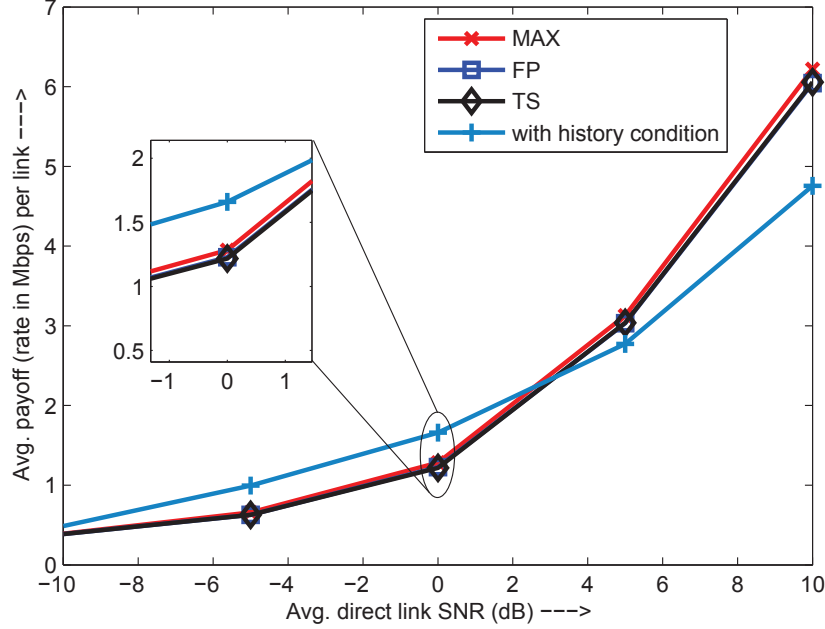
Figure 5.11: Average payoff per link comparisons when operating over single/multiple operating points.

Fig. 5.11 focuses on CF algorithm (initialized in singleton structure) based on (*self,no,no*) rule and highlights the effect of history condition (resulting in a *single* operating point) on the average achievable payoff per link and compares it with various exit options when a CF process ends up in a *cycle*. The three exit options considered are: (1) operating over multiple operating points through time sharing (TS), (2) operating over a network partition offering maximum sum-rate (MAX), and (3) operating over the first network partition (FP) in the cycle. Simulation results show that the three proposed exit options, with different degrees of computational complexity, result in very close average payoff per link over a wide range of SNR. However, in comparison to different exit procedures, CF

algorithm incorporating history condition provides an improved average payoff per link for $SNR < 3\ dB$ after which its performance starts degrading. This indicates that history condition offers stability at high SNR at the cost of reduced average payoff per link.
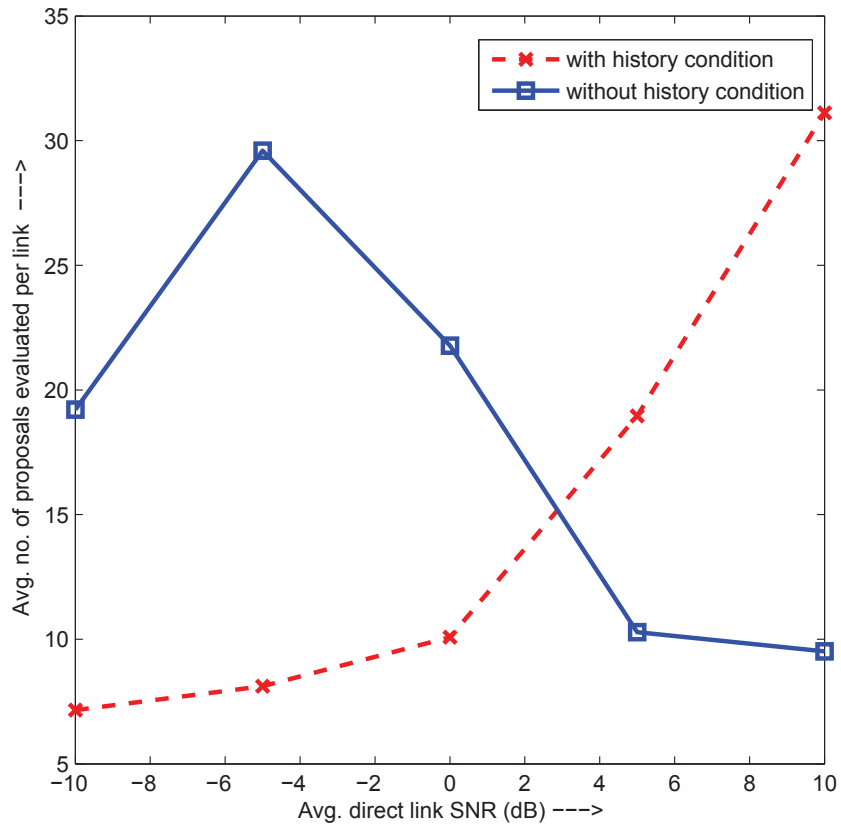
Figure 5.12: Avoiding cycles using history condition: Average number of proposals evaluated per link under (*self,no,no*) CF rule.

Fig. 5.12 shows the effect of using history condition, in (*self,no,no*) CF rule, on algorithm complexity in terms of average number of proposals evaluated per link before exiting the CF process. Simulation results show that for $SNR < 3\ dB$, history condition results in reduced complexity. However, it results in

much large number of proposals, as compared to the CF without incorporating history condition, are evaluated per link as SNR increases from 3 dB. This can be explained based on the fact that at high SNR, distributed players frequently find incentive to revisit coalitions in their history set, however, using history condition, players cannot join these coalitions, and hence, a large number of proposals are evaluated to find a suitable new coalition to join.

CHAPTER 6

CONCLUSIONS AND FUTURE WORK

This chapter summarizes the contributions of the thesis and provides future research directions.

6.1 Summary of Main Contributions

In this thesis, performance enhancement of cognitive radio networks (CRNs) based on dynamic and opportunistic spectrum access has been proposed via cooperative spectrum sensing/access. An in-depth comparative numerical analysis of various spectrum sensing (SS) techniques, presented in Chapter 2, indicated severe performance degradation of all single-user centric sensing schemes under multipath fading. Hence, CRNs must be equipped with cooperative sensing capabilities to improve the sensing reliability, and robustness to the RF environment. These cooperative sensing schemes require low-complexity detection algorithms that can

be applied locally at each radio in the network.

Based on the low-complexity requirement, energy detection (ED) based sensing has been investigated in details, in Chapter 3. The general form of test statistic for ED has been presented and the exact and approximate expressions for its distribution have been revisited to address some of the existing ambiguities in the literature. Exact closed-form expressions for false alarm rate and detection probability have been analyzed for various primary signal models. It has been shown that the detection probability expression of unknown deterministic signals can be extended to the random primary transmissions only for the case of equal energy primary signals. Exact and approximate ROC curves for deterministic and random primary signal models have been compared, and it has been found out that they converge for low SNR but differ significantly under high SNR scenario. Furthermore, the roles of SNR and sensing performance constraints are highlighted when Gaussian approximations are used in place of exact expressions.

Chapters 4 and 5 focus on the throughput-efficient cooperative spectrum access in CRNs. Coalitional game-theoretic framework has been used to model the joint coalition formation (CF) and bandwidth (BW) allocation problem. A closed-form expression of the optimal BW allocation among the coalition members is obtained, and both centralized and ad hoc network models have been considered, to develop efficient CF algorithms, that maximize spectrum reuse efficiency subject to interference constraints.

For centralized CRNs, the throughput-efficient network partitioning problem

has been modeled as a coordinated CF game and an efficient CF algorithm is developed to organize communication links into Nash-stable, throughput-efficient network partition. The performance of the proposed CF algorithm has been evaluated in terms of average network rate, and two initialization algorithms have been proposed to improve the convergence speed of the CF algorithm. On the other hand, for ad hoc CRNs, a fully distributed CF game is designed in which rational distributed CRs self-organize into throughput-efficient disjoint coalitions based on individual/group rate improvement. Different CF rules have been proposed and the convergence/stability properties of the algorithm under these rules have been analyzed. For the proposed CF rules that may lead to cycles in the CF process, the history condition has been introduced in the CF algorithm to guarantee Nash-stability, and different exit procedures have been described when a CF cycle is inevitable. Furthermore, the probabilistic analysis of the stability of grand coalition structure (GCS) and singleton coalition structure (SCS) has been provided to highlight the effectiveness of the proposed algorithm by evaluating a lower bound on the probability of a general network partition (other than GCS/SCS) being stable. Extensive simulations have been used to show that the proposed algorithm, with optimal bandwidth allocation, provide substantial payoff gains for moderate operating SNR, over other fixed CF structures, and over CF algorithms with suboptimal bandwidth allocation.

6.2 Future Research Directions

In the presented work, the payoff of a player has been defined solely in terms of its achievable rate and CF games have been designed to organize distributed players into disjoint groups/coalitions under the assumption that instantaneous channel state information (CSI) can be made available to all players. One possible extension to this work is to introduce individual players' rate constraints of some of the players in the CF process, to represent those users who might be using audio or video services. In this way, new CF rules may be developed to incorporate individual players' requirements according to their own priority of service. This would require changing the model and analyzing the convergence of the CF process to ensure that the required quality of service (QoS) is provided to the maximum number of players.

Another interesting dimension to explore is the self-organization of distributed players into stable, throughput-efficient coalition structure based on the average, instead of instantaneous, CSI. In this case, players may evaluate the expected rate. Furthermore, in some cases, the available CSI might be incomplete or outdated at some of the distributed players, and the effect of this needs to be taken into consideration while making coalitions.

Stability of the coalition structure evolving from the interactions of distributed players is an important parameter that can be incorporated in the CF rule. Probability that a proposed coalition structure would be stable might be considered as a weight given to the actual achievable payoff of each player in that coalition

structure.

Last but not the least, considering various costs of coalition formation process, in terms of energy and time consumed in self-organizing distributed links, is another interesting dimension to explore.

APPENDIX

A   Probability Density Function of $Y_i^{\{i,k\}}$

$Y_i^{\{i,k\}} = \sum_{j=1,j\neq i,k}^{N} Y_{ji}$ with $Y_{ji} \sim \beta_{ji}\exp(-\beta_{ji}y_{ji})$.   For the case of $\beta_{ji} = \beta, \ \forall \ i,j \in \mathcal{N}$,

$\hat{f}_{Y_i^{\{i,k\}}}(s) = \prod_{j=1,j\neq i,k}^{N} \hat{f}_{Y_{ji}}(s) = \prod_{j=1,j\neq i,k}^{N} \frac{\beta}{s+\beta} = \frac{\beta^{N-2}}{(s+\beta)^{N-2}}$ and hence,

$f_{Y_i^{\{i,k\}}}(\acute{y}_i) = \frac{\beta^{N-2}}{\Gamma(N-2)}(\acute{y}_i)^{N-3}\exp\left(-\beta\acute{y}_i\right)$. For the case of distinct $\beta_{ji}, \ \forall \ i,j \in \mathcal{N}$,

$\hat{f}_{Y_i^{\{i,k\}}}(s) = \prod_{j=1,j\neq i,k}^{N} \hat{f}_{Y_{ji}}(s) = \prod_{j=1,j\neq i,k}^{N}\left(\prod_{j=1,j\neq i,k}^{N}\beta_{ji}\right)\left(\sum_{j=1,j\neq i,k}^{N}\frac{1}{(s+\beta ji)\prod_{l=1,l\neq i,j,k}^{N}(\beta_{li}-\beta_{ji})}\right)$

and hence, $f_{Y_i^{\{i,k\}}}(\acute{y}_i) = \left(\prod_{j=1,j\neq i,k}^{N}\beta_{ji}\right)\left(\sum_{j=1,j\neq i,k}^{N}\frac{\exp(-\beta_{ji}\acute{y}_i)}{\prod_{l=1,l\neq i,j,k}^{N}(\beta_{li}-\beta_{ji})}\right)$.

B   Probability Distribution Function of $Y_i^{\{i\}}$

$Y_i^{\{i\}} = \sum_{j=1,j\neq i}^{N} Y_{ji}$ with $Y_{ji} \sim \beta_{ji} \exp(-\beta_{ji} y_{ji})$. For the case of $\beta_{ji} = \beta$, $\forall\, i,j \in \mathcal{N}$,

$f_{Y_i^{\{i\}}}(y_i) = \frac{\beta^{N-1}}{\Gamma(N-1)} (y_i)^{N-2} \exp\left(-\beta y_i\right)$ which gives:

$F_{Y_i^{\{i\}}}(y_i) = \int_0^{y_i} f_{Y_i^{\{i\}}}(\xi) d\xi = \frac{\beta^{N-1}}{\Gamma(N-1)} \int_0^{y_i} (\xi_i)^{N-2} \exp\left(-\beta \xi_i\right) d\xi_i = 1 - \frac{\Gamma(N-1,\beta y_i)}{\Gamma(N-1)}.$

For the case of distinct β_{ji}, $\forall\, i,j \in \mathcal{N}$,

$f_{Y_i^{\{i\}}}(y_i) = \left(\prod_{j=1,j\neq i}^{N} \beta_{ji}\right) \left(\sum_{j=1,j\neq i}^{N} \frac{\exp(-\beta_{ji} y_i)}{\prod_{l=1,l\neq i,j}^{N}(\beta_{li}-\beta_{ji})}\right)$ which gives:

$F_{Y_i^{\{i\}}}(y_i) = \int_0^{y_i} f_{Y_i^{\{i\}}}(\xi) d\xi = \left(\prod_{j=1,j\neq i}^{N} \beta_{ji}\right) \left(\sum_{j=1,j\neq i}^{N} \frac{1}{\beta_{ji} \prod_{l=1,l\neq i,j}^{N}(\beta_{li}-\beta_{ji})} \int_0^{y_i} \exp(-\beta_{ji} \xi_i) d\xi_i\right) =$

$\left(\prod_{j=1,j\neq i}^{N} \beta_{ji}\right) \left(\sum_{j=1,j\neq i}^{N} \frac{1-exp(-\beta_{ji} y_i)}{\beta_{ji} \prod_{l=1,l\neq i,j}^{N}(\beta_{li}-\beta_{ji})}\right).$

REFERENCES

[1] NTIA, "US frequency allocation chart," 2003. [Online]. Available: http://www.ntia.doc.gov/osmhome/allochrt.html

[2] R. W. Broderson, A. Wolisz, D. Cabric, S. M. Mishra, and D. Willkomm, "White paper: CORVUS: A Cognitive Radio Approach for Usage of Virtual Unlicensed Spectrum," University of California, Berkeley, Tech. Rep., 2004.

[3] M. McHenry, "NSF spectrum occupancy measurements project summary," Shared Spectrum Company, Tech. Rep., Aug. 2005.

[4] S. Shellhammer, A. Sadek, and W. Zhang, "Technical challenges for Cognitive Radio in the TV white space spectrum," *Information Theory and Applications Workshop*, Feb. 2009

[5] FCC,ET Docket No. 03-222 Notice of proposed rule making and order, Dec. 2003.

[6] I. F. Akyildiz, W. Y. Lee, M. C. Vuran, and S. Mohanty, "NeXt generation/dynamic spectrum access/ cognitive radio wireless networks: A survey," *Computer Networks Journal*, vol. 50, no. 13, pp. 2127-2159, 2006.

[7] J. Mitola, III, "Cognitive Radio for Flexible Multimedia Communications," *IEEE international Workshop on Mobile Multimedia Communications (MoMuC '99)*, pp. 310, 1999.

[8] J. O. Neel, "Analysis and design of cognitive radio networks and distributed radio resource management algorithms," Ph.D. dissertation, Virginia Polytechnic Institute and State University, Sept. 2006.

[9] ITU-R, WP8A, Working document towards a PDN Report: "Software Defined Radio in the Land Mobile Service," document 8A/228-E, 6 Sept., 2005.

[10] P. Kolodzy et al., "Next generation communications: Kickoff meeting," in Proc. DARPA, Oct. 17, 2001.

[11] S. Haykin, "Cognitive radio: brain-empowered wireless communications," *IEEE Journal on Selected Areas in Communications (JSAC '07)*, vol.23, no.2, pp. 201- 220, Feb. 2005.

[12] R. Tandra, S. M. Mishra, and A. Sahai, "What is a spectrum hole and what does it take to recognize one?," *Proceedings of the IEEE*, vol. 97, no. 5, pp. 824-848, May 2009.

[13] R. Umar, and A. U. H. Sheikh, "Spectrum access and sharing for cognitive radio," in *Developments in wireless network prototyping, design and deployment: Future generations*, IGI Global, 2012, ch. 12, pp. 241-271.

[14] S. J. Shellhammer, "A comparison of geo-location and spectrum sensing in cognitive radio," *18th International Conference on Computer Communications and Networks (ICCCN09)*, Aug. 2009.

[15] Y. Zhao, L. Morales, J. Gaeddert, K. K. Bae, J.-S. Um, and J. H. Reed, "Applying radio environment maps to cognitive wireless regional area networks," *2nd IEEE International Symposium on Dynamic Spectrum Access Networks (DySPAN '07)*, pp. 115-118, 17-20 April 2007.

[16] A. P. Hulbert, "Spectrum sharing through beacons," *16th IEEE International Symposium on Personal, Indoor and Mobile Radio Communications (PIMRC '05)*, pp. 989-993, Sept. 2005.

[17] M. Derakhshani, and T. Le-Ngoc, "Aggregate interference and capacity-outage analysis in a cognitive radio network," *IEEE Transactions on Vehicular Technology*, vol. 61, no. 1, pp. 196-207, Jan. 2012.

[18] E. Axell, G. Leus, and E. G. Larsson, "Overview of Spectrum Sensing for Cognitive Radio," *2nd International Workshop on Cognitive Information Processing*, 2010.

[19] B. Wang, and K. J. Ray Liu, "Advances in cognitive radio networks: a survey," *IEEE Journal of Selected Topics in Signal Processing*, vol. 5, no. 1, pp. 5-23, 2011.

[20] R. Umar, and A. U. H. Sheikh, "Cognitive radio oriented wireless networks: challenges and solutions," *IEEE International Conference on Multimedia Computing and Systems (ICMCS'12)*, pp. 992-997, Morocco, May 2012.

[21] R. Umar, and A. U. H. Sheikh, "A comparative study of spectrum awareness techniques for cognitive radio oriented wireless networks," *Physical Communications Journal Special Issue: Cognitive Radios*, vol. 9, pp. 148-170, Dec. 2013.

[22] I. F. Akyildiz, B. F. Lo, and R. Balakrishnan, "Cooperative spectrum sensing in cognitive radio networks: A survey," *Physical Communication Journal*, vol. 4, pp. 40-62, 2011.

[23] FCC,ET Docket No. 03-237,07-78 Termination order, 2007.

[24] Y. H. Zeng, Y. C. Liang, and R. Zhang, "A Review on Spectrum Sensing for Cognitive Radio: Challenges and Solutions," *EURASIP Journal on Advances in Signal Processing*, 2010.

[25] T. Yucek, and H. Arslan, " A survey of spectrum sensing algorithms for cognitive radio applications," *IEEE Communications Surveys and Tutorials*, Vol. 11 No. 1. First quarter 2009.

[26] E. Axell, G. Leus, and E. G. Larsson, "Spectrum Sensing for Cognitive Radio: state-of-the-art and recent advances," *IEEE Signal Processing Magazine*, vol. 29, no. 3, pp. 101-116, 2012.

[27] R. Umar, and A. U. H. Sheikh, "Unveiling the hidden assumptions of energy detector based spectrum sensing for cognitive radios," *IEEE Comm. Surveys and Tutorials*, vol. PP, no. 99, pp. 1-16, Sept. 2013.

[28] R. Umar, M. Deriche and A. U. H. Sheikh, "On the validity of Gaussian approximations to exact test statistics of energy detector based spectrum sensing for cognitive radios," *IEEE Region 10 Technical Symposium (TEN-SYMP '14)*, Kuala Lumpur, Malaysia, April 2014.

[29] H. Urkowitz, "Energy detection of unknown deterministic signals," *Proc. IEEE* , vol. 55, no. 4, pp. 523- 531, April 1967.

[30] A. Ghasemi, and E. S. Sousa, "Opportunistic spectrum access in fading channels through collaborative sensing," *J. Commun.*, vol.2, no.2, pp.71-82, March 2007.

[31] Y. H. Zeng, Y. C. Liang, A. T. Hoang, and E. C. Y. Peh, "Reliability of spectrum sensing under noise and interference uncertainty," *IEEE International Conference on Communications (ICC '09)*, June 2009.

[32] K.Arshad, M. A. Imran, and K. Moessner, "Collaborative spectrum sensing optimisation algorithms for cognitive radio networks," *International J. Digital Multimedia Broadcasting*, vol. 2010, Article ID 424036, 20 pages, 2010. doi:10.1155/2010/424036.

[33] M. Buddhikot, P. Kolodzy, S. Miller, K. Ryan, and J. Evans, "DIMSUMNet: New directions in wireless networking using coordinated dynamic spectrum

access," *Conference on the Economics, Technology and Policy of Unlicensed Spectrum*, East Lansing, MI, May 2005.

[34] V. Brik, E. Rozner, S. Banarjee, and P. Bahl, "DSAP: a protocol for coordinated spectrum access," *1st IEEE International Symposium on Dynamic Spectrum Access Networks (DySPAN '05)*, pp. 611-614, Nov. 2005.

[35] C. Raman, R.D. Yates, and N.B. Mandayam, "Scheduling variable rate links via a spectrum server," *1st IEEE International Symposium on Dynamic Spectrum Access Networks (DySPAN '05)*, pp. 110-118, Nov. 2005.

[36] L. Cao, and H. Zheng, "Distributed spectrum allocation via local bargaining," *IEEE International Conference on Sensor and Ad Hoc Communications and Networks (SECON '05)*, pp. 475486, Sept. 2005.

[37] J. Zhao, H. Zheng, and G.-H. Yang, "Distributed coordination in dynamic spectrum allocation networks," *1st IEEE International Symposium on Dynamic Spectrum Access Networks (DySPAN '05)*, pp. 259-268, Nov. 2005.

[38] Q. Zhao, L. Tong, and A. Swami, "Decentralized cognitive MAC for dynamic spectrum access," *1st IEEE International Symposium on Dynamic Spectrum Access Networks (DySPAN '05)*, pp. 224-232, Nov. 2005.

[39] J. Huang, R.A. Berry, and M.L. Honig, "Spectrum sharing with distributed interference compensation," *1st IEEE International Symposium on Dynamic Spectrum Access Networks (DySPAN '05)*, pp. 88-93, Nov. 2005.

[40] S. Sankaranarayanan, P. Papadimitratos, A. Mishra, and S. Hershey, "A bandwidth sharing approach to improve licensed spectrum utilization," *1st IEEE International Symposium on Dynamic Spectrum Access Networks (DySPAN '05)*, pp. 279-288, Nov. 2005.

[41] H. Zheng, and L. Cao, "Device-centric spectrum management," *1st IEEE International Symposium on Dynamic Spectrum Access Networks (DySPAN '05)*, pp. 56-65, Nov. 2005.

[42] C. Peng, H. Zheng, and B.Y. Zhao, "Utilization and fairness in spectrum assignment for opportunistic spectrum access," *ACM Mobile Networks and Applications (MONET '06)*, 2006.

[43] R. Menon, R.M. Buehrer, and J.H. Reed, "Outage probability based comparison of underlay and overlay spectrum sharing techniques," *1st IEEE International Symposium on Dynamic Spectrum Access Networks (DySPAN '05)*, pp. 101-109, Nov. 2005.

[44] S. Huang, X. Liu, and Z. Ding, "Optimal sensing-transmission structure for dynamic spectrum access," *IEEE International Conference on Computer Communications (INFOCOM'09)*, pp. 2295-2303, 19-25 April 2009.

[45] H. B. Salameh, "Rate-maximization channel assignment scheme for cognitive radio networks," *IEEE Global Telecommunications Conference (GLOBECOM '10)*, pp. 1-5, 6-10 Dec. 2010.

[46] M. Felegyhazi, and J. Hubaux, "Game theory in wireless networks: A tutorial," Technical Report LCA-REPORT-2006-002, 2006.

[47] B. Wang, Y. Wu, and K. Liu, "Game theory for cognitive radio networks: An overview," *Computer Networks*, vol. 54, no. 14, pp. 25372561, 2010.

[48] M. Felegyhazi, M. Cagalj, S. S. Bidokhti, and J-P Hubaux, "Non-cooperative multi-radio channel allocation in wireless networks," *IEEE International Conference on Computer Communications (INFOCOM'07)*,pp. 1442-1450, 6-12 May 2007.

[49] M. Maskery, V. Krishnamurthy, and Q. Zhao, "Decentralized dynamic spectrum access for cognitive radios: Cooperative design of a non-cooperative game," *IEEE Transactions on Communications*, vol. 57, no. 2, pp. 459469, 2009.

[50] C. Ghosh, D. Agrawal, and M. Rao, "Channel capacity maximization in cooperative cognitive radio networks using game theory," *ACM SIGMOBILE Mobile Computing and Communications Review*, vol. 13, no. 2, pp. 213, 2009.

[51] N. Nie, and C. Comaniciu, "Adaptive channel allocation spectrum etiquette for cognitive radio networks," *1st IEEE International Symposium on Dynamic Spectrum Access Networks (DySPAN '05)*, pp. 269-278, Nov. 2005.

[52] R. Etkin, A. Parekh, and D. Tse, "Spectrum sharing for unlicensed bands," *1st IEEE International Symposium on Dynamic Spectrum Access Networks (DySPAN '05)*, pp. 251-258, Nov. 2005.

[53] Z. Khan, J. Lehtomaeki, M. Codreanu, M. Latva-aho, and L. A. DaSilve, "Throughput efficient dynamic coalition formation in distributed cognitive radio networks," *EURASIP J. on Wireless Communications and Networking*, vol. 2010, article no. 87, April 2010.

[54] W. Saad, Z. Han, R. Zheng, A. Hjorungnes, T. Basar, and H. V. Poor, "Coalitional games in partition form for joint spectrum sensing and access in cognitive radio networks", *IEEE J. of Sel. Topics in Signal Processing*, vol. 6, no. 2, pp. 195-209, 2012.

[55] X. Hao, M. H. Cheung, V. W. S. Wong, and V. C. M. Leung, "Hedonic coalition formation game for cooperative spectrum sensing and channel access in cognitive radio networks," *IEEE Trans. on Wireless Communications*, vol. 11, no. 11, pp. 3968-3979, Nov. 2012.

[56] FCC, ET Docket No. 10-174 2nd memo. opinion and order, Sept. 2010.

[57] R. Umar, and W. Mesbah, "Throughput-efficient spectrum access in cognitive radio networks: A Game theoretic approach" in *Software-Defined and Cognitive Radio technologies for Dynamic spectrum access and management*, IGI Global, to be published in Sept. 2014 [under review].

[58] R. Umar, and W. Mesbah, "Joint coalition formation and bandwidth allocation in cognitive radio networks", *9th International Conference on Cognitive Radio Oriented Wireless Networks (CROWNCOM '14)*, Oulu, Finland, June 2014.

[59] R. Umar and W. Mesbah, "Throughput-efficient coordinated coalition formation games in cognitive radio networks", *Wiley Journal on Wireless Communications and Mobile Computing* [under review].

[60] R. Umar, and W. Mesbah, "Distributed coalition formation and bandwidth allocation in ad hoc cognitive radio networks", *IEEE Vehicular Technology Conference (VTC '14-Fall)*, Vancouver, Canada, Sept. 2014.

[61] R. Umar and W. Mesbah, "Distributed coalition formation for efficient spectrum sharing in cognitive radio ad-hoc networks", *IEEE Transactions on Wireless Communications* [under review].

[62] J. Ma, G. Y. Li, and B. H. Juang, "Signal Processing in Cognitive Radio," *Proceedings of the IEEE* , vol. 97, no. 5, pp. 805-823, May 2009.

[63] A. Sahai, N. Hoven, and R. Tandra, " Some fundamental limits in cognitive radio," *Allerton Conference on Communications, Control and Computing*, Urbana, Oct. 2004.

[64] A. Ghasemi, and E. S. Sousa, " Spectrum sensing in cognitive radio networks: requirements, challenges and design trade-offs," *IEEE Communications Magazine*, vol. 46, no. 4, pp. 32-39, April 2008.

[65] T. Basar, and G. J. Olsder, Dynamic Noncooperative Game Theory (Series in Classics in Applied Mathematics), Philadelphia, PA: SIAM, Jan. 1999.

[66] R. B. Myerson, Game Theory, Analysis of Conflict. Cambridge, MA: Harvard Univ. Press, Sept. 1991.

[67] W. Saad, Z. Han, M. Debbah, A. Hjoerungnes, and T. Basar, "Coalitional game theory for communication networks," *IEEE Signal Processing Magazine*, vol. 26, no. 5, pp. 7797 2009.

[68] D. Ray, A Game-Theoretic Perspective on Coalition Formation. New York: Oxford Univ. Press, Jan. 2007.

[69] J. von Neumann, and O. Morgenstern, Theory of Games and Economic Behavior. Princeton, NJ: Princeton Univ. Press, Sept. 1944.

[70] R. Thrall, and W. Lucas, "N-person games in partition function form," *Naval Res. Logistics Quart.*, vol. 10, no. 1, pp. 281298, 1963.

[71] R. J. Aumann, and B. Peleg, "Von neumann-morgenstern solutions to cooperative games without side payments," *Bull. Amer. Math. Soc.*, vol. 6, no. 3, pp. 173179, 1960.

[72] T. Sandholm, K. S. Larson, M. R. Andersson, O. Shehory, and F. Tohm, "Coalition structure generation with worst case guarantees," *Artificial Intelligence*, vol. 111, no. 1/2, pp. 209238, Jul. 1999.

[73] N. J. A. Sloane (Ed.), "Bell or exponential numbers: ways of placing n labeled balls into n indistinguishable boxes", *The On-Line Encyclopedia of Integer Sequence (OEIS)*.

[74] A. Bogomolnaia and M. O. Jackson, "The stability of hedonic coalition structures," *Games Economic Behavior*, vol. 38, pp. 201230, Feb. 2002.

[75] P. Stoica, and R.L. Moses, "Introduction to spectral Analysis". *Prentice Hall*, New Jersey 1997.

[76] F. Digham, M. S. Alouini, and M. K. Simon, "On the energy detection of unknown signals over fading channels," *5th IEEE International Conference on Communications (ICC '03)*, pp. 3575- 3579, 11-15 May 2003.

[77] H. P. Frank, Fitzek, and D. K. Marcos, *Cognitive wireless networks: concepts, methodologies and visions inspiring*, Springer, 2007.

[78] R. Tandra, and A. Sahai, "SNR Walls for Signal Detection," *IEEE Journal on Selected Topics in Signal Processing*, vol. 2, no. 1, pp. 4-17, Feb. 2008.

[79] F.-Boroujeny, "Filter Bank Spectrum Sensing for Cognitive Radios," *IEEE Transactions on Signal Processing*, vol. 56, no. 5, pp. 1801-1811, May 2008.

[80] D. J. Thomson, "Spectrum estimation and harmonic analysis," *Proceedings of the IEEE* , vol. 70, no. 9, pp. 1055- 1096, Sept. 1982.

[81] Z. Tian, and G. B. Giannakis, "A wavelet approach to wideband spectrum sensing for cognitive radios," *International Conference on Cognitive Ra-*

dio Oriented Wireless Networks and Communications (CROWNCOM '06), June 2006.

[82] Z. Tian, and G. G. Giannakis, "Compressed Sensing for Wideband Cognitive Radios," *IEEE International Conference on Accoustic, Speech and Signal Processing (ICASSP '10)*, pp. 1357-1360, 15-20 April 2007.

[83] W. A. Gardner, "Exploitation of spectral redundancy in cyclostationary signals," *IEEE Signal Processing Magazine*, vol. 8, no. 2, pp. 14-36, 1991.

[84] M. Oner, and F. K. Jondral, "Cyclostationarity-based methods for the extraction of the channel allocation information in a spectrum pooling system," *IEEE Radio and Wireless Conference*, pp. 279- 282, Atlanta, Georgia, USA, 19-22 Sept. 2004.

[85] D. Cabric, and R. W. Brodersen, "Physical layer design issues unique to cognitive radio systems," *16th IEEE International Symposium on Personal, Indoor and Mobile Radio Communications (PIMRC '05)*, pp. 759-763, 11-14 Sept. 2005.

[86] A. Fehske, J. Gaeddert, and J. H. Reed, "A new approach to signal classification using spectral correlation and neural networks," *1st IEEE International Symposium on Dynamic Spectrum Access Networks (DySPAN '05)*, Baltimore, MD, USA, pp. 144-150, 8-11 Nov. 2005.

[87] M. Ghozzi, F. Marx, M. Dohler, and J. Palicot, "Cyclostationarity-Based Test for Detection of Vacant Frequency Bands," *International Confer-*

ence on Cognitive Radio Oriented Wireless Networks and Communications (CROWNCOM '06), pp. 1-5, June 2006.

[88] K. Kim, I. A. Akbar, K. K. Bae, J. S. Urn, C. M. Spooner, and J. H. Reed, "Cyclostationary Approaches to Signal Detection and Classification in Cognitive Radio," *2nd IEEE International Symposium on Dynamic Spectrum Access Networks (DySPAN '07)*, pp. 212-215, 17-20 April 2007.

[89] J. Lunden, V. Koivunen, A. Huttunen, and H. V. Poor, "Spectrum Sensing in Cognitive Radios Based on Multiple Cyclic Frequencies," *International Conference on Cognitive Radio Oriented Wireless Networks and Communications (CROWNCOM '07)*, pp. 37-43, 1-3 Aug. 2007.

[90] A. Al-Habashna, O. A. Dobre, R. Venkatesan, and D. C. Popescu, "Second-Order Cyclostationarity of Mobile WiMAX and LTE OFDM Signals and Application to Spectrum Awareness in Cognitive Radio Systems," *IEEE Journal of Selected Topics in Signal Processing*, vol. 6, no.1, pp. 2642, 2012.

[91] D. Cabric, M. S. W. Chen, D. A. Sobel, S. Wang, J. Yang, and R. W. Brodersen, "Novel radio architectures for UWB, 60 GHz, and cognitive wireless systems," *EURASIP Journal on Wireless Communication and Networking*, pp. 1-18, Jan. 2006.

[92] S. Maleki, A. Pandharipande, and G. Leus, "Two-stage spectrum sensing for cognitive radios," *IEEE International Conference on Accoustic, Speech and Signal Processing (ICASSP '10)*, pp. 2946, 14-19 Mar. 2010.

[93] H. Tang, "Some physical layer issues of wide-band cognitive radio systems," *1st IEEE International Symposium on Dynamic Spectrum Access Networks (DySPAN '05)*, Baltimore, MD, USA, pp. 151-159, 8-11 Nov. 2005.

[94] A. Pandharipande, and J. P. M. G. Linnartz, "Performance Analysis of Primary User Detection in a Multiple Antenna Cognitive Radio," *IEEE Internationl Conference on Communications (ICC '07)*, pp.6482-6486, 24-28 June 2007

[95] Y. H. Zeng, Y. C. Liang, and R. Zhang, "Blindly combined energy detection for spectrum sensing in cognitive radio," *IEEE Signal Processing Letters*, vol. 15, pp. 649-652, 2008.

[96] B. Zayen, A. Hayar, and K. Kansanen, "Blind Spectrum Sensing for Cognitive Radio Based on Signal Space Dimension Estimation," *IEEE International Conference on Communications (ICC '09)*, pp. 1-5, 14-18 June 2009

[97] Y. H. Zeng, and Y. C. Liang, "Eigenvalue based spectrum sensing algorithms for cognitive radio," *IEEE Transactions on Communications*, vol. 57, no. 6, pp. 1784-1793, 2009.

[98] Y. H. Zeng, and Y. C. Liang, "Eigenvalue based sensing algorithms," IEEE 802.22-06/0118r0, July 2006.

[99] P. Bianchi, J. Najim, G. Alfano, and M. Debbah, "Asymptotics of eigen-based collaborative sensing," *IEEE Information Theory Workshop (ITW '09)*, Taormina, Sicily, Italy, Oct. 2009.

[100] M. Z. Shakir, W. Tang, M. A. Imran, and M. Alouini, "Collaborative spectrum sensing based on the upper bound on joint PDF of extreme eigenvalues," *European Conf. Signal Processing (EUSIPCO '11)*, Barcelona, Spain, Aug. 2011.

[101] M. Z. Shakir, W. Tang, A. Rao, M. A. Imran, and M. Alouini, "Eigenvalue Ratio Detection Based On Exact Analytical Moments Of Smallest And Largest Eigenvalues," *International Conference on Cognitive Radio Oriented Wireless Networks and Communications (CROWNCOM '11)*, pp. 46-50, May 2011.

[102] Y. H. Zeng, and Y. C. Liang, "Maximum-minimum eigenvalue detection for cognitive radio," *18th IEEE International Symposium on Personal, Indoor and Mobile Radio Communications (PIMRC '07)*, Athens, Greece, Sept. 2007.

[103] M.Maida, J. Najim, P. Bianchi, and M. Debbah, "Performance analysis of some eigen-based hypothesis tests for collaborative sensing," *IEEE Workshop on Statistical Signal Processing*, Cardiff,Wales, UK, Sept. 2009.

[104] F. Penna, R. Garello, and M. A. Spirito, "Cooperative spectrum sensing based on the limiting eigenvalue ratio distribution in wishartmatrices," *IEEE Communications Letters*, vol. 13, no. 7, pp. 507-509, 2009.

[105] Y. H. Zeng, and Y. C. Liang, "Covariance based signal detections for cognitive radio," *2nd IEEE International Symposium on New Frontiers in Dy-*

namic Spectrum Access Networks (DySPAN '07), pp. 202-207, Dublin, Ireland, April 2007.

[106] Y. H. Zeng, and Y. C. Liang, "Spectrum sensing algorithms for cognitive radio based on statistical covariances," *IEEE Transactions on Vehicular Technology (VTC '09)*, vol. 58, no. 4, pp. 1804-1815, May 2009.

[107] Y. H. Zeng, and Y. C. Liang, "Simulations for wireless microphone detection by eigenvalue and covariance based methods," IEEE 802.22-07/0325r0, July 2007.

[108] C. H. Lee, and W. Wolf, "Blind signal separation for cognitive radio," *Journal of Signal Processing Systems*, SpringerLink.

[109] X. Liu, X. Tan, and A. A. Anghuwo, "Spectrum detection of cognitive radio based on blind signal separation," *IEEE Youth Conference on Information, Computing and Telecommunication (YC-ICT '09)*, pp. 166-169, 20-21 Sept. 2009.

[110] G. Ganesan, and Y. Li, "Cooperative spectrum sensing in cognitive radio, part I: two user networks," *IEEE Transactions on Wireless Communications*, vol. 6, no. 6, pp. 2204-2213, June 2007.

[111] G. Ganesan, and Y. Li, "Cooperative spectrum sensing in cognitive radio, part II:Multiuser networks," *IEEE Transactions on Wireless Communications*, vol. 6, no. 6, pp. 2214-2222, June 2007.

196

[112] I. F. Akyildiz, B. F. Lo, and R. Balakrishnan, "Cooperative spectrum sensing in cognitive radio networks: A survey," *Physical Communication Journal*, vol. 4, pp. 40-62, 2011.

[113] G. Ganesan, and Y. Li, "Cooperative spectrum sensing in cognitive radio networks," *1st IEEE International Symposium on Dynamic Spectrum Access Networks (DySPAN '05)*, Baltimore, MD, USA, pp. 137-143, 8-11 Nov. 2005.

[114] S. M. Mishra, A. Sahai, and R. W. Brodersen, "Cooperative Sensing among Cognitive Radios," *IEEE International Conference on Communications (ICC '06)*, pp. 1658-1663, June 2006.

[115] J. Zhao, H. Zheng, and G. H. Yang, "Distributed coordination in dynamic spectrum allocation networks," *1st IEEE International Symposium on Dynamic Spectrum Access Networks (DySPAN '05)*, Baltimore, MD, USA, pp. 259-268, 8-11 Nov. 2005.

[116] A. F. Cattoni, I. Minetti, M. Gandetto, R. Niu, P. K. Varshney, and C. Regazzoni, "A spectrum sensing algorithm based on distributed cognitive models," *SDR Forum Technical Conference*, Orlando, Florida, USA, Nov. 2006.

[117] M. Gandetto, and C. Regazzoni, "Spectrum sensing: A distributed approach for cognitive terminals," *IEEE Journal on Selected Areas in Communications (JSAC '07)*, vol. 25, no. 3, pp. 546-557, April 2007.

[118] D. Cabric, S. Mishra, D. Willkomm, R. Brodersen, and A. Wolisz, "A cognitive radio approach for usage of virtual unlicensed spectrum," *IST Mobile and Wireless Communications Summit*, Dresden, Germany, June 2005.

[119] W. Zhang, R. K. Mallik, Ye Li, and K. B. Letaief, "Cooperative spectrum sensing optimization in cognitive radio networks," *IEEE International Conference on Communications (ICC '08)*,pp. 3411-3415, 2008.

[120] W. Zhang, and K. Letaief, "Cooperative spectrum sensing with transmit and relay diversity in cognitive radio networks," *IEEE Transactions on Wireless Communications*, vol. 7, no. 12, pp. 47614766, 2008.

[121] N. S. Shankar, C. Cordeiro, and K. Challapali, "Spectrum agile radios: utilization and sensing architectures," *1st IEEE International Symposium on Dynamic Spectrum Access Networks (DySPAN '05)*, Baltimore, MD, USA, pp. 160-169, 8-11 Nov. 2005.

[122] F. F. Digham, M. S. Alouini, and M. K. Simon, "On the energy detection of unknown signals over fading channels, *IEEE Trans. Commun.*, vol. 55, no. 1, pp. 2124, Jan. 2007.

[123] A. Ghasemi, and E. S. Sousa, "Collaborative spectrum sensing for opportunistic access in fading environments," *1st IEEE International Symposium on Dynamic Spectrum Access Networks (DySPAN '05)*, Baltimore, MD, USA, pp. 131-136,8-11 Nov. 2005.

[124] Z. Ye, G. Memik, and J. Grosspietsch, "Energy detection using estimated noise variance for spectrum sensing in cognitive radio networks," *IEEE Wireless Communications and Networking Conference (WCNC '08)*, pp.711-716, March 31 - April 3 2008.

[125] A. Sonnenschein, and P. M. Fishman, "Radiometric detection of spread-spectrum signals in noise of uncertain power," *IEEE Transactions on Aerospace and Electronic Systems*, vol. 28, no. 3, pp. 654-660, July 1992.

[126] D. Cabric, A. Tkachenko, and R. W. Brodersen, "Experimental study of spectrum sensing based on energy detection and network cooperation," *1st International Workshop on Technology and Policy for Accessing Spectrum (TAPAS 2006)*, Boston, August 2006.

[127] S. M. Kay, *Fundamentals of statistical signal Processing: Vol. II, Detection theory*. Prentice-Hall International Editions, Upper Saddle River, NJ, 1998.

[128] T. Trump and I. Muursepp, "An energy detector for spectrum sensing in impulsive noise environment," *IEEE 22nd International Symposium on Personal Indoor and Mobile Radio Communications (PIMRC'11)*, pp. 467-471, 11-14 Sept. 2011.

[129] W. Saad, Z. Han, T. Basar, M. Debbah, and A. Hjorungnes, "Coalition formation games for collaborative spectrum sensing," *IEEE Transactions on Vehicular Technology*, vol. 60, no. 1, pp. 276297, Jan. 2011.

[130] R. Umar, M. Fahham, M. Deriche and A. U. H. Sheikh, "Hybrid cooperative energy detection techniques in cognitive radio networks" in *Software-Defined and Cognitive Radio technologies for Dynamic spectrum access and management*, IGI Global, to be published in Sept. 2014 [under review].

[131] H. K. Kathuria, "A Hybrid Two-Threshold Spectrum Sensing Algorithm," *Master Thesis*, King Fahd University of Petroleum & Minerals, Dhahran, Saudi Arabia, 2012.

[132] R. La and V. Anantharam, "A game-theoretic look at the Gaussian multi-access channel," *DIMACS Series in Discrete Math. Theoretical Comp. Sci.*, vol. 66, pp.87106.

[133] Z. Khan, S. Glisic, L. DaSilva and J. Lehtomaki, "Modeling the dynamics of coalition formation games for cooperative spectrum sharing in an interference channel," *Trans. on Computational Intelligence and AI in Games*, vol. 3, no. 1, pp. 1730, 2011.

[134] Y. Yuan; P. Bahl, R. Chandra, P. A. Chou, J. I. Ferrell, T. Moscibroda, S. Narlanka, and W. Yunnan, "KNOWS: Cognitive Radio Networks Over White Spaces," *IEEE DySPAN'07*, pp. 416-427, April 2007.

[135] S. Boyd, and L. Vandengerghe, *Convex Optimization*. Cambridge University Press, 2005.

[136] M. Filo, A. Hossain, A. R. Biswas, and R. Piesiewics, "Cognitive pilot channel: Enabler for radio systmes coexistence," *Int. Workshop on Cognitive Radio and Advanced Spectrum Management*, Aalborg, Denmark, May 2009.

[137] A. Bogomolnaia and M. O. Jackson, "The stability of hedonic coalition structures," *Games Economic Behavior*, vol. 38, pp. 201230, Feb. 2002.

[138] S. Guruacharya, D. Niyato, M. Bennis, and Dong In Kim, "Dynamic coalition formation for network MIMO in small cell networks," *IEEE Trans. on Wireless Communications*, vol.12, no.10, pp. 5360,5372, Oct. 2013.

[139] A. Papoulis, and S. U. Pillai, Proability, Random variables and Stochastic Processes. McGraw-Hill, 4th Ed. 2002.

Vitae

- Name: Raza Umar

- Nationality: Pakistani

- Date of Birth: December 21, 1977

- Present Address: P.O. Box 8661, KFUPM, Dhahran 31261, Saudi Arabia.

- Permanent Address: 41-E Block, Model Town, 54700 Lahore, Pakistan.

- Telephone: (+966) 53 156 1042

- Email: *raza.umar@gmail.com*

Education:

- Ph.d. Electrical Engineering: May, 2014

- M.Sc. Information Technology: Jun, 2005

- B.Sc. Electrical Engineering: Sept, 2000

Industrial Experience:

- Research Fellow Oct, 2004 - Jun, 2005

  Alcatel, Research and Innovation center, Weilimdorf, Germany

- Research Internee Jun, 2004 - Sept, 2004

  BKtel systems GmbH & Co. KG, Kornwestheim, Germany

- Senior Design Engineer Sept, 2000 - Jan, 2003

  AVAZ networks Inc., formerly Communications Enabling Technologies, Islamabad, Pakistan (HQ: Irvine, CA, USA)

- **Book chapters:**

  1. R. Umar, and W. Mesbah, **Throughput-efficient spectrum access in cognitive radio networks: A Game theoretic approach** in *Software-Defined and Cognitive Radio technologies for Dynamic spectrum access and management, IGI Global*, to be published in Sept. 2014 (under 2nd review).

  2. R. Umar, M. Fahham, M. Deriche and A. U. H. Sheikh, H**ybrid cooperative energy detection techniques in cognitive radio networks** in *Software-Defined and Cognitive Radio technologies for Dynamic spectrum access and management, IGI Global*, to be published in Sept. 2014 (under 2nd review).

  3. R. Umar, and A. U. H. Sheikh, **Spectrum access and sharing for cognitive radio in Developments** in *wireless network prototyping, design and deployment: Future generations, IGI Global*, 2012, ch. 12, pp. 241-271. doi:10.4018/978-1-4666-1797-1.ch012.

- **Journal publications:**

1. R. Umar and W. Mesbah, **Distributed coalition formation for efficient spectrum sharing in cognitive radio ad-hoc networks**, *IEEE Transactions on Wireless Communications* (expected submission by the end of June 2014).

2. R. Umar and W. Mesbah, **Throughput-efficient coordinated coalition formation games in cognitive radio networks**, *Wiley Journal on Wireless Communications and Mobile Computing* (under review).

3. R. Umar, and A. U. H. Sheikh, **A comparative study of spectrum awareness techniques for cognitive radio oriented wireless networks**, *Elsevier Physical Communications Journal Special Issue: Cognitive Radios*, vol. 9, pp. 148-170, Dec. 2013. doi:10.1016/j.phycom.2012.07.005.

4. R. Umar, A. U. H. Sheikh and M. A. Deriche, **Unveiling the hidden assumptions of energy detector based spectrum sensing for cognitive radios**, IEEE Communications Surveys and Tutorials, vol. 16, no. 2, pp. 713-728, Second Quarter 2014. doi:10.1109/SURV.2013.081313.00054.

- **International Conference publications:**

1. R. Umar, and W. Mesbah, **Distributed coalition formation and bandwidth allocation in ad hoc cognitive radio networks**, accepted at *IEEE Vehicular Technology Conference (VTC '14-Fall)*, Vancouver, Canada, Sept. 14-17 2014.

2. R. Umar, and W. Mesbah, **Joint coalition formation and bandwidth allocation in cognitive radio networks**, accepted at *9th International Conference on Cognitive Radio Oriented Wireless Networks (CROWNCOM '14)*, Oulu, Finland, June 2-4 2014.

3. R. Umar, M. Deriche and A. U. H. Sheikh, **On the validity of Gaussian approximations to exact test statistics of energy detector based spectrum sensing for cognitive radios**, *IEEE Region 10 Technical Symposium (TENSYMP '14)*, Kuala Lumpur, Malaysia, April 14-16 2014.

4. R. Umar, **Spectrum sensing for cognitive radio**, *15th Saudi Technical Exchange Meeting (STEM'12)*, Dhahran, Saudi Arabia, Dec. 18-20, 2012.

5. R. Umar, and A. U. H. Sheikh, **Cognitive radio oriented wireless networks: challenges and solutions**, *International workshop on cognitive radio networks in conjunction with IEEE International Conference on Multimedia Computing and Systems (ICMCS'12)*, Tangier, Morocco, May 10-12, 2012.